Trinity College Dublin
Coláiste na Tríonóide, Baile Átha Cliath
The University of Dublin

Investigating the Role of Altered Energy Metabolism in the Therapeutic Response of Rectal Cancer

Croí Ellyn Buckley (B.Sc., M.Sc.)

Ph.D. Thesis (Volume 2)

Submitted to Trinity College Dublin for the degree of

Doctor of Philosophy

September 2022

Department of Surgery, Trinity St. James's Cancer Institute, Trinity Translational Medicine Institute, Trinity College Dublin and St. James' Hospital

Thesis supervisors: Dr Niamh Lynam-Lennon (Primary Supervisor)

Prof. Jacintha O'Sullivan (Secondary Supervisor)

Chapter 6: Multi-Omic profiling of pre-treatment sera and tumour tissue from rectal cancer patients and non-cancer rectal tissue controls

6.1. Introduction

The identification of biomarkers that predict response to neoCRT, prior to initiation of treatment, are crucial for improved stratification, quality of life and outcomes for rectal cancer patients. Resistance to neoCRT is a major clinical problem in the management of rectal cancer, with a conservative estimate of 15-30% of patients achieving a pCR, which is associated with favourable prognosis in rectal cancer (44-47). The majority of patients who are resistant to standard of care treatments, are subject to therapy-associated toxicities, a delay in surgery and no apparent therapeutic gain. Currently, standard clinicopathological parameters do not predict patient response to treatment, highlighting the need for novel biomarkers predicting response to neoCRT, prior to initiation of treatment, for improved patient stratification.

Altered tumour metabolism has been demonstrated as a mechanism underlying the resistance to radiation and chemotherapy (177-181), suggesting a potential role for metabolic markers as biomarkers predicting response to treatment. In chapters 2-4, altered energy metabolism was demonstrated to be associated with radioresistance in an *in vitro* model of radiosensitive/radioresistant CRC. However, the role of altered metabolism in the response to neoCRT *in vivo* is largely unknown. A number of studies have utilised metabolomic profiling to identify biomarkers predictive of therapeutic response in rectal cancer (423-425). In a recent study conducted by Rodriguez-Tomas *et al.,* metabolomic profiling of sera from rectal cancer patients, identified two metabolites, succinate and valine, as preliminary biomarkers predictive of patient response to neoadjuvant CRT and relapse (423). Furthermore, another study of pre-treatment rectal cancer sera identified a multi-metabolite panel predictive of therapeutic response by metabolomic profiling (424). These findings highlight the role of altered metabolism in rectal cancer and the potential utility of metabolomic profiling in the identification of predictive biomarkers in rectal cancer.

Initial research to identify potential predictive biomarkers often involves the use of *in vitro* models, as they are cost-effective, easily powered, and accessible. However, there are a number of limitations to the use of *in vitro* models, primarily that they are an over-simplification of a much more complex biological system (426). One approach to validate findings of *in vitro* studies, and to enhance the translation of laboratory-based research to the patient setting is the use of *ex vivo* samples. *Ex vivo* tumour tissue samples more accurately reflect the diverse cellular components of a tumour, including cancer cells, immune cells and stromal cells. Furthermore, the 3D structure of the tumour is maintained in *ex* vivo tumour

tissue biopsies, more accurately reflecting the tumour composition *in vivo,* when compared to 2D *in vitro* models. In addition, as an ideal biomarker is easily accessible, the identification of minimally-invasive circulating biomarkers are of particular interest in biomarker discovery and development (315). Another beneficial strategy to identify and validate predictive biomarkers is to assess potential biomarkers in non-cancer tissue, to further elucidate the role of these biomarkers in tumour pathogenesis.

In recent years, 'omic' platforms have become more accessible, and have been widely utilised for the identification of biomarkers, and to give a more comprehensive view of biological systems and diseases (316). Transcriptomic analysis is the study of relative RNA transcript abundance (317). Metabolomic profiling is the quantitation of small metabolites in a system, and gives an indication of the metabolic pathways being utilised (325). Evidence suggests that combining data from an 'upstream' omic platform, such as transcriptomics, with that from a 'downstream' omic platform, such as metabolomics, can provide a more detailed, dynamic and accurate portrayal of the flux of biological pathways in a system or disease (317). Multi-omic profiling has been performed to identify predictive and prognostic biomarkers of CRC (427-429). One study demonstrated that the integration of multi-omic data from metabolomic, gene expression, and copy number variation analyses, permitted identification of reliable biomarkers highly predictive of relapse in CRC patients, and highlighted the immune response as a biological signature of relapse in CRC (427). The authors also highlighted that the integration of multi-omic data permitted the elimination of redundant molecular features.

In this chapter, the role of altered metabolism in both the development and therapeutic response of rectal cancer was investigated by profiling the metabolome, secretome and transcriptome of pre-treatment sera and tumour samples from rectal cancer patients and rectal tissue samples from non-cancer controls.

6.2. Overall Objective and Specific Aims of Chapter 6

The specific aims of this chapter were:

- Investigate whether the metabolome in pre-treatment sera samples from rectal cancer patients is associated with subsequent pathological response to neoCRT and other clinicopathological characteristics.
- Investigate if the metabolome and transcriptome of pre-treatment rectal cancer biopsies is associated with subsequent pathological response to neoCRT, and other clinicopathological characteristics.
- Evaluate the real-time metabolic rate of pre-treatment rectal tumour and non-cancer rectal tissue biopsies, to investigate the basal metabolic phenotype
- Characterise the metabolome of rectal cancer tissue, tumour conditioned media, and compare to that of non-cancer rectal tissue.
- Profile and compare the inflammatory secretome of rectal cancer and non-cancer rectal tissue, and correlate with clinicopathological characteristics.
- Characterise the basal transcriptome of rectal cancer tissue and non-cancer rectal tissue.
- Investigate whether the altered metabolome and transcriptome of rectal cancer permit predictive clustering into cancer and non-cancer cohorts.

6.3. Materials and Methods

6.3.1. *Patient Cohort*

Ethical approval for patient sample collection for this study was granted by the Joint St. James's Hospital/AMNCH ethical review board and the Beacon Hospital Research Ethics Committee. Patients undergoing lower gastrointestinal investigations or endoscopy for rectal cancer diagnosis were recruited between January 2018 and October 2021 from St. James's Hospital, Dublin and Beacon Hospital, Dublin (*n*=36 cancers, *n*=31 non-cancers). A separate cohort of pre-treatment sera samples (*n*=52) from consenting rectal adenocarcinoma patients were also obtained in collaboration with Ahus and Oslo University Hospitals, Norway, collected between October 2013 and November 2017.

6.3.2. *Tissue Collection*

Pre-treatment rectal tumour biopsies were obtained from consenting patients by a qualified endoscopist at diagnostic endoscopy, prior to neoCRT. Normal (non-cancer) rectal tissue biopsies were obtained by a qualified endoscopist during colonoscopy from consenting patients who did not have a cancer diagnosis. Specimens were immediately placed in RNA-*later* (Ambion, Warrington, UK) and refrigerated for 24 h, before removal of RNA-*later* and storage at -80^{o}C. Biopsies were also snap-frozen in liquid nitrogen for 1-2 min, and stored at -80°C. Patient data was pseudo-anonymised and coded with a unique biobank identifier. Histological confirmation of tumour tissue and non-malignant tissue in biopsies was performed by an experienced GI pathologist using haematoxylin and eosin staining. Patient data was pseudonymised and coded with unique biobank identifier.

6.3.3. *Patient treatment*

Rectal cancer patients from St. James's Hospital or the Beacon hospital received either neoCRT, neoCT, neoRT, surgery only, or CT only. All rectal cancer patients from the Norway sera cohort received neoadjuvant chemoradiation therapy (neoCRT), prior to surgery. Chemotherapy consisted of capecitabine, FLOX (fluorouracil, leucovorin, oxaliplatin) or FLV (5-FU, leucovorin). Radiation therapy was delivered in either 25 fractions of 2 Gy, or 5 fractions of 5 Gy.

6.3.4. *Pathological response*

Response to neoCRT was determined pathologically. All resected rectal specimens were assessed by an experienced pathologist who was blinded to the clinical data. Tumour regression score (TRS) in the Norwegian cohort was assessed using the college of American

pathologists/American joint committee of cancer (CAP/AJCC) four-point TRS scale. This scale is identical to the modified Ryan TRS scale used in the UK and Ireland, which was utilised in this study for patient samples obtained from St. James's Hospital and the Beacon Hospital. In these scales TRS 0 (complete response) refers to no remaining viable cancer cells, TRS 1 (moderate response) refers to only a small cluster or single cancer cells remaining, TRS 2 (minimal response) refers to residual cancer remaining with fibrosis, and TRS 3 (poor response) refers to minimal or no tumour kill with extensive residual cancer (430).

6.3.5. *Generation of tumour conditioned media and non-cancer conditioned media*

Tumour conditioned media (TCM) and non-cancer conditioned media (NCM) was generated using fresh pre-treatment rectal cancer biopsies and normal rectal tissue biopsies, respectively. Biopsies were washed gently three times in PBS supplemented with 1% penicillin-streptomycin, 0.1% gentamycin and 1% Fungizone™ (amphotericin B) (Merck, Sigma Aldrich). The biopsy was then placed in 1 mL M199 media, supplemented with FBS (10%), penicillin-streptomycin (1%), Fungizone™ (1%), gentamycin (0.1%) and insulin (1 µg/mL) in a 12-well plate. The plate was incubated at 37°C at 5% CO_2/ 95% atmospheric air overnight. Following 24 h, the TCM or NCM was collected and stored at -80°C. Matched tissue biopsies were collected, snap-frozen in liquid nitrogen and stored at -80°C.

6.3.6. *Metabolite extraction from tissue*

Frozen tissue was weighted and grinded with liquid nitrogen followed by addition of ice-cold extraction solvent (Ethanol: PBS = 85:15). The samples were subsequently centrifuged at 10000 × *g* for 5 min at 4°C. The supernatant was collected and stored at -80°C for metabolite measurement.

6.3.7. *TCM, NCM and serum sample preparation for metabolomic analysis*

TCM and serum samples were thawed and centrifuged at 2750 × *g* for 5 min at 4°C prior to metabolomic analysis.

6.3.8. *AbsoluteIDQ® p180 assay*

Metabolites were identified and quantified using the AbsoluteIDQ® p180 assay (Biocrates Life Sciences, Innsbruck, Austria) according to the manufacturers' instructions. Detailed sample preparation and analysis were previously described (431). Briefly, 10 µL of sample supernatant from TCM, NCM, serum and tissue were added to the 96-well plate and dried under a stream of nitrogen. A total of 50 µL of 5% phenyl isothiocyanate solution was added and incubated for 25 min at room temperature. Following incubation, the plate was dried for 60 min under

the nitrogen stream. The extraction solvent (5 mM ammonium acetate in methanol, 300 µL) was added to each well and the plate was subsequently incubated for 30 min with shaking. The plate was centrifugated at 500 × *g* for 2 min to obtain the eluate, and 150 µL of eluate was diluted with 150 µL of HPLC grade water for liquid chromatography-tandem mass spectrometry (LC-MS/MS) run. A total of 50 µL of eluate was diluted with 450 µL mobile phase for the flow injection analysis-tandem mass spectrometry (FIA-MS/MS) run.

The data was acquired on a SCIEX QTRAP 6500plus mass spectrometer coupled to SCIEX ExionLC™ Series UHPLC capability. During LC-MS/MS run, a UHPLC column provided with AbsoluteIDQ® p180 kit was installed for metabolite separation, and water and acetonitrile (both added 0.2% formic acid) were used as mobile phase A and B, respectively. Amino acids (*n*=21) and biogenic amines (*n*=21) were identified and quantified in positive mode. For the FIA-MS/MS analyses, methanol was employed as the running solvent, and 40 acylcarnitines, 14 lysophosphatidylcholines (lysoPC), 38 acyl/acyl phosphatidylcholines (PC aa), 38 acyl/alkyl phosphatidylcholines (PC ae), 15 sphingomyelins (SMs), and the sum of hexoses (H1) were identified and quantified in positive mode. In this assay, all metabolites were quantified by multiple reaction monitoring (MRM) method which was optimized and provided by Biocrates Life Sciences. Data acquisition was conducted by the software of AB Sciex Analyst® version1.7.2.

6.3.9. *Data processing and metabolite quantification*

Amino acids and biogenic amines were quantified based on isotopically labelled internal standards and 7-point calibration curves using AB Sciex Analyst® version1.7.2 software. Other metabolites, such as acylcarnitines, lysoPCs, PCs, SMs and hexose were semi-quantified by using 14 internal standards in the MetIDQ™ software (Biocrates Life Sciences). Data quality was evaluated by checking the accuracy and reproducibility of QC samples included in the p180 kit. Finally, the concentrations of metabolites were reported in µM. For further statistical analyses, metabolites were included only when the concentrations of metabolites were above the limit of detection (LOD) in more than 50% of samples.

6.3.10. *Real-time metabolic profiling of rectal tumour and non-cancer rectal tissue biopsies*

Following informed consent, 2 biopsies per patient (either rectal cancer or non-cancer rectal tissue) were collected at colonoscopy, placed on saline-soaked gauze, and transported to the laboratory. Each biopsy was placed into an individual well of an XF24 Islet Capture Microplate (Agilent Technologies) and secured into place by islet capture screens. A volume of 1 mL

complete M199 (Gibco) supplemented with FBS (10%), penicillin-streptomycin (1%), Fungizone™ (1%), gentamycin (0.1%) and insulin (1 µg/mL) was placed in each well. The plate was placed at 37°C, in 5% CO_2/95% atmospheric air for 30 min to equilibrate.

Three basal measurements of OCR and ECAR were measured over 24 min, of three repeats of mix (3 min)/ wait (2 min) / measurement (3 min) using the Seahorse XFe24 analyser. Biopsies and matching TCM or NCM were collected, snap-frozen in liquid nitrogen, and stored at -80°C until required. Metabolic rates were normalised to protein content using the BCA assay (Pierce) (**Section 5.2.15).**

6.3.11. ***Multiplex enzyme-linked immunosorbent assay (ELISA) profiling of TCM and NCM***

The protein secretome of rectal cancer and non-cancer rectal tissue biopsies was assessed in TCM and NCM using the Meso Scale Diagnostics (MSD) Discovery multiplex ELISA platform. Angiogenic, vascular injury, pro-inflammatory, cytokine and chemokine protein secretions were assessed, as previously described (**Section 5.2.16**). Data was normalised to total protein content of matching biopsies, using the BCA assay (**Section 5.2.14**).

6.3.12. ***Isolation and quantification of RNA***

Tissue biopsies were immediately placed in 600 µL RNAlater™ (Sigma Aldrich) following collection and stored at 4 °C for 24 h. Following 24 h, RNAlater™ liquid was removed to waste and the biopsy stored at -80 °C until required. To isolate RNA, the MiRNeasy Mini Kit (Qiagen) was utilised, as previously described (**Section 5.2.9**). RNA was quantified using a Nanodrop 1000 spectrophotometer, as described previously (**Section. 5.2.10**).

6.3.13. ***Transcriptomic analysis of pre-treatment rectal and non-cancer rectal tissue biopsies***

Transcriptomic profiling by RNA-Seq, was conducted using Lexogen QuantSeq 3'mRNA-Seq, and a NovaSeq 6000 sequencing platform, as previously described (**Section 2.3.16**).

Briefly, RNA libraries were prepared for sequencing using the QuantSeq 3' mRNA-Seq Library prep kit (Lexogen), according to the manufacturers instructions. First strand synthesis of RNA samples was conducted, and RNA samples were denatured. The RNA template was degraded prior to initiation of second strand synthesis of cDNA. The dsDNA library was purified using magnetic beads, to remove contaminants from reaction components. The library was amplified by PCR, using an optimised number of 15 PCR cycles, as described (**Section 2.3.16**). An equal molar amount was pooled for sequencing, with 320 pM loaded onto the NovaSeq flow cell for sequencing using the NovaSeq 6000 and an SP v1.5 sequencing kit, with 1 x 100

bp reads. Raw sequencing files were uploaded to the BlueBee platform for analysis (**Section 5.2.12**).

6.3.14. *IPA analysis*

Significantly differentially expressed genes, and corresponding Log2 Fold Change values were imported to IPA bioinformatics software. Core analysis in IPA was performed, which utilises the Qiagen Knowledge Base, to identify networks and predict specific biological function and pathway involvement in the uploaded experimental transcriptomic dataset. Downstream Effects Analysis in IPA was utilised to predict alterations to downstream biological functions in uploaded experimental datasets. Canonical Pathway Analysis in IPA, utilising the Qiagen Knowledge Base, was used to predict involvement and activation or inhibition of specific biological pathways in the experimental dataset, as previously described (**Section 5.2.13)**.

6.3.15. *Hierarchical clustering analysis*

Normalised, matched metabolomics and transcriptomics data were scaled individually before being integrated to create a single data matrix. Unsupervised hierarchical clustering with supporting heatmap and dendrograms were generated in R Studio (v21.09.0) using packages 'ComplexHeatmap' (v2.6.2), 'RColorBrewer' (v1.1-2), 'gplots' (v3.1.1) and 'pheatmap' (v1.0.12).

6.3.16. *Statistical analysis*

All statistical analysis and graphing were performed using GraphPad Prism v9 software. Data is presented as mean ± SEM throughout. Metabolomic data analysis was performed by un-paired *t*-testing, GLM analysis or as stated in the figure or table legends. For transcriptomic data analysis, BlueBee, DESeq2 R extension and IPA software were utilised for statistical analysis. DESeq2 utilised Wald testing, while IPA utilised Fisher's Exact Test, as stated in figure/table legends. Analysis of MSD or seahorse data using patient samples used Mann-Whitney U or Wilcoxon signed rank test, as appropriate. Spearman correlations were carried out using R software version 3.6.2 (432). Spearman correlations were generated using R package 'Hmisc' version 4.4-0 (433). Graphical representations of correlations were generated with the R package 'corrplot' version 0.84(434). All correlations with an associated p-value < 0.05 following Holm-Bonferroni correction were considered statistically significant. Results were considered significant where probability (p) ≤ 0.05.

Table 6.1: **Overview of patient samples utilised in each analysis in chapter**

Experiment	Cohort	Type of Sample	Cancer (*n*)	Non-Cancer (*n*)
Metabolomics	Norway	Pre-treatment sera	52	
	SJH/Beacon	Pre-treatment tissue	32	20
		Matching conditioned media	24 (of 32)	15 (of 20)
Transcriptomics	SJH/Beacon	Pre-treatment tissue	36	31
Real-time metabolic profiling	SJH/Beacon	Pre-treatment tissue	11	12
Secretome profiling	SJH/Beacon	Conditioned media	12	12

Abbreviations: SJH, St. James's Hospital

6.4. Results

6.4.1. *The metabolome of pre-treatment sera is significantly altered in rectal cancer patients having a poor response to neoCRT*

Having demonstrated in Chapters 1-3 that a radioresistant phenotype is associated with altered metabolism in rectal cancer *in vitro*, the potential role of altered energy metabolism in the response of rectal tumours to neoCRT was investigated. The metabolome of pre-treatment sera samples from rectal adenocarcinoma patients (n = 52) was assessed by LC-MS and correlated with subsequent pathological response to neoCRT and other key clinical parameters to investigate the potential role for circulating metabolites as biomarkers predicting response to neoCRT. Patient characteristics are outlined in **Table 6.2**.

Generalised Linear Model (GLM) analysis was applied to estimate the significantly different features based on four clinicopathological features; tumour regression score (TRS) college of American pathologists/American joint committee of cancer (CAP/AJCC), lymph node involvement, differentiation stage or clinical T stage with BMI and sex used as covariates in the analysis. Adjusted p-values (FDR corrected) were corrected for multiple comparisons using the Benjamini-Hochburg (BH) procedure.

No altered metabolites were demonstrated to be associated with tumour differentiation status or tumour stage. One metabolite, PC ae C38:1 was significantly associated with lymph node involvement in pre-treatment sera from rectal cancer patients (p = 0.047) (**Table 6.3).**

Interestingly, 16 metabolites were demonstrated to be significantly altered depending on TRS (**Table 6.3)**. These 16 metabolites significantly associated with therapy response were all phosphatidylcholines (PCs). Post-hoc multiple comparisons GLM analysis demonstrated the significant differences in metabolite concentrations, when comparing each TRS (**Fig. 6.1**).

Lyso PC a C28:0, was demonstrated to be significantly lower in pre-treatment sera from patients with a subsequent TRS 2 and TRS 3, when compared to those with a complete response TRS 0 (p = 0.02, p = 0.013, respectively) (**Fig. 6.1A**). Six diacyl (aa) PC metabolites were significantly altered depending on TRS. Levels of PC aa C36:2 was significantly lower in the sera of patients with a TRS 1, 2 and 3, when compared to those with a complete response (TRS 0) (p = 0.012, p = 0.045, p = 0.011, respectively) (**Fig. 6.1B**). PC aa C40:2 levels were significantly decreased in sera from patients with TRS 2 and 3, when compared to those with TRS 0 (p = 0.007, p = 0.012, respectively) (**Fig. 6.1C**). Levels of PC aa C40:3 was significantly

lower in patients with no response to treatment (TRS 3), when compared to those with a complete response (TRS 0) (p = 0.024) (**Fig. 6.1D**). PC aa C42:1 levels were significantly lower in the sera from patients with a TRS 1, 2 and 3, when compared to TRS 0 (p = 0.025, p = 0.019, p = 0.04, respectively) (**Fig. 6.1E**). Sera levels of PC aa C42:2 were also significantly reduced in patients with a TRS of 1, 2, and 3, when compared to patients with a complete response to neoCRT (TRS 0) (p = 0.014, p = 0.009, p = 0.013, respectively) (**Fig. 6.1F**).

Nine acyl alkyl (ae) PCs were significantly reduced in the sera of patients with increasing TRS. PC ae 34:2 levels were significantly reduced in the sera of patients with TRS 1, 2 and 3, when compared to those with TRS 0 (p = 0.031, p = 0.012, p = 0.004, respectively) (**Fig. 6.1G**). A significant decrease in the concentration of PC ae C34:3 in the sera of rectal cancer patients with TRS 2 or 3 was demonstrated, when compared to those with TRS 0 (p = 0.039, p = 0.02, respectively) (**Fig. 6.1H**). Levels of PC ae C36:0 were significantly higher in patients with TRS 0, when compared to TRS 1, 2, and 3 (p = 0.003, p = 0.004, p = 0.002, respectively) (**Fig. 6.2A**). Furthermore, PC ae C36:3 concentration was significantly lower in patients with TRS 1, 2 and 3, when compared to those with TRS 0 (p = 0.03, p = 0.034, p = 0.006) (**Fig. 6.2B**). Levels of PC ae C38:1 were demonstrated to be significantly lower in the pre-treatment sera of rectal patients with a TRS of 1, 2 or 3, when compared to those with TRS 0 (p = 0.007, p = 0.047, p = 0.013, respectively) (**Fig. 6.2C**). Sera concentrations of PC ae C38:2 were significantly reduced in patients with TRS 1, 2 or 3, when compared to TRS 0 (p = 0.008, p = 0.019, p = 0.003, respectively) (**Fig. 6.2D**). Levels of PC ae C40:1 were significantly lower in the sera of patients with TRS 1, 2 or 3, when compared to those with TRS 0 (p = 0.004, p = 0.012, p = 0.001, respectively) (**Fig. 6.2E**). The concentration of PC ae C40:3 were significantly higher in patients with TRS 0, when compared to those with TRS 1, 2 and 3 (p = 0.048, p = 0.049, p = 0.02, respectively) (**Fig. 6.2F**). Sera levels of PC ae C42:2 were demonstrated to be significantly lower in the pre-treatment sera of patients with TRS 1, 2, and 3, when compared to TRS 0 (p = 0.003, p = 0.001, p = 0.0002, respectively) (**Fig. 6.2G**). The concentration of PC ae C42:3 in the pre-treatment sera of rectal cancer patients with a TRS 0 was significantly higher than those with TRS 1, 2 or 3 (p= 0.005, p = 0.007, p = 0.001, respectively) (**Fig. 6.2H**).

Together, these data demonstrate that significant alterations in the levels of 16 metabolites in the pre-treatment sera of rectal cancer patients is associated with subsequent

pathological response to neoCRT, supporting a potential role for these 16 metabolites as novel circulating predictive markers of treatment response in rectal cancer.

Table 6.2: **Patient characteristics of rectal cancer patients used in metabolomic analysis of pre-treatment sera samples**

		Cancer (*n*=52)
Gender	**Male (*n*)**	35
	Female (*n*)	17
Age	**Mean (y)**	62
	Range (y)	41-79
Histology	**Adenocarcinoma *(n)***	52
Differentiation	**Low (*n*)**	3
	Mean/Moderate (*n*)	30
	High (*n*)	9
	N/A (*n*)	10
BMI	**Underweight <18.5 (*n*)**	2
	Normal 18.5-24.9 (*n*)	21
	Overweight 25-29.9 (*n*)	19
	Obese >30	10
Clinical T stage	**2 (*n*)**	3
	3 (*n*)	25
	4 (*n*)	24
Pathological Nodal involvement	**Yes (*n*)**	25
	No (*n*)	27
Treatment	**NeoCRT (*n*)**	52
TRS (CAP/AJCC Scale)	**0 (*n*)**	4
	1 (*n*)	14
	2 (*n*)	22
	3 (*n*)	12

Abbreviations; y, years; N/A, not available; BMI, body mass index; T stage, tumour stage neoCRT, neoadjuvant chemoradiation therapy; TRS, tumour regression score

Table 6.3: **GLM analysis of metabolite alterations in pre-treatment sera from rectal cancer patients significantly associated with clinical parameters** (OxyTarget cohort)

Metabolites	**TRS (CAP/AJCC Scale)** ***p*-value (FDR Corrected)**	**Lymph node positivity** ***p*-value (FDR corrected)**
LysoPC a C28:0	0.0143	
PC aa C36:2	0.0322	
PC aa C40:2	0.0143	
PC aa C40:3	0.025	
PC aa C42:1	0.0322	
PC aa C42:2	0.0243	
PC ae C34:2	0.0184	
PC ae C34:3	0.0250	
PC ae C36:0	0.0072	
PC ae C36:3	0.0322	
PC ae C38:1	0.0207	0.0473
PC ae C38:2	0.0207	
PC ae C40:1	0.0033	
PC ae C40:3	0.0322	
PC ae C42:2	0.0010	
PC ae C42:3	0.0021	

GLM analysis was used to estimate the significantly different features based on TRS (CAP/AJCC) or lymph node positivity, with sex and BMI used as covariates. Based on metabolite levels from pre-treatment sera of *n*=52 rectal adenocarcinoma patients. TRS 0 *n*=4, TRS 1 *n*=14, TRS 2 *n*=22, TRS 3 *n*=12. Positive lymph nodes; Yes *n*=25, No *n*=27. *p*-value (FDR corrected) are corrected for multiple comparisons using the Benjamini-Hochburg (BH) procedure.

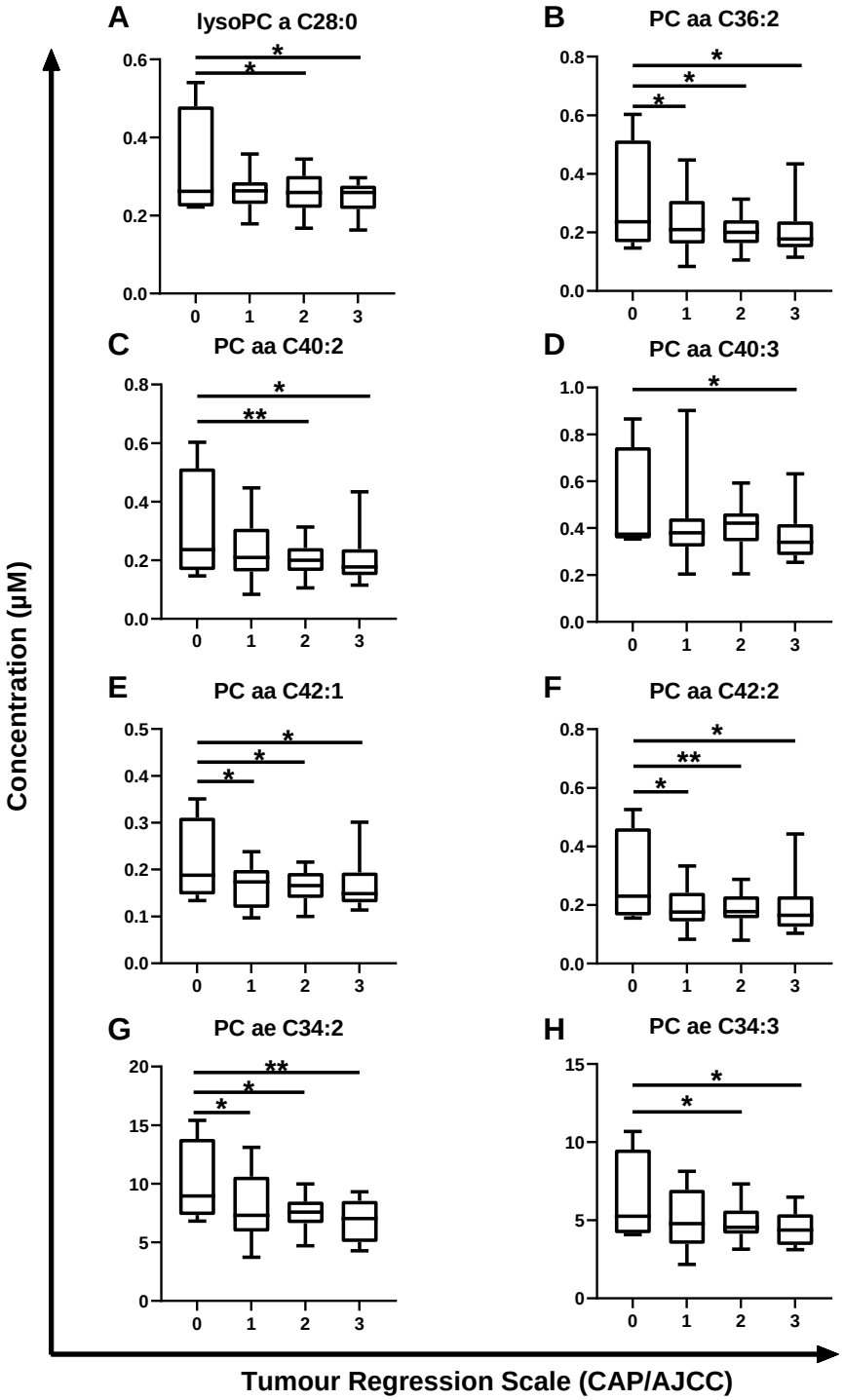

***Fig. 6.1*: Pre-treatment sera metabolite levels are significantly altered across tumour regression score in rectal cancer patients.** Metabolite levels in pre-treatment sera from rectal adenocarcinoma patients (*n* =52) were assessed by liquid chromatography mass spectrometry (LC-MS) and correlated with subsequent pathological response to neoCRT. **A)** lysoPC a C28:0, **B)** PC aa C36:2, **C)** PC aa C40:2, **D)** PC aa C40:3, **E)** PC aa C42:1, **F)** PC aa C42:2, **G)** PC ae C34:2 and **H)** PC ae C34:3 levels are significantly decreased with increasing TRS and worse therapeutic response. TRS 0 *n*=4, TRS 1 *n*=14, TRS 2 *n*=22, TRS 3 *n*=12. Data is presented as median ± minimum/maximum. Statistical analysis was performed by post-hoc unpaired GLM analysis. **p*<0.05, ***p* < 0.01**.**

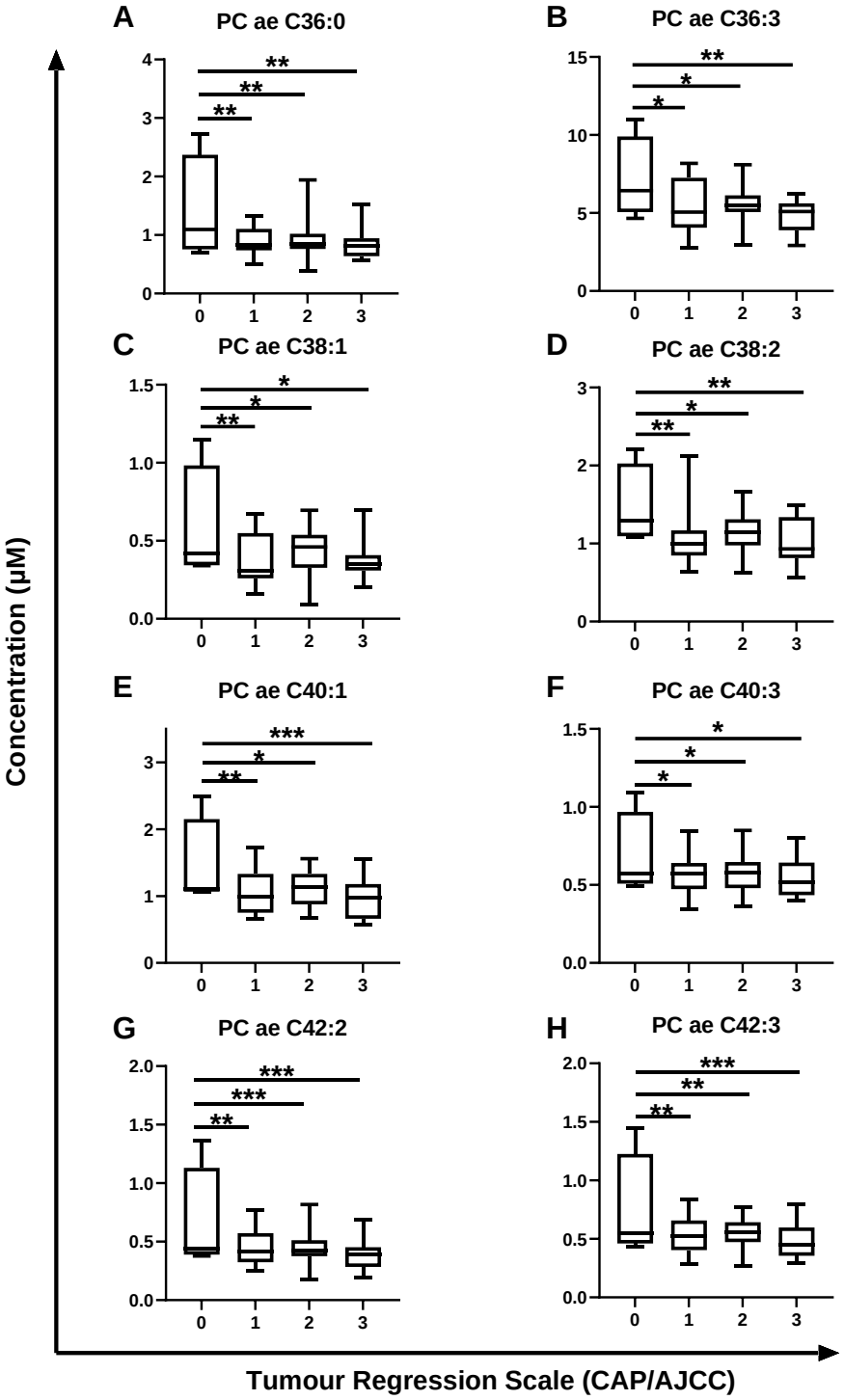

Fig. 6.2: **Pre-treatment sera metabolite levels are significantly altered across tumour regression score in rectal cancer patients.** Metabolite levels in pre-treatment sera from rectal adenocarcinoma patients (*n* =52) were assessed by liquid chromatography mass spectrometry (LC-MS) and correlated with subsequent pathological response to neoCRT. **A)** PC ae C36:0, **B)** PC ae C36:3, **C)** PC ae C38:1, **D)** PC ae C38:2, **E)** PC ae C40:1, **F)** PC ae C40:3, **G)** PC ae C42:2 and **H)** PC ae C42:2 levels are significantly decreased with increasing TRS and worse therapeutic response. TRS 0 *n*=4, TRS 1 *n*=14, TRS 2 *n*=22, TRS 3 *n*=12. Data is presented as median ± minimum/maximum. Statistical analysis was performed by post-hoc unpaired GLM analysis. **p*<0.05, ***p* < 0.01, ****p* < 0.001.

6.4.2. *The intracellular and secreted metabolome of pre-treatment rectal tumour biopsies is significantly correlated with response to neoadjuvant treatment*

Having demonstrated that the circulating metabolome of pre-treatment sera is significantly altered in rectal cancer patients having a poor response to treatment, the intracellular metabolome of rectal tumour tissue (*n*=32) was profiled by LC-MS, and metabolite levels correlated with subsequent pathological response and other clinicopathological parameters.

The patient characteristics of the cohort used in the intracellular metabolome profiling of pre-treatment rectal cancer biopsies are demonstrated in **Table 6.4.** The levels of two metabolites in rectal tumour tissue were demonstrated to be significantly associated with subsequent TRS. Decreased levels of serotonin were demonstrated to be significantly associated with worsening TRS in rectal tumour tissue (p = 0.034, R value = -0.53). In addition, increasing lyso PC a C16:1 levels were significantly associated with worsening response to treatment (TRS) (p = 0.02, R-value = 0.57) (**Fig. 6.3**). The levels of three metabolites, C16, C18 and putrescine were demonstrated to display significant positive correlation with advancing clinical T stage (**Fig. 6.3**). Seven metabolite levels were significantly negatively correlated with advancing N stage (C0, C2, C3, C3-DC(C4-OH), C4, alanine (ala) and symmetric dimethylarginine (SDMA)) (**Fig. 6.3**). Furthermore, while four intracellular metabolites were demonstrated to be positively correlated with pathological T stage (C4:1, lysoPC a 16:1, lysoPC a C20:4 and PC aa C28:1), one metabolite, lysoPC a C20:3 was significantly negatively correlated with pathological T stage (**Fig. 6.3**). In addition, levels of spermine, lysoPC a C16:1 and lysoPC a C18:2 were associated with a significant positive correlation with pathological T stage (**Fig. 6.3**). Five metabolites were significantly negatively correlated with pathological N stage in rectal tumour tissue (PC ae C40:6, PC ae C42:3, PC ae C44:3, PC ae C44:4 and SM C26:0) (**Fig. 6.3**). Fifteen metabolites were demonstrated to be significantly correlated with BMI in rectal tumour tissue, including 11 amino acids (**Fig. 6.3**).

To investigate whether the secreted metabolome of rectal tumour tissue was associated with response to treatment and key clinical characteristics, the levels of metabolites secreted from rectal tumour was assessed in TCM (*n*=24) by LC-MS. The patient characteristics of this cohort are demonstrated in **Table 6.5**. The levels of one metabolite, PC aa C32:3 displayed significant positive correlation with worsening response to treatment (TRS) (p = 0.031, R-value = 0.65). Two metabolites, asparagine (Asn) and PC aa C30:2 were demonstrated not only to have a significant negative correlation with clinical N stage, but also

pathological N stage (**Fig. 6.4**). Eleven secreted metabolites were demonstrated to display a significant positive correlation with clinical T stage (C0, Ala, Clt, Glu, Gly, sarcosine, SDMA, PC aa C28:1, SM C16:0, SM C16:1 and SM C18:0) (**Fig. 6.4**). Secreted levels of two metabolites, threonine (Thr) and creatinine were demonstrated to have a positive correlation with pathological T stage (**Fig. 6.4**).

Together these data demonstrate that the intracellular and secreted metabolome of rectal cancer is significantly associated with subsequent pathological response to treatment and other key clinical and pathological parameters, further supporting a role for altered metabolism in the pathogenesis and therapeutic response of rectal cancer and highlighting the potential for metabolomic biomarkers predicting response to neoadjuvant treatment.

Table 6.4: **Patient characteristics of rectal cancer patients used in intracellular metabolomic profiling of pre-treatment rectal tumour biopsies**

		Cancer (*n*=32)
Gender	**Male (*n*)**	20
	Female (*n*)	12
Age	**Mean ± SEM (y)**	63.8 ± 1.7
	Range (y)	48-89
Histology	**Adenocarcinoma (*n*)**	32
Differentiation	**Poor-Moderate (*n*)**	2
	Moderate (*n*)	28
	Well (*n*)	1
	Unknown (*n*)	1
Clinical T stage	**1 (*n*)**	1
	1/2 (*n*)	1
	2 (*n*)	8
	3 (*n*)	18
	3/4 (*n*)	1
	4 (*n*)	3
Clinical N stage	**0 (*n*)**	17
	1 (*n*)	9
	1/2 (*n*)	1
	2 (*n*)	5
Pathological T stage*	**0 (*n*)**	3
	1 (*n*)	4
	2 (*n*)	7
	3 (*n*)	10
	4 (*n*)	1
Pathological N stage**	**0 (*n*)**	20
	1 (*n*)	4
Treatment received	**NeoCRT (*n*)**	16
	NeoRT (*n*)	2

	NeoCT (*n)*	1
	Surgery only (*n)*	7
	CT + RT only (*n)*	4
	CT only (*n)*	1
	Awaited (*n)*	1
TRS (Modified Ryan Scale) (neoCRT or neoRT)* **	**0 (*n)***	3
	1 (*n)*	7
	2 (*n)*	5
	3 (*n)*	1

*Pathological T stage available for *n*=25 patients only. **Pathological N stage available for *n*=24 patients only. ***TRS available for *n*=16 patients only, receiving either neoCRT or neoRT. Abbreviations; SEM, standard error of the mean; y, years; T stage, tumour stage; N stage, nodal stage; TRS, tumour regression score; neo, neoadjuvant; CRT, chemoradiation therapy; RT, radiation therapy; CT, chemotherapy.

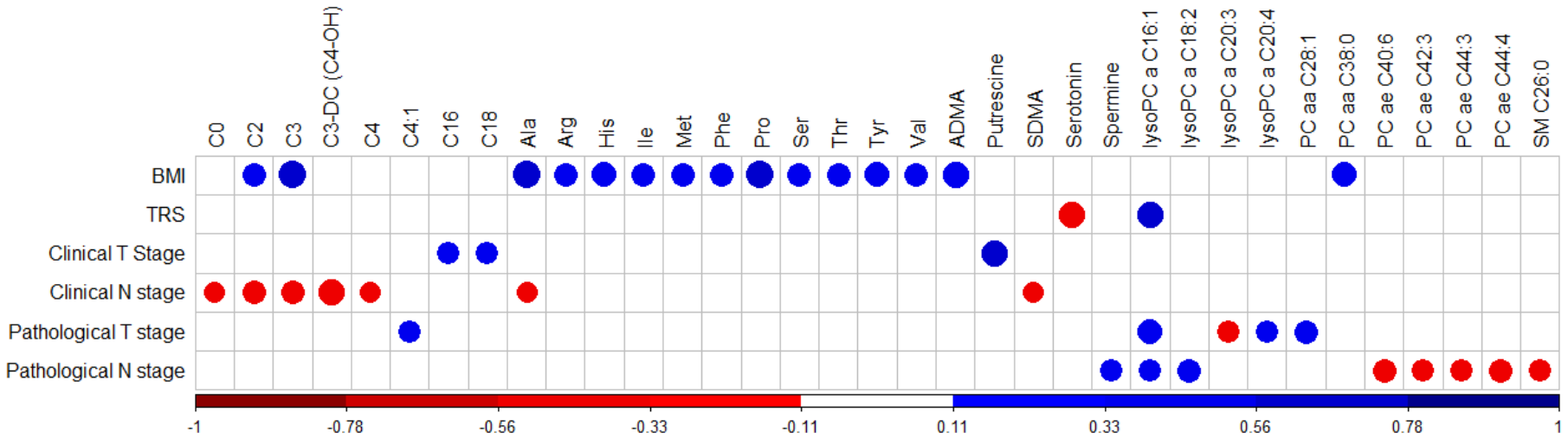

Fig. 6.3: **Intracellular metabolite levels of rectal tumour biopsies significantly correlate with clinical and pathological characteristics.** Intracellular metabolite levels of pre-treatment rectal tumour biopsies (*n* = 32) were assessed by LC-MS, and correlated with clinical and pathological characteristics, using R software. Blue dots represent significant positive correlations, while red dots represent significant negative correlations. The x-axis demonstrates the R value denoting strength of correlations with increasing colour.

Table 6.5: **Patient characteristics of rectal cancer patients used in secreted metabolomic profiling of pre-treatment rectal tumour biopsies (TCM)**

		Cancer (*n*=24)
Gender	**Male (*n*)**	14
	Female (*n*)	10
Age	**Mean (y)**	63
	Range (y)	48-78
Histology	**Adenocarcinoma (*n*)**	24
Differentiation	**Poor-Moderate (*n*)**	2
	Moderate (*n*)	14
	Well (*n*)	1
	Unknown (*n*)	1
Clinical T stage	**1 (*n*)**	0
	1/2 (*n*)	1
	2 (*n*)	8
	3 (*n*)	11
	3/4 (*n*)	1
	4 (*n*)	3
Clinical N stage	**0 (*n*)**	14
	1 (*n*)	6
	1/2 (*n*)	1
	2 (*n*)	3
Pathological T stage*	**0 (*n*)**	2
	1 (*n*)	2
	2 (*n*)	6
	3 (*n*)	8
	4 (*n*)	1
Pathological N stage**	**0 (*n*)**	15
	1 (*n*)	4
TRS (Modified Ryan Scale) (neoCRT or neoRT)***	**0 (*n*)**	2
	1 (*n*)	4

	2 (*n)*	5
	3 (*n)*	0

*Pathological T stage available for *n*=19 patients only. **Pathological N stage available for *n*=19 patients only. ***TRS available for *n*=11 patients only, receiving either neoCRT or neoRT. Abbreviations; SEM, standard error of the mean; y, years; T stage, tumour stage; N stage, nodal stage; TRS, tumour regression score; neo, neoadjuvant; CRT, chemoradiation therapy; RT, radiation therapy; CT, chemotherapy.

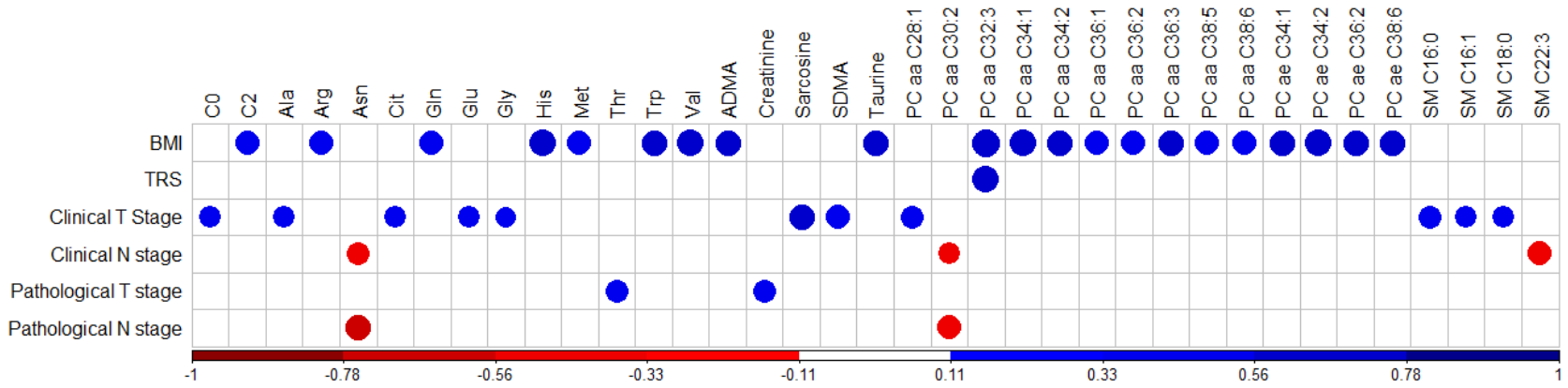

Fig. 6.4: **Secreted metabolite levels in rectal TCM significantly correlate with clinical characteristics.** Secreted metabolite levels of pre-treatment rectal tumour biopsies were assessed in TCM (*n*=24) by LC-MS, and correlated with clinical characteristics (BMI, TRS, Clinical T/N stage, pathological T/N stage), using R software. Blue dots represent significant positive correlations, while red dots represent significant negative correlations. The x-axis demonstrates the R value denoting strength of correlations with increasing colour

6.4.3. *The transcriptome of pre-treatment rectal tumour biopsies is significantly altered in patients with a poor response to neoadjuvant treatment*

Having demonstrated significant alterations to the circulating and tumour metabolome of rectal cancer patients with a poor response to treatment, the transcriptome of pre-treatment rectal tumour tissue (*n* = 36) was assessed using a Lexogen QuantSeq 3' mRNA FWD sequencing kit to assess upstream alterations. Differential expression analysis was performed using BlueBee™ software and the DESeq2 R script extension.

The patient characteristics of the patient cohort utilised in this study are demonstrated in **Table 6.6**. When comparing patients with a good response to neoadjuvant treatment [TRS 0 (*n*=2) or TRS 1 (*n*=4)] to those with a poor response to treatment [TRS 2 (*n*=5)], two genes were demonstrated to be significantly differentially expressed between good and poor responders. H1-3, a histone coding gene, was demonstrated to be significantly downregulated in patients with a poor therapeutic response (TRS 2), when compared to those with a good response (TRS 0 and 1) (*p*-adj = 0.0002, Log_2 fold change = -1.76) (**Table 6.7**). In addition, RNA-Y, an RNA gene was demonstrated to be significantly downregulated in patients with a poor response to treatment (TRS 2), when compared to good responders (TRS 0 and 1) (*p*-adj = 0.03, Log_2 fold change = -1.68) (**Table 6.7**).

In addition, these two genes were also the only genes significantly differentially expressed between patients with TRS 1 and those with TRS 2 (**Table 6.7**). H1-3 was demonstrated to be significantly downregulated in patients with TRS 2, when compared to those with TRS 1 (*p*-adj = 0.027, Log_2 Fold Change = -1.65) (**Table 6.7**). In addition, RNA-Y expression was also demonstrated to be significantly downregulated in patients with TRS 2, when compared to those with TRS 1 (*p*-adj = 0.027, log2 fold change = -1.72) (**Table 6.7**).

Five genes were demonstrated to be significantly altered in patients with a poor response to treatment (TRS 2), when compared to those with a complete response to treatment (TRS 0). Two genes were significantly downregulated in patients with poor response (TRS 2). Dual oxidase 2 (DUOX2), which is a member of the NADPH oxidase (NOX) family of proteins, was demonstrated to be significantly downregulated in patients with TRS 2, when compared to those with a TRS 0 (*p*-adj = 0.003, log_2 Fold change = -2.58) (**Table 6.7**). Expression of apolipoprotein E (APOE), involved in regulation of lipid metabolism, was also significantly downregulated in patients with a poor response to treatment (TRS 2), when compared to

those with a complete response to treatment (TRS 0) (*p*-adj = 0.026, $\log_2$ Fold Change = -2.18) (**Table 6.7**).

The expression of three ribosomal protein genes was demonstrated to be significantly upregulated in rectal tumour tissue of patients with a poor response to treatment (TRS 2), when compared to those with a complete response to treatment (TRS 0). Ribosomal protein L30 (RPL30) and RPL7A gene expression were demonstrated to be significantly upregulated in patients with a poor response to treatment (TRS 2), when compared to those with TRS 0 (*p*-adj = 0.017, *p* = 0.023, respectively) ($\log_2$ fold change = 1.68, $\log_2$ fold change = 1.78, respectively) (**Table 6.7**). Ribosomal protein S21 (RPS21) was also demonstrated to be significantly upregulated in tumour tissue of patients with a poor response to treatment (TRS 2), when compared to those with a complete response (TRS 0) (**Table 6.7**).

Interestingly, the transcriptome was also demonstrated to be significantly altered based on pathological T stage. Differential expression analysis demonstrated a total of 78 genes significantly differentially expressed in tumour tissue from rectal cancer patients with a pathological T stage of T3/T4, when compared to those with a pathological T stage of T0. In total, 55 genes were significantly upregulated in patients with a pathological T stage of T3/4, when compared to those with a pathological T stage of T0. Twenty-three genes were demonstrated to be significantly downregulated in patients with a pathological T stage of T3 or 4, when compared to those with a pathological T stage of T0. Of the significantly altered genes, the top 20 upregulated and downregulated genes in patients with an advanced pathological T stage (T3/4), when compared to those with a pathological T stage of T0 are demonstrated (**Fig. 6.5A-B**). DEFA5 (Defensin Alpha 5), which is involved in host defence, was the most downregulated gene (as determined by fold change, Log2 Fold Change = -2.14) in patients with a pathological T stage of T3/4, when compared to those with a pathological T stage of T0 (**Fig. 6.5A**). RPL22L1 (Ribosomal protein L22 Like 1) was demonstrated to be the most upregulated gene (as determined by fold change, Log2 fold change = 2.24) in tumour tissue from patients with a higher pathological T stage (T3/4), when compared to those with a pathological T stage of T0. (**Fig. 6.5B**).

The top 30 most significantly altered genes in patients with a pathological T stage of T3/T4, when compared to those with a pathological T stage of T0 (**Table 6.8**). FAU gene, which encodes the 40S ribosomal protein S30, was the most significantly upregulated gene in patients with high pathological T stage (T3/4), when compared to those with a pathological T

stage of T0 (as determined by *p*-adj, *p*-adj = 0.0002). LCN2 (Lipcalin 2) was demonstrated to be the most significantly downregulated gene in patients with a pathological T stage of T3/4, when compared to those with a pathological T stage of T0 (as determined by *p*-adj, *p*-adj = 0.006) (**Table 6.8**).

These data demonstrate that the transcriptome of rectal cancer patients with a poor response to neoadjuvant treatment is significantly altered, when compared to good responders. These data also demonstrate significant alterations in the transcriptome of patients with an advanced pathological T stage of 3/4, when compared to those with no residual tumour.

***Table 6.6*: Patient characteristics of patient cohort used in transcriptomic analysis of pre-treatment rectal tumour tissue biopsies**

		Cancer (*n*=36)
Gender	**Male (*n*)**	23
	Female (*n*)	13
Age at diagnosis	**Median (y)**	63
	Range (y)	48-89
Histology	**Adenocarcinoma (*n*)**	36
Differentiation	**Poor-Moderate (*n*)**	3
	Moderate (*n*)	31
	Well (*n*)	1
	Unknown (*n*)	1
Body Mass Index (BMI) at diagnosis	**Normal (*n*)**	3
	Overweight (*n*)	12
	Obese (*n*)	10
	N/A (*n*)	11
Pathological T stage	**0 (*n*)**	4
	1 (*n*)	6
	2 (*n*)	6
	3 (*n*)	7
	4 (*n*)	1
Treatment received	**NeoCRT (*n*)**	18
	NeoRT (*n*)	2
	NeoCT (*n*)	1
	Surgery only (*n*)	8
	CT + RT (no surgery) (*n*)	4
	CT only (*n*)	1
	Awaited (*n*)	2

TRS (Modified Ryan Scale) (neoCRT or neoRT)*	**0**	5
	1	7
	2	5
	3	1

Abbreviations; N/A, not available; BMI, body mass index; clinical T stage, clinical tumour stage; clinical N stage, clinical nodal stage; clinical M stage, clinical metastasis stage; MX, metastasis cannot be measured; neoCRT, neoadjuvant chemoradiation therapy; neoRT, neoadjuvant radiation therapy; neoCT, neoadjuvant chemotherapy; TRS, tumour regression score. *****TRS only available for *n*=18 patients, (*n*=16 received neoCRT, *n*=2 received neoRT).

Table 6.7: **The transcriptome of pre-treatment rectal tumour tissue is significantly altered in patients with a poor response to treatment**

Good response (TRS 0 +1) vs Poor response (TRS 2)		
Gene	**Log2FoldChange**	***p*-adj**
RNA-Y	-1.76	0.000242
H1-3	-1.67	0.0335
TRS 1 vs TRS 2		
Gene	**Log2FoldChange**	***p*-adj**
RNA-Y	-1.73	0.0267
H1-3	-1.65	0.0267
TRS 0 vs TRS 2		
Gene	**Log2FoldChange**	***p*-adj**
DUOX2	-2.58	0.0025
RPL30	1.68	0.0165
RPL7A	1.78	0.023
APOE	-2.18	0.026
RPS21	1.89	0.026

Log_2 Fold Change indicated the differential expression of each gene in patients with a good response, when compared to those with a poor response, with negative values indicating genes downregulated in poor responders, and positive values indicating genes upregulated in poor responders, when compared to good responders. The *p*-adj values indicate the statistical significance of the differential expression of each gene between good and poor responders. Statistical analysis performed using the Wald test, with corrections for multiple comparisons performed by the Benjamini-Hochberg correction (FDR).

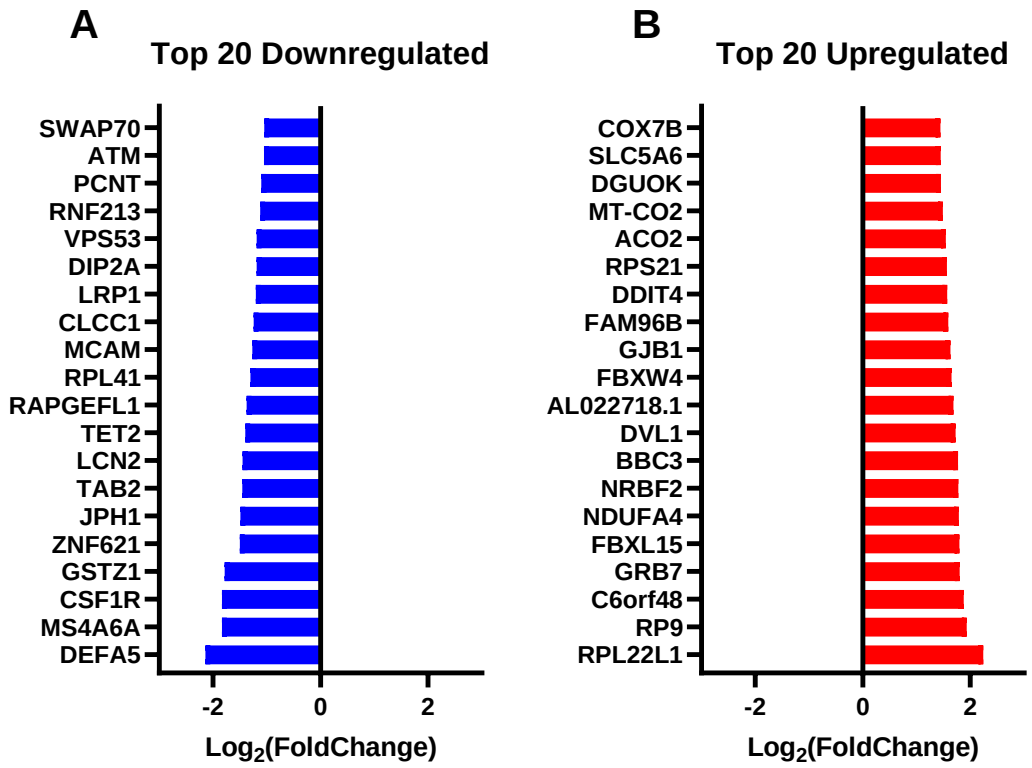

Fig. 6.5: **The basal transcriptome is significantly altered in pre-treatment rectal tumour biopsies from patients with pathological T stage of T3/4, when compared to those with pathological T stage T0.** Transcriptomic profiling was performed on RNA isolated from pre-treatment rectal cancer biopsies. Differential expression analysis was performed using BlueBee™ Software, using the DESeq2 R extension script. **A)** The top 20 downregulated genes (by fold change) in patients with pathological T stage T3/4, when compared to those with pathological T stage T0. **B)** The top 20 upregulated genes (by fold change) in in patients with pathological T stage T3/4, when compared to those with pathological T stage T0. Data is presented from patients with a pathological T stage of T0 (*n*=4) or T3/4 (*n*=8) patients. Statistical analysis was performed using the Wald test, with corrections for multiple comparisons performed by the Benjamini-Hochberg correction (FDR).

Table 6.8: **Top 30 most significantly altered genes in rectal cancer patients with a pathological T stage of T3/4, when compared to those with a pathological T stage of T0**

Gene	Up/Downregulated in pathological T stage T3/4	Log_2 Fold Change	*p*-adj
FAU	Up	1.077705	0.000181
RPL30	Up	1.412689	0.001647
RPL22L1	Up	2.240567	0.002839
ACO_2	Up	1.547734	0.00528
MT-CO_2	Up	1.488552	0.006113
ATP5F1B	Up	1.255563	0.006113
TUBA1C	Up	1.199871	0.006113
LCN2	Down	-1.45057	0.006113
TAB2	Down	-1.45282	0.006113
DVL1	Up	1.727825	0.007844
RPS2	Up	1.301386	0.008871
ATM	Down	-1.05221	0.010529
ZNF621	Down	-1.49793	0.010529
RPL41	Down	-1.30196	0.011402
BBC3	Up	1.774344	0.012276
COX7B	Up	1.44649	0.012276
RPL7A	Up	1.396214	0.012276
RP9	Up	1.934482	0.012635
DDIT4	Up	1.572787	0.012635
RPS21	Up	1.564903	0.012635
CLDN4	Up	1.360476	0.012635
RAC1	Up	1.163133	0.012635
FBXL15	Up	1.795973	0.013586
CALM3	Up	1.118701	0.015639
HNRNPL	Up	1.165144	0.017714
VPS53	Down	-1.18669	0.017714
FBXW4	Up	1.652337	0.018784
C6orf48	Up	1.87756	0.019038
NDUFA4	Up	1.788272	0.021041
SLC5A6	Up	1.450858	0.022409

Log_2 Fold Change indicated the differential expression of each gene in patients with a pathological T stage T0, when compared to those with a pathological T stage T3/4, with negative values indicating genes downregulated in those with pathological T3/4, and positive values indicating genes upregulated in those with pathological T3/4, when compared to good responders. The *p*-adj values indicate the statistical significance of the differential expression of each gene between patients with pathological T0 and pathological T3/4. Statistical analysis performed using the Wald test, with corrections for multiple comparisons performed by the Benjamini-Hochberg correction (FDR).

6.4.4. *Pre-treatment rectal tumour biopsies from patients having a poor response to neoadjuvant treatment demonstrate significant alterations in biological function and canonical pathways*

To further interrogate the transcriptomic alterations demonstrated in pre-treatment rectal tumour biopsies from patients with a poor response to treatment, genes with a log2 fold change > 1.5 were assessed by IPA analysis, to predict and identify pathways altered in patients with a TRS 2 (n = 5), when compared to those with a complete response (TRS 0 (n = 5). The p-values represent the statistical probability that selecting genes associated with each function is due to chance alone. As each biological function is comprised of multiple functional pathways, significance is represented as p-value range.

In total, 29 genes were altered by ≥1.5 $\log_2$ fold change in rectal tumour tissue from patients with a poor response to treatment (TRS 2), when compared to those with a complete response (TRS 0), including 5 genes, which were significantly altered (**Section 2.4.3**).

Molecular and cellular function analysis by IPA predicted significant alterations to numerous functional pathways (**Fig. 6.6**). The pathway most significantly altered in patients with a poor response to treatment (TRS 2) was 'RNA damage and repair' (p = 3.8 x 10^{-9}- 2.14 x10^{-2}). In addition, multiple pathways associated with cellular growth and survival were predicted to be significantly altered in patients with a poor response to treatment (TRS 2), when compared to complete responders (TRS 0), including 'cell cycle' (p = 1.2 x10^{-4} – 4.25 x 10^{-2}), 'cell death and survival' (p = 4.2 x10^{-4}–3.86 x 10^{-2}) and 'cellular growth and proliferation' (p = 2.54x10^{-3}- 4.88x10^{-2}). Interestingly, a number of metabolic pathways were also predicted to be significantly altered in patients with a poor response to treatment, when compared to good responders, including 'carbohydrate metabolism', 'lipid metabolism', 'energy production', and 'nucleic acid metabolism' (**Fig. 6.6**).

Canonical pathway analysis by IPA also demonstrated canonical pathways predicted to be altered in patients with a poor response to treatment (TRS 2) (**Table 6.9).** The canonical pathway, eukaryotic initiation factor-2 (EIF2) signalling, involved in pro-inflammatory and stress response signalling was predicted to be significantly activated in patients with a poor response (TRS 2), when compared to those with a complete response (TRS 0) (Z-score = 2, -log(p-value) = 6.65) (**Table 6.9**). Interestingly, oxidative phosphorylation and mitochondrial dysfunction were predicted to be significantly altered in patients with a poor response to treatment (TRS 2), when compared to those with a complete response (TRS 0) (**Table 6.9**).

IPA analysis was also performed on the 78 significantly altered genes in patients with pathological T stage T3/4, when compared to those with a pathological T stage T0. Similarly, molecular functions related to cellular growth and survival were demonstrated to be significantly altered in patient tissue who went on to have a high pathological T stage following treatment (T3/4), when compared to those with a pathological T stage of T0, including 'cell death and survival', 'cellular growth and proliferation' and 'cell cycle' (**Fig. 6.7)**. In addition, numerous metabolic functions were also demonstrated to be significantly altered in patients with a pathological T stage of T3/4, when compared to those with pathological T stage T0, including 'lipid metabolism', 'carbohydrate metabolism', 'amino acid metabolism' and 'nucleic acid metabolism'. Interestingly, 'cellular response to therapeutics' was also highlighted as a significantly altered biological process in samples from patients with a high pathological T stage (T3/4), when compared to those with a pathological T stage of T0. (**Fig. 6.7**).

To further investigate specific pathways predicted to be altered in the transcriptome of tumour tissue from patients who went on have a poor pathological T stage, canonical pathway analysis was performed in IPA. Interestingly, 'oxidative phosphorylation' was predicted to be significantly activated in tissue from patients who went on to have a poor pathological T stage (T3/4), when compared to those with a good pathological T stage (T0)(-log10(*p*-value) = 5.63, Z-score = 2.44), with 6 oxidative phosphorylation related genes being significantly altered (**Table 6.10**). In addition, mitochondrial dysfunction, and the TCA cycle II pathways were also demonstrated to be significantly altered in these poor responders.

These data demonstrate significant alterations in the molecular and biological functions of pre-treatment rectal cancer tissue, from patients who have a poor response to treatment, when compared to good responders and in patients with a pathological T stage of T3/4. Furthermore, many of these pathways and processes are related to energy metabolism, supporting altered metabolism in the therapeutic response and pathogenesis of rectal cancer and highlighting the potential role for metabolic markers as novel biomarkers predicting the response to treatment.

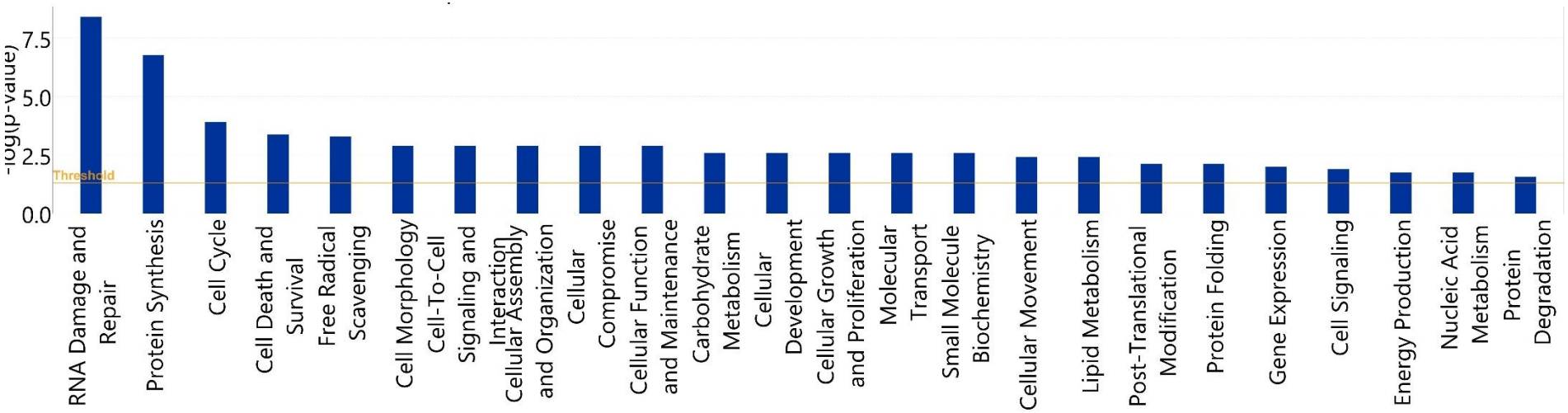

Fig. 6.6: **Biological functions are significantly altered in pre-treatment rectal tumour biopsies from patients having a subsequent poor response to neoadjuvant treatment (TRS 2), when compared to good responders (TRS 0).** Transcriptomic profiling was performed on pre-treatment rectal tumour biopsies. Biostatistical analysis was performed on genes with ≥1.5 $\log_2$ fold change difference between good responders [TRS 0 (*n*=5)] and poor responders [TRS 2 (*n*=5)], by IPA analysis to identify predicted altered biological functions. Statistical analysis was performed by right-tailed Fisher's exact test using IPA analysis.

Table 6.9: **Canonical pathways significantly altered in rectal cancer patients with a poor response to treatment (TRS 2), when compared to those with TRS 0.**

Ingenuity Canonical Pathways	-log(*p*-value)	Genes
EIF2 Signalling	6.65	RPL30,RPL37,RPL7A,RPL9,RPS2,RPS21
mTOR Signalling	2.67	DDIT4,RPS2,RPS21
SPINK1 General Cancer Pathway	2.57	MT1E,MT1G
Oxidative Phosphorylation	2.1	MT-CO_2,NDUFA4
Aldosterone Signalling in Epithelial Cells	1.76	HSPA1A/HSPA1B,HSPE1
Mitochondrial Dysfunction	1.73	MT-CO_2,NDUFA4
Regulation of eIF4 and p70S6K Signalling	1.69	RPS2,RPS21
Coronavirus Pathogenesis Pathway	1.6	RPS2,RPS21
Glucocorticoid Receptor Signalling	1.52	CD163,HSPA1A/HSPA1B,NDUFA4
Protein Ubiquitination Pathway	1.34	HSPA1A/HSPA1B,HSPE1

Biostatistical analysis was performed on genes with ≥1.5 $\log_2$ fold change difference between good responders [TRS 0 (*n*=5)] and poor responders [TRS 2 (*n*=5)] by IPA analysis to identify projected altered biological functions between the two groups. Statistical analysis performed by right-tailed Fisher's exact test using IPA analysis.

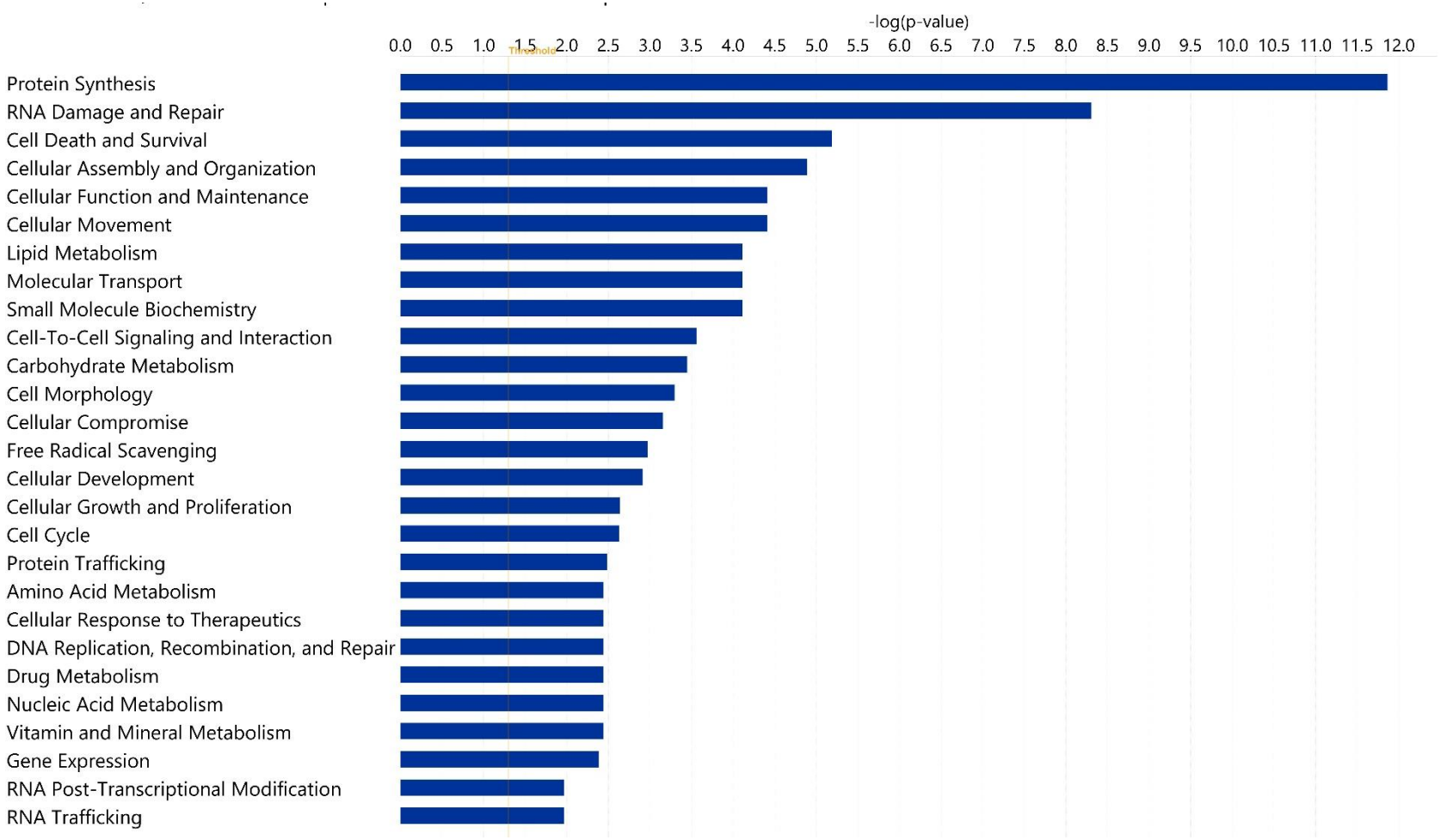

Fig. 6.7: **Biological functions are significantly altered in rectal cancer patients with a pathological T stage of T3/4, when compared to those with a pathological T stage of T0.** Biostatistical analysis was performed on significantly altered genes between patients with a pathological T stage of T0 (*n*=4) and those with a pathological T stage of T3/4 (*n*=8), by IPA analysis to identify predicted altered biological functions. Statistical analysis was performed by right-tailed Fisher's exact test using IPA analysis

Table 6.10: **Top 15 canonical pathways significantly altered in rectal cancer patients with a pathological T stage T3/4, when compared to those with a pathological T stage of 0.**

Ingenuity Canonical Pathways	-log(*p*-value)	Genes
EIF2 Signaling	13.5	EIF1,EIF1AX,EIF4G3,FAU,RPL22L1,RPL30,RPL36AL,RPL41,RPL7A,RPL9,RPS13,RPS16,RPS2,RPS21
mTOR Signaling	7.28	DDIT4,EIF4G3,FAU,RAC1,RHOA,RPS13,RPS16,RPS2,RPS21
Regulation of eIF4 and p70S6K Signaling	6.64	EIF1,EIF1AX,EIF4G3,FAU,RPS13,RPS16,RPS2,RPS21
Mitochondrial Dysfunction	5.65	ACO2,ATP5F1B,COX7A2L,COX7B,MT-CO2,NDUFA4,UQCRC2
Oxidative Phosphorylation	5.63	ATP5F1B,COX7A2L,COX7B,MT-CO2,NDUFA4,UQCRC2
Sumoylation Pathway	3.31	PCNA,RAC1,RAN,RHOA
Coronavirus Pathogenesis Pathway	3.16	FAU,RPS13,RPS16,RPS2,RPS21
Molecular Mechanisms of Cancer	2.98	ATM,BBC3,DVL1,LRP1,RAC1,RHOA,TAB2
Role of Osteoblasts, Osteoclasts and Chondrocytes in Rheumatoid Arthritis	2.92	CALM1 (includes others),CSF1R,DVL1,LRP1,TAB2
PCP (Planar Cell Polarity) Pathway	2.87	DVL1,RAC1,RHOA
Macropinocytosis Signaling	2.58	CSF1R,RAC1,RHOA
TCA Cycle II (Eukaryotic)	2.55	ACO2,IDH3G

Biostatistical analysis was performed on significantly altered genes between patients with a pathological T stage of T0 (*n*=4) and those with a pathological T stage of T3/4 (*n*=8) by IPA analysis to identify projected altered biological functions between the two groups. Statistical analysis performed by right-tailed Fisher's exact test.

6.4.5. *Pre-treatment rectal tumour and non-cancer rectal biopsies display elevated oxidative phosphorylation*

Having demonstrated that significant alterations to the circulating and tumour metabolome of rectal cancer patients is associated with therapy response, and that enhanced reliance on oxidative phosphorylation is associated with enhanced radioresistance in rectal cancer *in vitro* (Chapter 2), the metabolic phenotype of rectal cancer was assessed and compared to the metabolic phenotype of non-cancer rectal tissue.

The baseline metabolic phenotype of pre-treatment *ex vivo* rectal cancer and non-cancer rectal tissue biopsies were assessed in real-time using the Seahorse XFe24 analyser, within an hour of the patient undergoing colonoscopy.

Rectal cancer patient characteristics are outlined in **Table 6.11**. Non-cancer rectal tissue biopsies were obtained from a total of 12 patients [Male (*n*=6), Female (*n*=6)] with a histological confirmation of normal rectal tissue. The median age of non-cancer patients was 41.5 years, with a range of 26-81 years.

Real-time metabolic profiling of live pre-treatment rectal cancer and non-cancer rectal tissue demonstrated heterogenous rates of oxygen consumption rate (OCR), a marker of oxidative phosphorylation and extracellular acidification rate (ECAR), a measure of glycolysis, across patient samples, with consistently higher OCR rates than ECAR rates in both tumour and non-cancer biopsies (**Fig. 6.8A-B**). Non-cancer rectal biopsies demonstrated significantly higher OCR, when compared to ECAR (p = 0.0015) (Mean ± SEM; OCR 267.4 ± 42.16 vs 109 ± 20.16) (**Fig. 6.8C**). Furthermore, in rectal cancer biopsies, OCR was significantly higher than ECAR (p = 0.001) (Mean ± SEM; OCR 166.3 ± 19.06 vs ECAR 84.57 ± 15.76) (**Fig. 6.8C**). In addition, significantly higher OCR was demonstrated in non-cancer rectal biopsies, when compared to rectal cancer biopsies (p = 0.0374) (Mean normalised OCR ± SEM; non-cancer 267.4 ± 42.16 vs cancer 166.3 ± 19.06) (**Fig. 6.8C**). No significant differences were demonstrated in ECAR rates, when comparing non-cancer rectal biopsies to rectal cancer tissue.

These data demonstrate that non-cancer rectal tissue display elevated oxidative phosphorylation rates, when compared to rectal cancer tissue. However, real-time metabolic profiling also demonstrates that in both cancer and non-cancer tissue, there is an enhanced reliance on oxidative phosphorylation, when compared to glycolysis.

Table 6.11: **Patient characteristics of rectal cancer patients used in live real-time metabolic profiling of pre-treatment tumour biopsies.**

		Cancers (*n*=11)
Gender	**Male (*n*)**	5
	Female (*n*)	6
Age at diagnosis	**Median (range) (y)**	69 (47-78)
BMI at Diagnosis*	**Median**	28.45
	Normal (18.5-24.9) (*n*)	3
	Overweight (25-29.9) (*n*)	3
	Obese (≥30) (*n*)	4
Clinical T stage*	**2 (*n*)**	3
	3 (*n*)	6
	4 (*n*)	1
Clinical N stage*	**0 (*n*)**	6
	2 (*n*)	3
	3 (*n*)	1
Differentiation Stage	**Moderate-poor (*n*)**	2
	Moderate (*n*)	5
	Well (*n*)	1
	Awaiting (*n*)	3
Treatment received	**NeoCRT (*n*)**	5
	Surgery only (*n*)	3
	CT only (*n*)	1
	Awaiting (*n*)	2
TRS (of neoCRT patients)	**0 (*n*)**	2
	1 (*n*)	1
	2 (*n*)	2

*BMI at diagnosis, clinical tumour stage, clinical nodal stage only available for *n*=9 patients. Abbreviations; BMI, body mass index; Clinical T stage, clinical tumour stage, clinical N stage, clinical nodal stage; TRS, tumour regression score; neoCRT, Neoadjuvant chemoradiation therapy; CT, chemotherapy

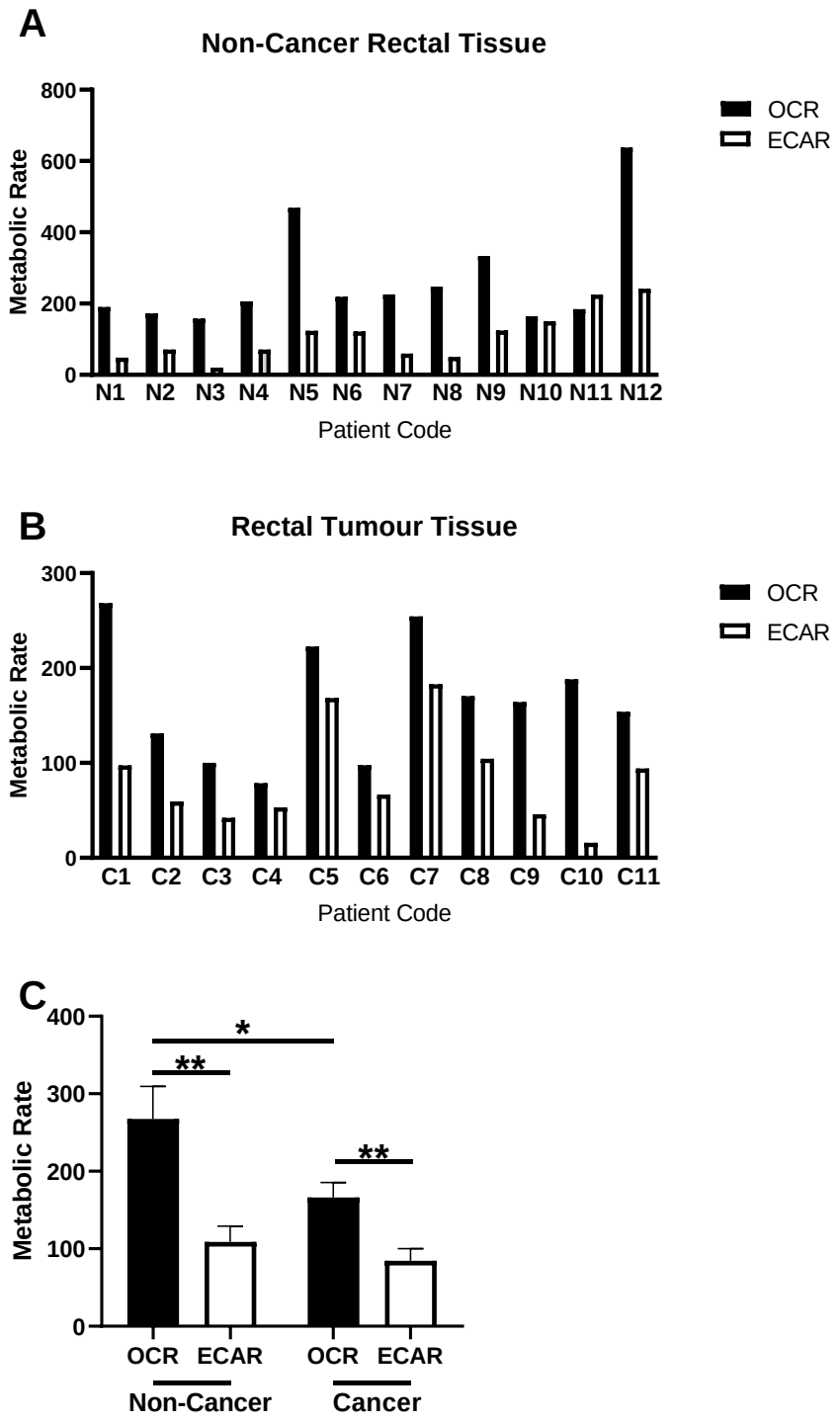

***Fig. 6.8*: Oxidative phosphorylation is significantly higher than glycolysis in pre-treatment rectal cancer biopsies and non-cancer rectal tissue.** The metabolic rate of pre-treatment rectal cancer biopsies and non-cancer rectal tissue biopsies were assessed using the Seahorse Biosciences XFe24 analyser. **A)** Basal OCR and ECAR rates in non-cancer rectal tissue biopsies. **B)** Basal OCR and ECAR rates in pre-treatment rectal cancer tissue biopsies. **C)** OCR is significantly elevated in non-cancer rectal tissue and rectal cancer tissue, when compared to ECAR. Data is normalised to protein content and presented as mean ± SEM from non-cancer (*n*=12) and rectal cancer (*n*=11) patients. Statistical analysis was performed by Wilcoxon ranked testing or Mann Whitney U testing as appropriate. **p*<0.05, ***p*<0.01.

6.4.6. *Real-time metabolic rates of pre-treatment rectal cancer biopsies is not dependent on clinical parameters*

Having demonstrated that pre-treatment rectal cancer biopsies display heterogenous metabolic rates, and display elevated OCR, when compared to ECAR, the impact of clinical parameters on metabolic rates was assessed.

The clinical characteristics of this pre-treatment rectal cancer cohort are displayed in **Table 6.11**. OCR and ECAR rates were not significantly altered depending on clinical T stage, clinical N stage, BMI or TRS (**Fig. 6.9A-H).**

These data suggest that the metabolic phenotype of rectal cancer biopsies is not dependent on any examined clinical or pathological characteristic.

6.4.7. *Pre-treatment rectal tumour tissue has a distinct metabolome from non-cancer rectal tissue*

Having demonstrated that the real-time metabolic phenotype of rectal tumour tissue is distinct from non-cancer rectal tissue (**Section 6.4.5**), the intracellular metabolome of non-cancer rectal tissue and rectal cancer was profiled by LC-MS. Treatment naïve tissue biopsies were obtained from rectal adenocarcinoma patients (*n*=32) undergoing diagnostic colonoscopy. Clinical data from these patients are demonstrated in **Table 6.4.** In addition, normal non-cancer rectal tissue was obtained from 20 patients undergoing endoscopic assessment, who did not have rectal cancer. The median age for non-cancer patients was 60.95 years, with *n* =12 males, and *n* =8 females.

In total, twenty-three metabolites were demonstrated to be significantly altered in rectal cancer tissue, when compared to non-cancer rectal tissue (**Table 6.12**). Of these 23 metabolites, 9 were demonstrated to be significantly increased in rectal cancer tissue, when compared to non-cancer tissue. These increased metabolites were primarily made up of phosphatidylcholines (PCs). Five PC diacyl metabolites, PC aa C32:2 (*p*-adj = 0.0019), PC aa C24:0 (*p*-adj = *0*.0041), PC aa C32:1 (*p*-adj = 0.0041), PC aa C30:2 (*p*-adj = 0.036) and PC C42:6 (*p*-adj = 0.042) were significantly increased in rectal cancer tissue, when compared to non-cancer rectal tissue. In addition, two PC acyl alkyl metabolites were also demonstrated to be significantly increased in rectal cancer tissue, when compared to non-cancer rectal tissue; PC ae C30:0 (*p*-adj = 0.023) and PC ae C44:5 (*p*-adj = 0.029). In addition, the lysophosphatidylcholine, LysoPC a C16:1 was also demonstrated to be significantly upregulated in rectal cancer tissue, when compared to non-cancer rectal tissue (*p*-adj = 0.036).

Putrescine, a polyamine, was also demonstrated to be significantly increased in rectal cancer tissue, when compared to non-cancer rectal tissue (*p*-adj = 0.026).

In contrast, a total of 14 metabolites were significantly downregulated in rectal cancer tissue, when compared to non-cancer rectal tissue (**Table 6.12**). The most significantly downregulated metabolite in rectal cancer tissue was serotonin (*p*-adj = 5.9 x 10^{-14}). Sphingolipids, including sphingomyelin (SM) species were significantly decreased in cancer tissue, when compared to non-cancer tissue, including SM (OH) C22:1 (*p*-adj = = 5.18 x10^{-6}), SM C18:0 (*p*-adj = 5.18 x10^{-6}), SM C26:0 (*p*-adj = 0.0037), SM (OH) C16:1 (*p*-adj = 0.0138), SM C24:0 (*p*-adj = 0.041), SM (OH) C24:1 (*p*-adj = 0.048) and SM C20:2 (*p*-adj = 0.048). The polyamine spermine was also demonstrated to be significantly decreased in rectal cancer tissue, when compared to non-cancer rectal tissue (*p*-adj = 0.036). In addition, histamine, a biogenic amine, was demonstrated to be significantly decreased in rectal tumour tissue (*p*-adj = 0.042). Two PC metabolites were demonstrated to be significantly decreased in rectal cancer tissue, when compared to non-cancer tissue; PC ae C34:3 (*p*-adj = 0.0019) and lysoPC C16:0 (*p*-adj = 0.042). In addition, the acylcarnitine C3-DC (C4-OH) was also demonstrated to be significantly reduced in rectal cancer tissue (*p*-adj = 0.042).

These data demonstrate significant alterations to the metabolome of rectal adenocarcinoma tissue, when compared to non-cancer rectal tissue.

6.4.8. *Significantly altered metabolites in rectal cancer tumour tissue permit predictive clustering into cancer and non-cancer cohorts*

Given that the intracellular metabolome of rectal cancer is distinct from that of non-cancer rectal tissue, unsupervised hierarchical clustering analysis was performed on the significantly altered metabolites between rectal cancer and non-cancer rectal tissue to assess the role of altered metabolism in the development of rectal cancer.

Unsupervised hierarchical clustering analysis was utilised using R software, based on the 10 most significantly altered metabolites distinguishing non-cancer and cancer tissue, as these provided the most accurate clustering (**Fig. 6.10)**. Of the 20 non-cancer patients assessed, *n*=7 were misclassified as cancer samples by unsupervised hierarchical clustering. This analysis led to a clustering accuracy of 86.5%, with more false-positives than false-negative cancer predictions based on the dataset.

These data demonstrate that the metabolome of cancer and non-cancer rectal tissue may be useful in distinguishing cancer and non-cancer.

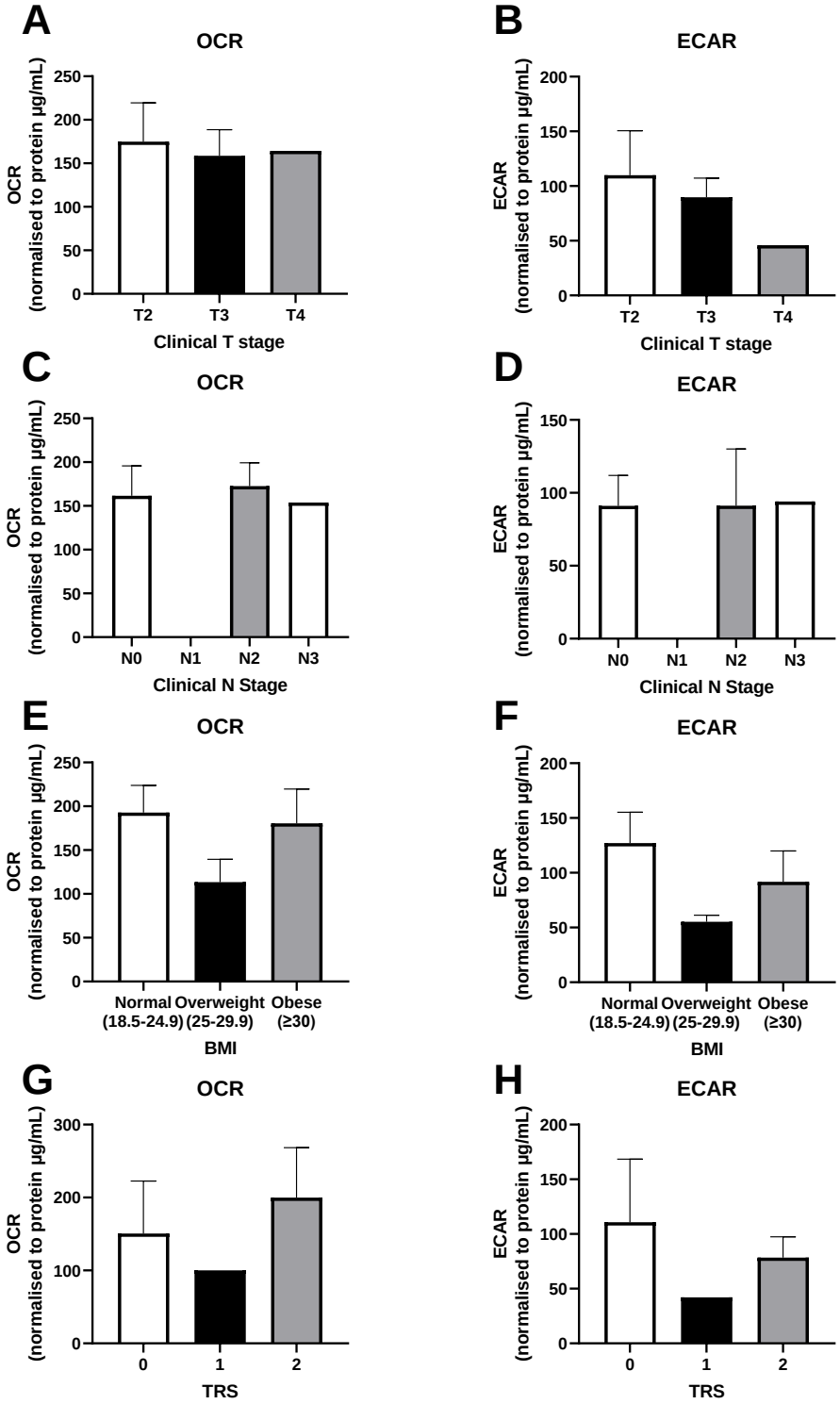

Fig. 6.9: **OCR and ECAR of pre-treatment rectal tumour biopsies are not significantly associated with T stage, N stage, BMI or TRS.** OCR and ECAR were measured in pre-treatment rectal cancer biopsies using the Seahorse XFe24 analyser. OCR in biopsies was sub-divided according to **A)** Clinical T stage (*n*=10), **C)** Clinical N stage (*n*=10), **E)** BMI (*n*=10) and **G)** TRS (*n* = 6). ECAR in rectal cancer biopsies was sub-divided according to **B)** Clinical T stage (*n*=10), **D)** Clinical N stage (*n* = 10), **F)** BMI (*n*=10) and **H)** TRS (*n*=6). Data is presented as mean ± SEM. Statistical analysis was performed by un-paired Mann-Whitney U or Kruskal-Wallis testing with post-hoc multiple comparisons, as appropriate.

***Table 6.12*: Twenty-three metabolites are significantly altered between rectal cancer tissue and non-cancer tissue biopsies.**

Metabolite	Increased or decreased in cancer	*p*-value (FDR corrected)
Serotonin	Decreased	5.9071E-14
SM (OH) C22:1	Decreased	5.1883E-6
SM C18:0	Decreased	5.1883E-6
PC aa C32:2	Increased	0.0018849
PC ae C34:3	Decreased	0.0018849
SM C26:0	Decreased	0.0037346
PC aa C24:0	Increased	0.0041348
PC aa C32:1	Increased	0.0041348
SM (OH) C16:1	Decreased	0.013915
PC ae C30:0	Increased	0.023149
Putrescine	Increased	0.025906
PC ae C44:5	Increased	0.028952
lysoPC a C17:0	Decreased	0.03602
Spermine	Decreased	0.03602
lysoPC a C16:1	Increased	0.03602
PC aa C30:2	Increased	0.03602
SM C24:0	Decreased	0.041349
Histamine	Decreased	0.041954
PC aa C42:6	Increased	0.042075
C3-DC (C4-OH)	Decreased	0.042075
lysoPC a C16:0	Decreased	0.042075
SM (OH) C24:1	Decreased	0.048006
SM C20:2	Decreased	0.048365

Statistical analysis performed by unpaired *t*-testing, on log transformed data. *p*-adjusted (FDR)<0.05. Cancer biopsies (*n*=32) non-cancer rectal tissue biopsies (*n*=20). Abbreviations; SM, sphingomyelin; PC, phosphatidylcholine.

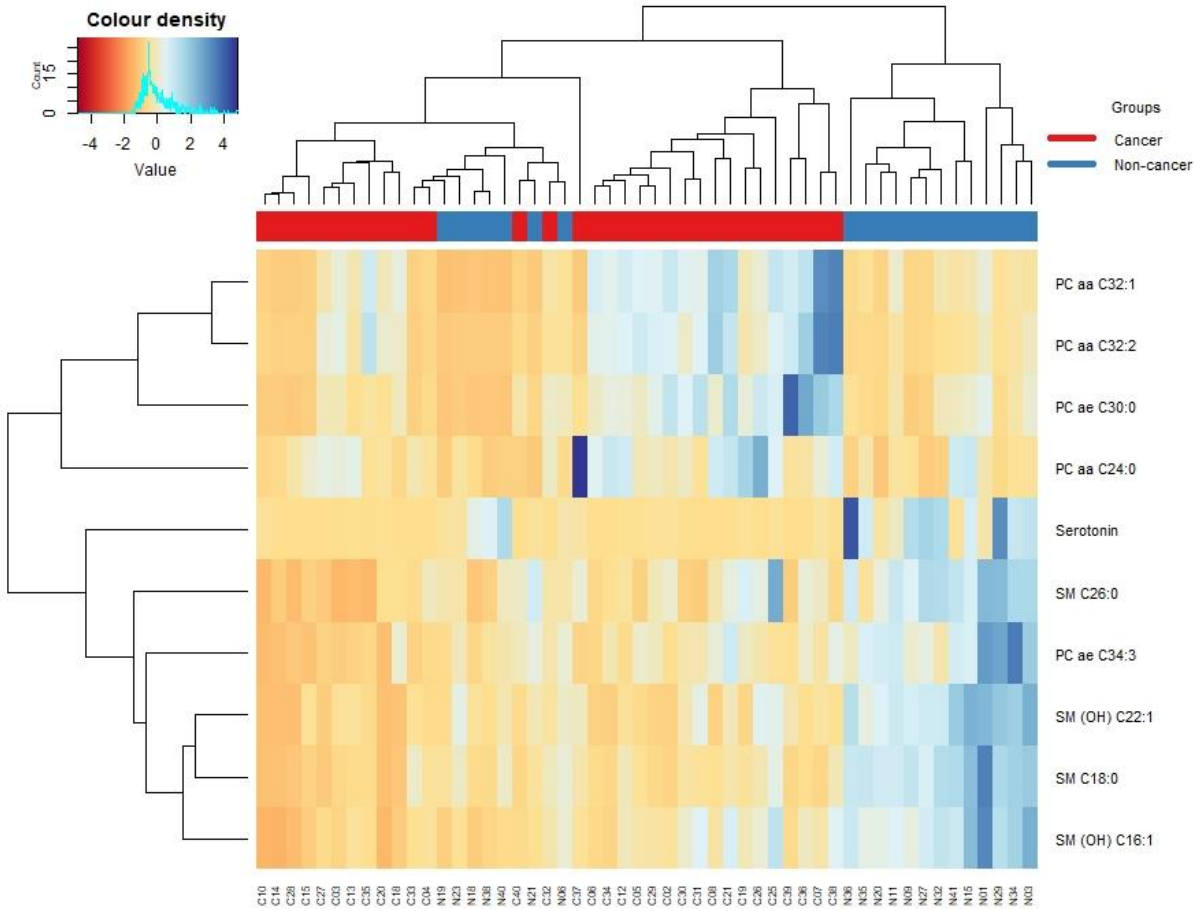

***Fig. 6.10*: Hierarchical clustering analysis of metabolites significantly altered between pre-treatment rectal tumour biopsies and non-cancer rectal tissue biopsies.** Metabolites from rectal tumour biopsies (*n*=32), and non-cancer rectal tissue biopsies (*n*=20) were assessed by LC-MS. Hierarchical clustering analysis was performed using R software to demonstrate the accuracy of clustering into non-cancer and cancer, based on the 10 most significantly altered metabolites between rectal cancer and non-cancer rectal tissue biopsies.

6.4.9. *The secreted metabolome from rectal cancer tissue is significantly altered, when compared to non-cancer rectal tissue*

Having demonstrated that the intracellular metabolome of rectal cancer tissue is significantly altered, when compared to non-cancer rectal tissue (**Section 6.4.7**), the levels of metabolites secreted from rectal tumour and non-cancer tissue was assessed using TCM and NCM by LC-MS.

In total, the secreted levels of 4 metabolites were demonstrated to be significantly altered in rectal TCM, when compared to NCM (**Fig. 6.11**) (**Table 6.13**). Two biogenic amines, dopamine (DOPA) and methionine sulfoxide (Met-SO) were demonstrated to be significantly increased in the conditioned media of rectal cancer tissue, when compared to that of non-cancer tissue (*p*-adj = 0.0058, = 0.009 respectively) (**Fig. 6.11A-B) (Table 6.13**). In addition, the secretion of two lysoPC metabolites were demonstrated to be significantly reduced from rectal cancer tissue, when compared to non-cancer tissue. Lyso-PC a C17:0 levels were significantly lower in TCM, when compared to NCM (*p*-adj = 0.019) (**Fig. 6.11C)**. Lyso PC a C18:0 levels were also demonstrated to be significantly reduced in TCM, when compared to NCM (*p*-adj = 0.048) (**Fig. 6.11D).**

These data demonstrate that there are significant alterations in metabolites secreted from rectal cancer tissue, when compared to non-cancer rectal tissue.

6.4.10. *Significantly altered metabolites in rectal cancer TCM permit predictive clustering into cancer and non-cancer cohorts*

Given that the secreted metabolome of rectal cancer is distinct from that of non-cancer rectal tissue, unsupervised hierarchical clustering analysis was performed on the four metabolites altered between TCM and NCM to further assess altered metabolism in rectal cancer pathogenesis.

Two patients of the 15 non-cancer patients were misclassified into the cancer cohort based on the secreted metabolome (**Fig. 6.12**). Of the 24 cancer patients, *n*=7 patients were misclassified into the non-cancer cohort based on the secreted metabolome (**Fig. 6.12**). In total, a clustering accuracy of 76.9% was demonstrated.

These data demonstrate moderate clustering accuracy based on differentially secreted metabolites between TCM and NCM.

Table 6.13: **Four metabolites are significantly altered between rectal TCM and NCM**

Metabolite Name	Increased or decreased in cancer	p-value (FDR corrected)
DOPA	Increased	0.005781
Met-SO	Increased	0.0089648
lysoPC a C17:0	Decreased	0.019384
lysoPC a C18:0	Decreased	0.048125

Statistical analysis performed by unpaired *t*-testing, on log-transformed data, normalised by sum. *p*-adjusted (FDR)<0.05. Rectal cancer TCM (*n*=24), non-cancer NCM (*n*=15). Abbreviations; DOPA, dopamine; Met-SO, methionine sulfoxide; PC, phosphatidylcholine.

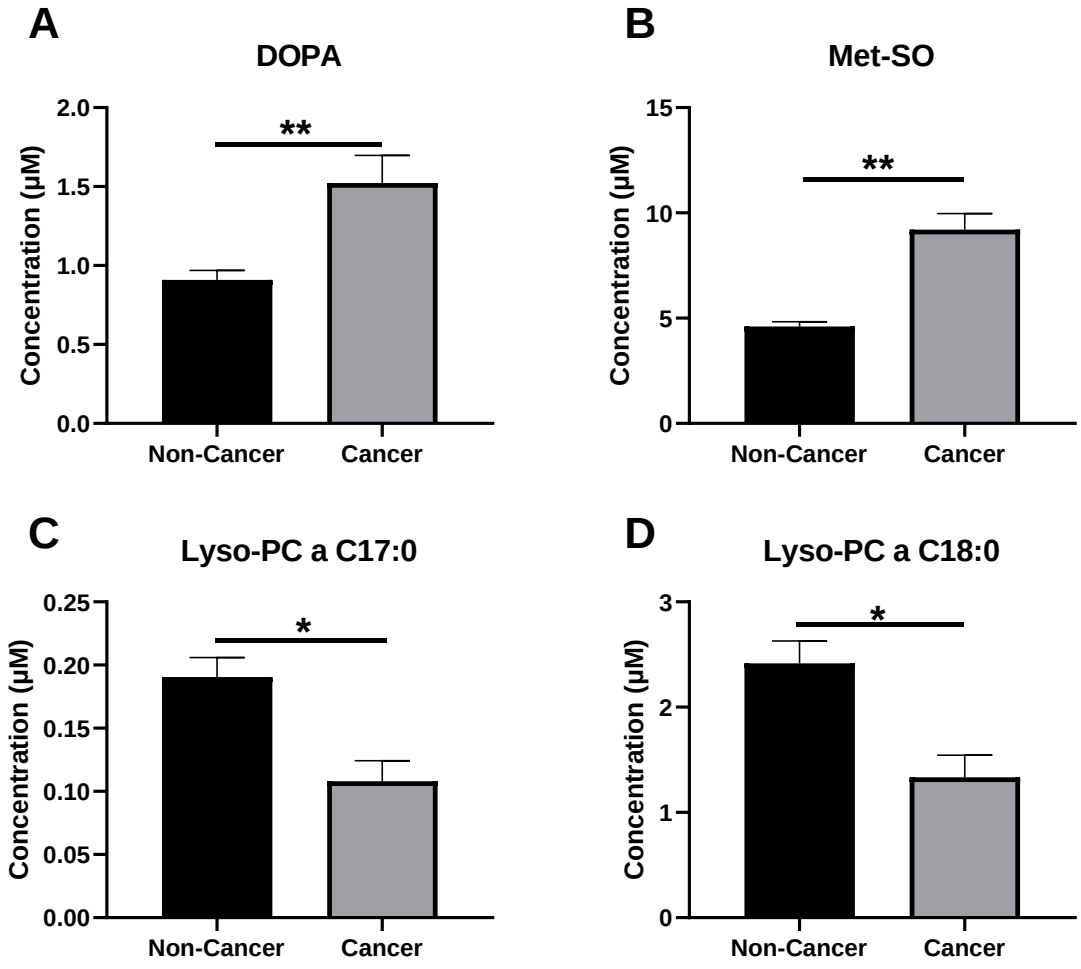

Fig. 6.11: **Four metabolites are significantly altered in rectal cancer TCM, when compared to non-cancer NCM.** The levels of secreted metabolites in TCM and NCM from rectal cancer and non-cancer rectal tissue, respectively, was assessed by LC-MS. Concentration of **A)** dopamine (DOPA), **B)** methionine sulfoxide (Met-SO), **C)** Lyso-PC a C17:0 and **D)** Lyso-PC C18:0 in rectal NCM and TCM. Data is presented as mean ± SEM for TCM samples (*n*=24), or NCM samples (*n*=15). Statistical analysis performed by unpaired *t*-testing, on log-transformed data, normalised by sum. *p*-adjusted (FDR)<0.05. **p*-adj<0.05, ***p*-adj<0.01.

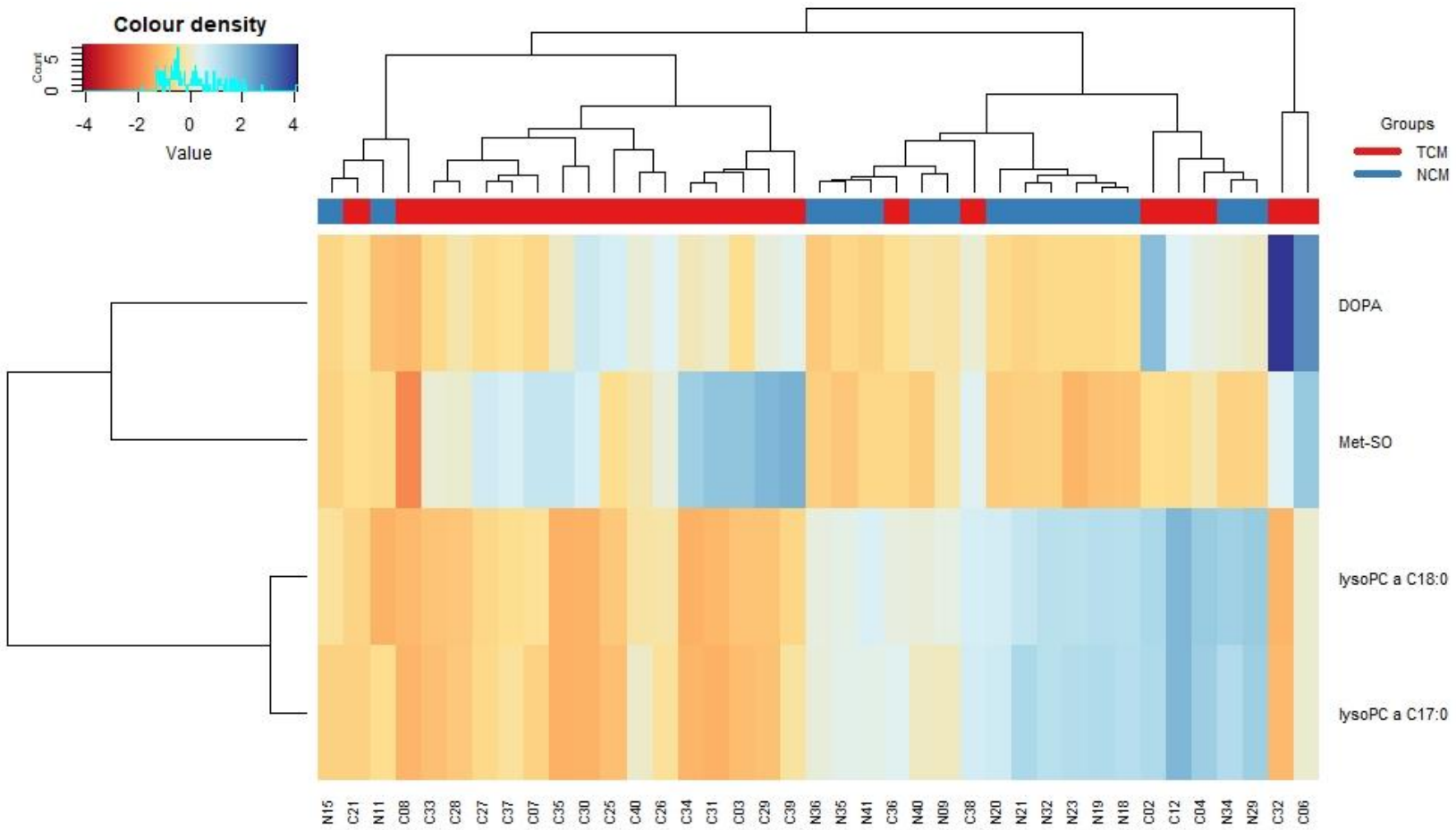

***Fig.6.12*: Hierarchical clustering analysis of secreted metabolites significantly altered between rectal cancer and non-cancer rectal tissue.** Secreted metabolites from non-cancer rectal tissue, and rectal cancer tissue biopsies were measured in TCM (*n*=15) and NCM (*n*=24), respectively by LC-MS. Hierarchical clustering analysis was performed using R software to demonstrate the accuracy of clustering into non-cancer and cancer, based on significantly altered metabolites in the secreted metabolome from rectal cancer and non-cancer rectal tissue biopsies. The y-axis denotes metabolites assessed. The x-axis denotes the patient sample, with N representing non-cancer patients, and C representing rectal cancer patients.

6.4.11. *The protein secretome is significantly altered in pre-treatment rectal tumour biopsies, when compared to non-cancer rectal tissue*

Having demonstrated distinct alterations to the metabolic phenotype and metabolome of rectal cancer tissue (**Sections 6.4.5, 6.4.7** and **6.4.9**), the protein secretome of pre-treatment rectal cancer biopsies and non-cancer rectal tissue biopsies was assessed. TCM and NCM samples were profiled for inflammatory, angiogenic, chemokine and cytokine secretions using the MSD 54 multiplex ELISA systems.

The characteristics of the cancer patient cohort used in this study are demonstrated in **Table 6.14**. In the non-cancer cohort (*n*=12; Male *n*=6 and Female *n*=6), the median age was 41.5 years, with a range from 26–81 years.

In total, the levels of 10 proteins were demonstrated to be significantly altered in TCM, when compared to NCM (**Fig. 6.13** and **6.14**). Of these 10, 3 proteins were related to angiogenesis. Flt-1, also referred to as vascular endothelial growth factor receptor 1 (VEGFR-1), was demonstrated to be significantly increased in TCM, when compared to NCM (p = 0.0036) (Mean concentration (pg/mL) per µg of protein ± SEM; NCM 434.2 ± 47.09 vs TCM 1263 ± 233) **(Fig. 6.13A).** Placental growth factor (PIGF) was also demonstrated to be significantly increased in TCM, when compared to NCM (p = 0.012) (NCM 16.1 ± 3.4 vs TCM 47.9 ± 10.99) (**Fig. 6.13B).** VEGF-C was significantly increased in TCM, when compared to NCM (p = 0.016) (NCM 61.86 ± 20.85 vs TCM 210.1 ± 51.66) (**Fig. 6.13C**).

The secreted levels of two TH17-related proteins, interleukin (IL)-23, and macrophage inflammatory protein -3 alpha (MIP-3α) were demonstrated to be significantly altered in TCM. MIP-3α was significantly increased in TCM, when compared to NCM (p = 0.0009) (NCM 12.4 ± 1.76 vs TCM 62.25 ± 18.28) (**Fig. 6.13D**). In contrast, IL-23 levels were significantly decreased in TCM, when compared to NCM (p = 0.004) (NCM 11.45 ± 2.17 vs TCM 4.52 ± 1.47) (**Fig. 6.13E)**. A trend towards lower levels of IL-21, another TH-17 related cytokine, in TCM, when compared to NCM was demonstrated, but did not reach statistical significance (p = 0.057) (NCM 5.28 ± 1.8 vs TCM 1.27 ± 0.43) (**Fig. 6.13F**).

The levels of three other cytokines were significantly altered in the secretome of rectal cancer, when compared to non-cancer rectal tissue. Granculocyte-macrophage colony stimulating factor (GM-CSF) levels were demonstrated to be significantly increased in TCM, when compared to NCM (p = 0.004) (NCM 40.82 ± 9.3 vs TCM 753.8 ± 314.1) (**Fig. 6.14A**). IL-5 levels were significantly lower in TCM, when compared to NCM (p = 0.033) (NCM 28.4 ± 3.89

vs TCM 19.28 ± 3.78) (**Fig. 6.14B**). Levels of a pro-inflammatory cytokine, IL-8, were also demonstrated to be significantly lower in TCM, when compared to NCM (p = 0.002) (NCM 45922 ± 17731 vs TCM 7226 ± 6433) (**Fig. 6.14C**).

C-reactive protein (CRP), a marker of vascular injury, was demonstrated to be significantly increased in TCM, when compared to NCM (p = 0.004) (NCM 18,774 ± 4,088 vs TCM 168,946 ± 109,816) (**Fig. 6.14D**). In addition, interferon γ-induced protein (IP-10), also known as CXCL10, was demonstrated to be significantly increased in cancer TCM, when compared to NCM (p = 0.0008) (NCM 3.53 ± 1.91 vs TCM 151.7 ± 74.6) (**Fig. 6.14E**). A trend towards increased secretion of another chemokine, MIP1α, from cancer biopsies, when compared to non-cancer rectal biopsies was demonstrated, however this did not reach statistical significance (p = 0.056) (**Fig. 6.14F**).

Together these data demonstrate significant alterations to the protein secretome of rectal cancer, when compared to non-cancer rectal tissue.

6.4.12. *The secretome of rectal cancer is significantly associated with subsequent pathological response to neoadjuvant treatment and other clinicopathological parameters*

Having demonstrated significant alterations to the protein secretome in rectal cancer, these factors were correlated to key clinical and pathological characteristics.

sVCAM-1, was demonstrated to be significantly positively correlated with TRS in rectal cancer patients (p = 0.014, R-value = 0.95). In addition, sVCAM-1 was also demonstrated to have a significant positive correlation with pathological T stage (p = 0.0058, R-value 0.83). Secreted levels of IL-16 were also demonstrated to be significantly associated with pathological T stage (p = 0.038, R-value = 0.69) (**Table 6.15**).

These data demonstrate that alterations in the secretome of rectal cancer are significantly associated with tumour response to therapy and pathological T stage.

Table 6.14: **Patient characteristics of rectal cancer patients used in multiplex ELISA profiling of the secretome of rectal tumour biopsies.**

		Cancers (*n*=12)
Gender	**Male (*n*)**	6
	Female (*n*)	6
Age at diagnosis	**Median (y)(range)**	69 (47-78)
BMI at diagnosis*	**Median**	27.7
	Normal (18.5-24.9) (*n*)	3
	Overweight (25-29.9) (*n*)	4
	Obese (≥30) (*n*)	4
Clinical T stage*	**1/2 (*n*)**	1
	2 (*n*)	3
	3 (*n*)	6
	4 (*n*)	1
Clinical N stage*	**0 (*n*)**	7
	2 (*n*)	3
	3 (*n*)	1
Differentiation stage	**Moderate-poor(*n*)**	2
	Moderate (*n*)	6
	Well (*n*)	1
	Awaiting (*n*)	3
Treatment received	**NeoCRT (*n*)**	5
	Surgery only (*n*)	4
	CT only (*n*)	1
	Awaiting (*n*)	2
TRS (of neoCRT patients)	**0 (*n*)**	2
	1 (*n*)	1
	2 (*n*)	2

*BMI at diagnosis, clinical tumour stage, clinical nodal stage only available for *n* = 11 patients. Abbreviations; y, years; BMI, body mass index; clinical T stage, clinical tumour stage; clinical N stage, clinical nodal stage; NeoCRT, neoadjuvant chemoradiation therapy; CT, chemotherapy; TRS, tumour regression score.

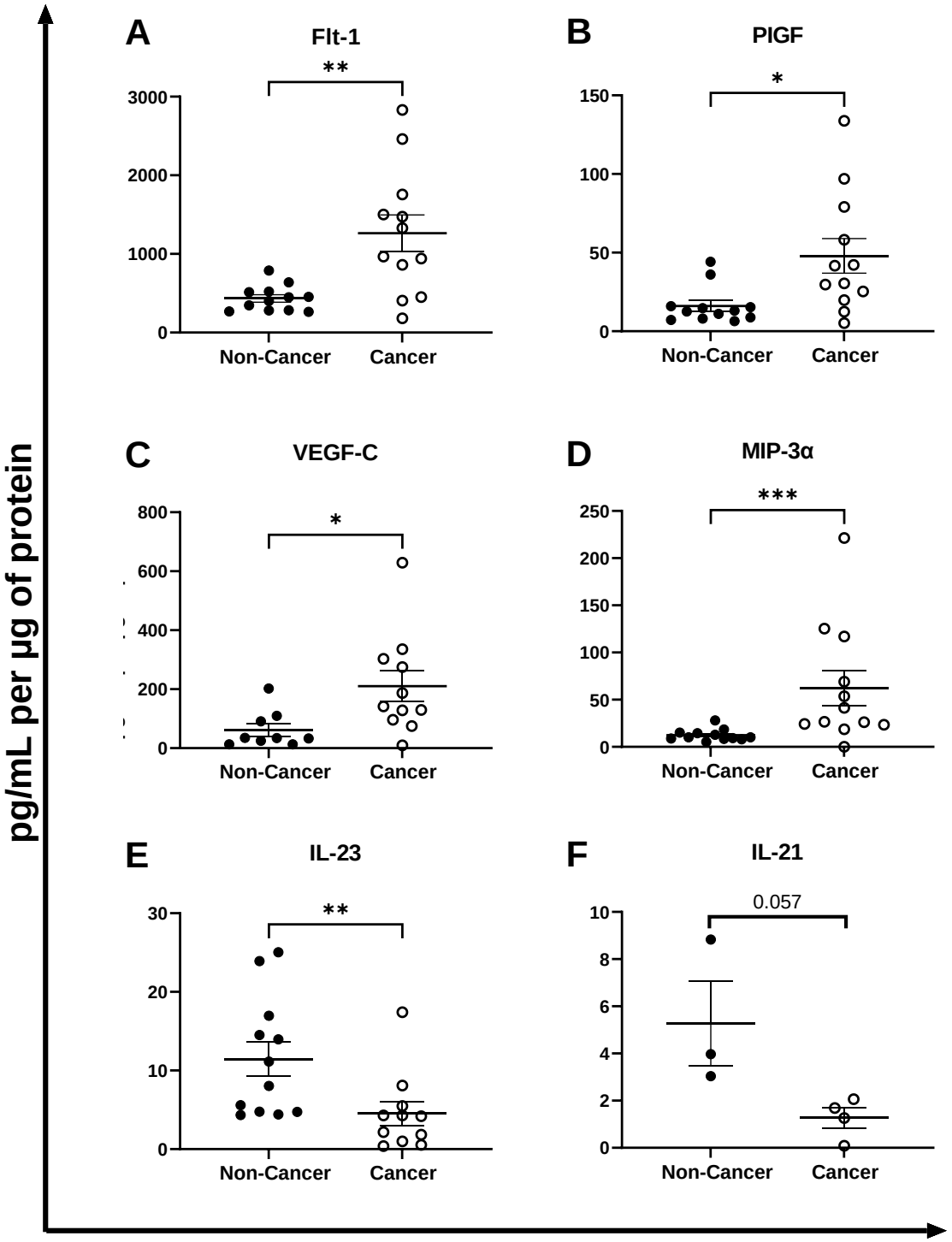

Fig. 6.13: **The protein secretome of rectal cancer is significantly altered, when compared to non-cancer rectal tissue.** The protein secretome of non-cancer rectal tissue and rectal cancer tissue was assessed by multiplex ELISA, assessing levels of 54 proteins. Secreted levels of angiogenic proteins **A)** Flt-1, **B)** PIGF and **C)** VEGF-C from non-cancer rectal tissue and pre-treatment rectal cancer biopsies. Secreted levels of TH17 pathway proteins **D)** MIP-1α, **E)** IL-23 and **F)** IL-21 from non-cancer rectal tissue and pre-treatment rectal cancer biopsies. Data is normalised to protein content and presented ± SEM from non-cancer (*n*=12) and rectal cancer (*n*=12) patients. Statistical analysis was performed by Mann-Whitney U testing. **p*<0.05, ***p*<0.01, ****p*<0.001.

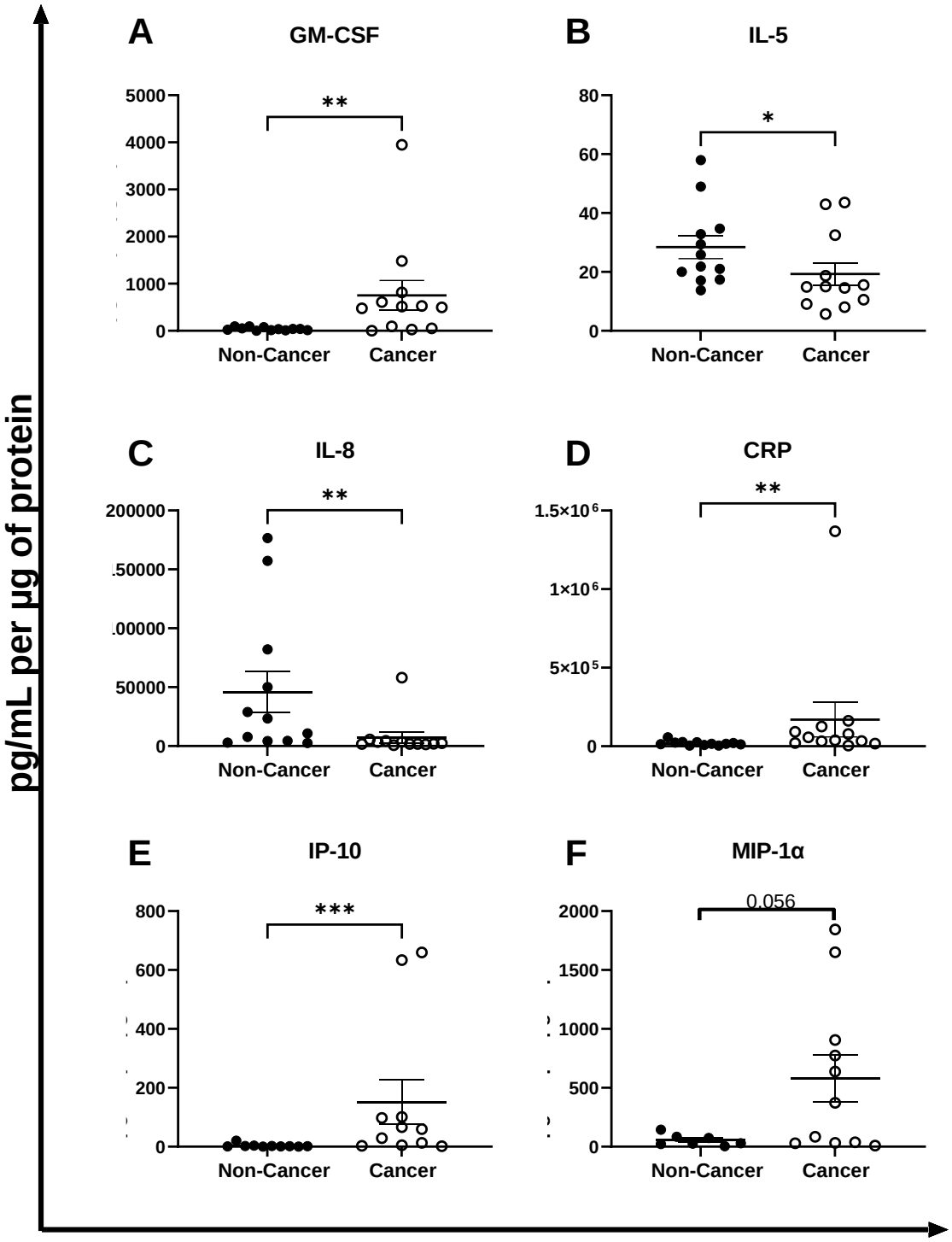

Fig. 6.14: **The protein secretome of rectal cancer is significantly altered, when compared to non-cancer rectal tissue.** The protein secretome of non-cancer rectal tissue and rectal cancer tissue was assessed by multiplex ELISA, assessing levels of 54 proteins. Secreted levels of cytokines **A)** GM-CSF and **B)** IL-5 and **C)** IL-8 from non-cancer rectal tissue and pre-treatment rectal cancer biopsies. Secreted levels of vascular injury protein **D)** CRP and chemokines **E)** IP-10 and **F)** MIP-1α from non-cancer rectal tissue and pre-treatment rectal cancer biopsies. Data is normalised to protein content and presented ± SEM from non-cancer (*n*=12) and rectal cancer (*n*=12) patients. Statistical analysis was performed by Mann-Whitney U testing. **p*<0.05, ***p*<0.01, ****p*<0.001.

Table 6.15: **Correlation analysis of rectal cancer secretome with patient characteristics**

	IL-16		sVCAM-1	
	***p*-value**	**R-value**	***p*-value**	**R-value**
BMI	0.433441	-0.26364	0.957685	-0.01818
TRS	0.111367	0.790569	0.013847	0.948683
Clinical T Stage	0.377373	-0.29567	0.605965	-0.1754
Clinical N stage	0.135398	-0.4797	0.390751	-0.28782
Pathological T stage	0.037741	0.694879	0.00579	0.82851
Pathological N stage	0.725369	-0.13693	0.475797	0.273861

Abbreviations; BMI, body mass index; TRS, tumour regression score; Clinical/pathological T stage, Clinical/pathological tumour stage; clinical/pathological N stage, clinical pathological nodal stage. Values in red denote significantly correlated factors.

6.4.13. *The transcriptome of rectal cancer is significantly altered, when compared to non-cancer rectal tissue*

Having demonstrated alterations to the secretome and metabolome of rectal tumour tissue, the transcriptome of rectal tumour tissue (*n*=36) and non-cancer rectal tissue (*n*=31) was assessed using a Lexogen QuantSeq 3' mRNA FWD sequencing kit. Differential expression analysis was performed using BlueBee™ software and the DESeq2 R script extension.

The patient characteristics of the cancer patient cohort used in this study are demonstrated in **Table 6.6**. The non-cancer cohort was composed of 51.6% (*n*=16) males, and 48.4% (*n*=15) females. The median age of patients in the non-cancer cohort was 59 years, with a range from 28-81 years.

In total, 33,383 genes were expressed across cancer and non-cancer samples. Differential expression analysis demonstrated that 470 genes were differentially expressed between non-cancer and cancer samples. In total, 207 genes were significantly downregulated, and 263 genes were upregulated in rectal cancer tissue, when compared to non-cancer rectal tissue (p-adj < 0.05) (**Fig. 6.15A**). Of the significantly altered genes, the top 25 downregulated and upregulated genes in cancer, when compared to non-cancer tissue are demonstrated in **Fig. 6.15B-C**. ITLN1 (Intelectin1), also known as Omentin, which is involved in carbohydrate binding in the intestine, was the most downregulated gene (as determined by fold change, Log2 Fold Change = -2.64) in rectal cancer tissue, when compared to non-cancer rectal tissue (**Fig. 6.15B**). MMP3 (matrix metallopeptidase 3), which is involved in tissue remodelling, was the most upregulated gene (as determined by fold change Log2 Fold Change = 2.35) in rectal cancer, when compared to non-cancer tissue (**Fig. 6.15C**).

The top 30 genes most significantly altered in rectal cancer tissue, when compared to non-cancer rectal tissue are displayed in **Table 6.16.** ITLN1 was again the most significantly downregulated gene (as determined by p-adj, p-adj = 1.33×10^{-9}) in rectal cancer, when compared to non-cancer rectal tissue. COL1A1 (collagen type I alpha 1 chain), which encodes for type I collagens, was demonstrated to be the most significantly upregulated gene in rectal cancer, when compared to non-cancer rectal tissue (as determined by p-adj, p-adj = 1.7×10^{-8}).

These data demonstrate that the transcriptome of rectal cancer tissue is significantly altered from that of non-cancer rectal tissue.

6.4.14. *Rectal cancer has significantly altered biological functions, when compared to non-cancer rectal tissue*

Having demonstrated significant alterations in the transcriptome of rectal cancer, the differentially expressed genes were analysed by IPA to predict and identify altered biological functional pathways in rectal cancer.

The top 15 significantly altered biological and cellular functions identified in rectal cancer tissue, when compared to non-cancer rectal tissue are demonstrated in **Fig. 6.16.** The *p*-values represent the statistical probability that selecting genes associated with each function is due to chance alone. As each biological function is comprised of multiple functional pathways, significance is represented as *p*-value range.

The most significantly altered biological function in rectal cancer, when compared to non-cancer rectal tissue was 'cellular movement' (*p*-adj range $1.08x10^{-32}$ - $6.33x10^{-5}$). Other functions, and hallmarks of cancer predicted to be altered in rectal cancer tissue included 'cell death and survival' (*p*-adj range $1.34x10^{-09}$ - $5.73x10^{-05}$) and 'cellular growth and proliferation (*p*-adj range $1.97x10^{-15}$ - $1.65x10^{-05}$). Interestingly, metabolic pathways were also predicted to be significantly altered in rectal cancer, when compared to non-cancer tissue, including carbohydrate metabolism (*p*-adj range $2.52x10^{-06}$ - $1.13x10^{-05}$) and lipid metabolism (*p*-adj range $5.89x10^{-05}$ - $5.89x10^{-05}$) (**Fig. 6.16**).

These data demonstrate significant alterations in the molecular and cellular functions in rectal cancer, when compared to non-cancer rectal tissue, including functions related to energy metabolism.

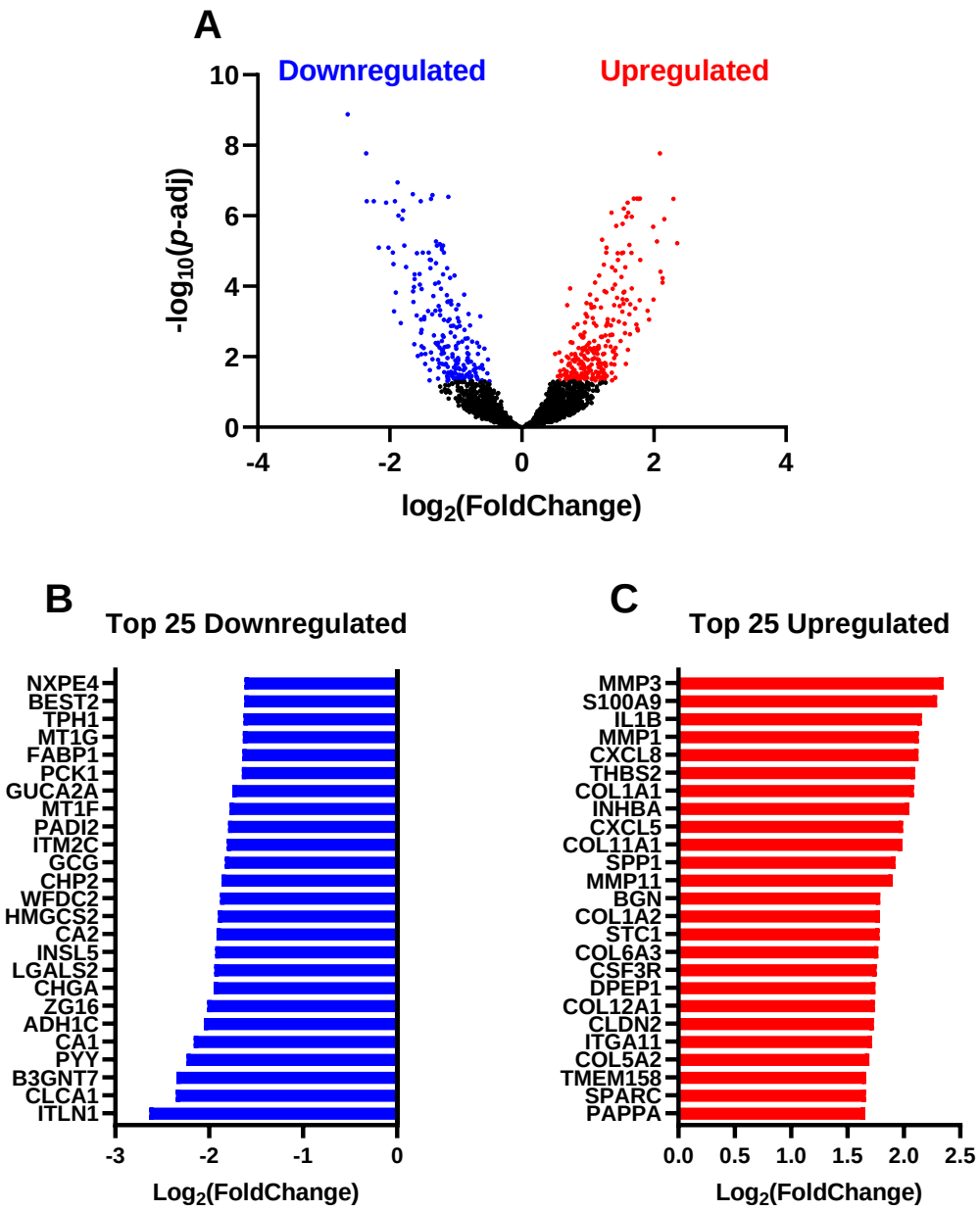

***Fig. 6.15*: The basal transcriptome is significantly altered in rectal cancer, when compared to non-cancer rectal tissue.** Transcriptomic profiling was performed on RNA isolated from non-cancer rectal tissue and pre-treatment rectal cancer biopsies. Differential expression analysis was performed using BlueBee™ Software, using the DESeq2 R extension script. **A)** Volcano plot demonstrating 470 genes significantly altered in rectal cancer tissue, when compared to non-cancer rectal tissue. The y-axis corresponds to the -log10(*p*-adj), and the x-axis demonstrates the Log2 (Fold Change). Dots in blue and red represent the significantly downregulated/upregulated genes in rectal cancer, respectively, when compared to non-cancer rectal tissue. Dots in black represent the genes that did not reach statistical significance (*p*-adj > 0.05). **B)** The top 25 downregulated genes (by fold change) in rectal cancer tissue, when compared to non-cancer rectal tissue biopsies. **C)** The top 25 upregulated genes (by fold change) in rectal cancer tissue, when compared to non-cancer rectal tissue biopsies. Data is presented from non-cancer (*n*=31) and rectal cancer (*n*=36) patients. Statistical analysis was performed using the Wald test, with corrections for multiple comparisons performed by the Benjamini-Hochberg correction (FDR).

Table 6.16: **Top 30 most significantly altered genes in rectal tumour biopsies, when compared to non-cancer rectal tissue**

Gene	Upregulated or downregulated in rectal cancer	Log2 Fold Change	*p*-adj
ITLN1	Downregulated	-2.63911	1.33E-09
CLCA1	Downregulated	-2.3561	1.70E-08
COL1A1	Upregulated	2.089303	1.70E-08
WFDC2	Downregulated	-1.88241	1.13E-07
PCK1	Downregulated	-1.65268	2.42E-07
MAOA	Downregulated	-1.35166	2.60E-07
PDCD4	Downregulated	-1.11212	2.88E-07
COL5A2	Upregulated	1.694068	3.25E-07
COL12A1	Upregulated	1.744134	3.25E-07
COL1A2	Upregulated	1.787971	3.25E-07
ST6GALNAC1	Downregulated	-1.37758	3.33E-07
COL6A3	Upregulated	1.772576	3.33E-07
S100A9	Upregulated	2.294154	3.33E-07
B3GNT7	Downregulated	-2.34964	3.87E-07
PYY	Downregulated	-2.24218	3.87E-07
CA2	Downregulated	-1.92174	3.87E-07
SLC26A2	Downregulated	-1.52927	3.87E-07
ADH1C	Downregulated	-2.05658	4.26E-07
COL3A1	Upregulated	1.601953	4.26E-07
RAB31	Upregulated	1.542433	6.27E-07
PADI2	Downregulated	-1.79996	7.21E-07
VCAN	Upregulated	1.357066	8.20E-07
COL4A1	Upregulated	1.610918	8.20E-07
CHP2	Downregulated	-1.8692	9.99E-07
COL4A2	Upregulated	1.583106	1.07E-06
SPARC	Upregulated	1.663728	1.07E-06
IL1B	Upregulated	2.159954	1.25E-06
ITM2C	Downregulated	-1.81272	1.25E-06
COL18A1	Upregulated	1.525965	1.69E-06

Log2 Fold Change indicated the differential expression of each gene in pre-treatment rectal tumour biopsies, when compared to non-cancer rectal tissue, with negative values indicating genes downregulated in cancer, and positive values indicating genes upregulated in cancer. The *p*-adj values indicate the statistical significance of the differential expression of each gene between rectal cancer and non-cancer rectal tissue. Statistical analysis performed using the Wald test, with corrections for multiple comparisons performed by the Benjamini-Hochberg correction (FDR).

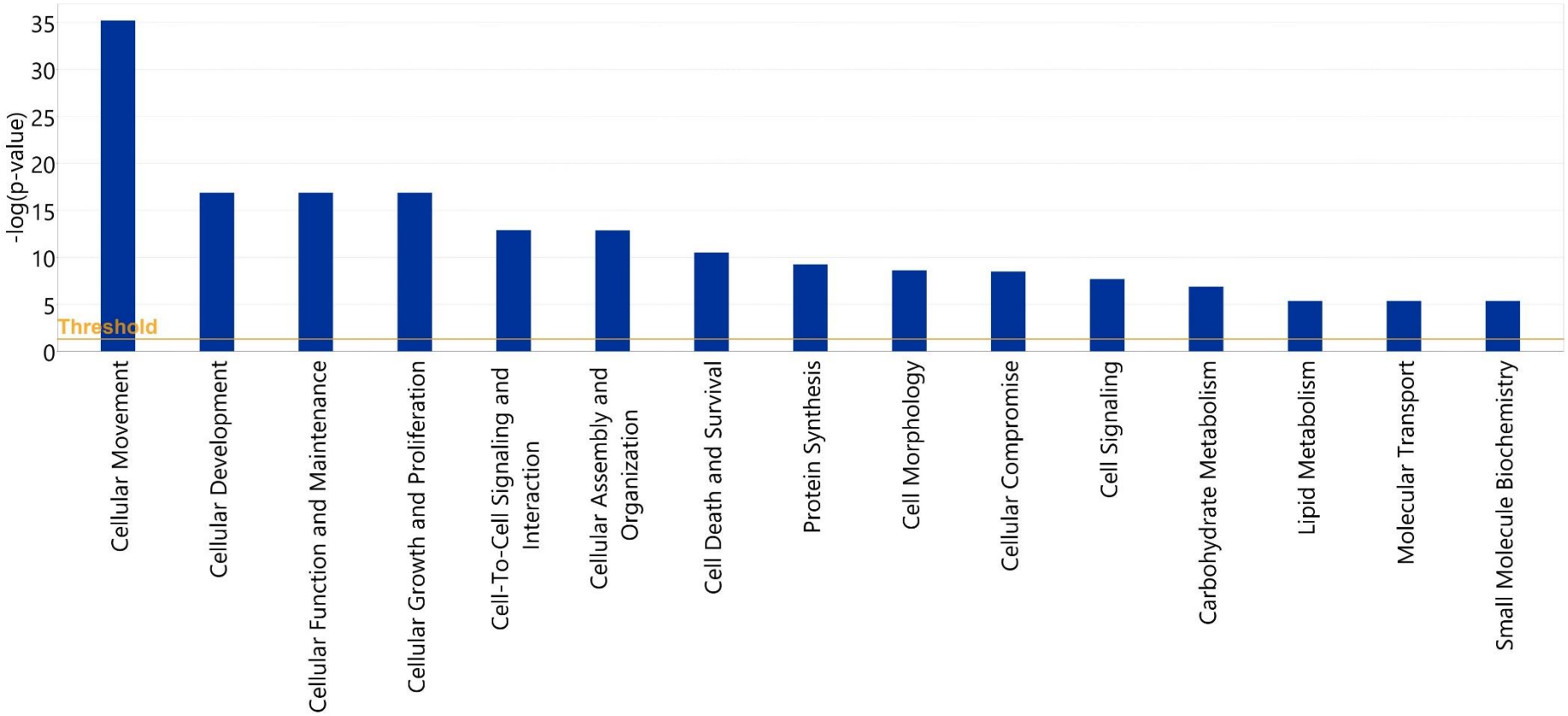

***Fig. 6.16*: Biological functions are significantly altered in rectal cancer, when compared to non-cancer rectal tissue.** Biostatistical analysis was performed on genes significantly altered between non-cancer rectal tissue and rectal cancer tissue by IPA analysis to identify predicted altered biological functions. Statistical analysis was performed by right-tailed Fisher's exact test using IPA analysis.

6.4.15. *Canonical pathways are significantly altered in rectal cancer, when compared to non-cancer rectal tissue*

As biological functions were demonstrated to be significantly altered in rectal cancer, when compared to non-cancer rectal tissue, the specific pathways involved in these processes were assessed. Transcriptomic data was analysed using IPA canonical pathway analysis, which predicts activation or inhibition of pathways in a dataset, based on the dataset itself, and the Ingenuity Knowledge Base.

The top 40 most significantly altered canonical pathways in rectal cancer tissue, when compared to non-cancer rectal tissue are demonstrated in **Table 6.17**. The *p*-value represents the significance in the overlap of the dataset and the ingenuity knowledge base, which indicates the confidence in the involvement of each pathway. The Z-score refers to software prediction of the activation or inhibition of each affected canonical pathway, with a Z-score ≥ 2, or ≤ -2 indicating significant activation or inhibition of each pathway, respectively.

The canonical pathway most significantly predicted to be altered in rectal cancer, when compared to non-cancer tissue, was demonstrated to be 'hepatic fibrosis/hepatic stellate cell activation' indicating that rectal cancer may share signalling patterns with this canonical pathway. The 'GP6 signalling pathway' was predicted to be significantly activated in rectal cancer (Z-score = 4.796). Other pathways significantly altered in rectal cancer biopsies included the 'tumour microenvironment' canonical pathway, which was predicted to be significantly activated in rectal cancer, when compared to non-cancer tissue (-log10(*p*-value) = 7.87, Z-score = 4.123). 'Molecular mechanisms of cancer' was also demonstrated to be significantly altered in rectal cancer, when compared to non-cancer tissue (-log10(*p*-value) = 1.78)**.** 'Wound healing signalling pathway' was also predicted to be significantly upregulated in rectal cancer, when compared to non-cancer (-log10(*p*-value) = 12.4, Z-score = 4.158) (**Table 6.17**).

Several pathways associated with metastasis and extracellular matrix remodelling were predicted to be altered in rectal cancer biopsies, when compared to non-cancer rectal tissue, including activation of 'colorectal cancer metastasis signalling pathway' (-log10(*p*-value) = 2.68, Z-score 2.53), inhibition of 'inhibition of matrix metalloproteases' (log10(*p*-value) = 8.22, Z-score = -1) and activation of 'integrin signalling' (log10(*p*-value) = 1.83, Z-score 1.4) (**Table 6.17**).

These data demonstrate alterations to multiple canonical signalling pathways in rectal cancer tissue, when compared to non-cancer tissue.

6.4.16. *Significantly altered genes in rectal cancer tissue correlate with pathological response to treatment, and clinical and pathological T and N stage*

Having demonstrated significant alterations in the transcriptome of rectal cancer, when compared to non-cancer rectal tissue, the correlation between significantly altered genes and clinicopathological factors were examined by spearman correlation in R software.

Of the 263 genes significantly upregulated in rectal cancer (**Section 6.4.13**), when compared to non-cancer rectal tissue, 17 genes were significantly positively correlated with TRS (**Table 6.18**). The R values of these correlations ranged from 0.49 to 0.66, indicating moderate correlation.

In addition, significantly upregulated genes in rectal cancer were demonstrated to significantly correlate with other clinicopathological factors (**Table 6.19**). One gene, PDE4B significantly positively correlated with clinical T stage. Another gene, CEMIP displayed a significant negative correlation with clinical N stage. NCL, was demonstrated to have a significant positive correlation with pathological T stage. Eleven genes upregulated in rectal cancer were demonstrated to significantly correlate with pathological N stage (**Table 6.19**).

In addition, of the 207 genes demonstrated to be significantly downregulated in rectal cancer (**Section 6.4.13**), when compared to non-cancer rectal tissue, five were significantly correlated with TRS (ANTXR1, CD9, INSL5, MT-TT and TST) (**Table 6.20**). Four genes were demonstrated to be significantly positively correlated with clinical T stage (CHGA, KIAA1324, TGFBI, and TPH1) (**Table 6.20**)**.** In addition, two genes displayed a significant positive correlation with clinical N stage (SLC28A2, and TPH1). One gene, SEMA4G, was demonstrated to have a significant negative correlation with pathological N stage (**Table 6.20**).

These data demonstrate that genes, which are significantly altered in rectal cancer also display significant correlations to patient characteristics, including patient pathological response to treatment.

Table 6.17: **Top 40 canonical pathways predicted to be significantly altered between non-cancer rectal tissue and rectal tissue biopsies**

Ingenuity Canonical Pathways	-log(*p*-value)	z-score
Hepatic Fibrosis / Hepatic Stellate Cell Activation	18.7	N/A
GP6 Signalling Pathway	14.5	4.796
Pulmonary Fibrosis Idiopathic Signalling Pathway	12.7	5.745
Wound Healing Signalling Pathway	12.4	4.158
Agranulocyte Adhesion and Diapedesis	11.8	N/A
Osteoarthritis Pathway	10.3	1.886
Granulocyte Adhesion and Diapedesis	9.63	N/A
Inhibition of Matrix Metalloproteases	8.22	-1
Tumour Microenvironment Pathway	7.87	4.123
Role of IL-17A in Psoriasis	6.57	2.449
Hepatic Fibrosis Signalling Pathway	6.32	3.962
Atherosclerosis Signalling	6.17	N/A
Semaphorin Neuronal Repulsive Signalling Pathway	6.17	0.535
Leukocyte Extravasation Signalling	6.04	2.84
Axonal Guidance Signalling	5.4	N/A
HOTAIR Regulatory Pathway	4.97	3.464
GPCR-Mediated Integration of Enteroendocrine Signalling Exemplified by an L Cell	4.49	-1.134
GPCR-Mediated Nutrient Sensing in Enteroendocrine Cells	4.29	-1
Apelin Liver Signalling Pathway	3.66	2.236
Role of IL-17A in Arthritis	3.64	N/A
Role of Osteoblasts, Osteoclasts and Chondrocytes in Rheumatoid Arthritis	3.47	N/A
Adrenomedullin signalling pathway	3.46	1.155
Endocannabinoid Cancer Inhibition Pathway	3.44	-2.121
Role of IL-17F in Allergic Inflammatory Airway Diseases	3.33	2
IL-17 Signalling	3.23	3.464
P2Y Purigenic Receptor Signalling Pathway	3.19	0
Cardiac Hypertrophy Signalling (Enhanced)	3.19	1.414
Hepatic Cholestasis	3.11	N/A
LXR/RXR Activation	2.82	-1.633
Endocannabinoid Neuronal Synapse Pathway	2.81	1.414
Role of Macrophages, Fibroblasts and Endothelial Cells in Rheumatoid Arthritis	2.78	N/A
Sertoli Cell-Sertoli Cell Junction Signalling	2.78	N/A
BEX2 Signalling Pathway	2.74	1.633
Intrinsic Prothrombin Activation Pathway	2.72	1.342
PPAR Signalling	2.7	-1.89
Colorectal Cancer Metastasis Signalling	2.68	2.53
SPINK1 General Cancer Pathway	2.68	2.449
Signalling by Rho Family GTPases	2.67	3

Table 6.18: **Significantly upregulated genes in rectal cancer are positively correlated with patient pathological response to treatment**

	TRS	
Gene	***p*-value**	**R-value**
ACTA2	0.012	0.578
ADAMDEC1	0.005	0.636
COL18A1	0.038	0.493
COLGALT1	0.003	0.656
DDX52	0.016	0.558
ITGA2	0.006	0.623
METTL7A	0.025	0.525
NCL	0.013	0.571
NCOR2	0.012	0.578
PCDH17	0.021	0.538
PMEPA1	0.021	0.538
POMP	0.002	0.669
PTPN12	0.015	0.565
SCD	0.021	0.538
TFF3	0.025	0.525
TLN1	0.041	0.486
ZNF91	0.023	0.532

Abbreviations: TRS, tumour regression score.

Table 6.19: **Significantly upregulated genes in rectal cancer are significantly correlated with patient characteristics**

	Clinical T stage		Clinical N stage		Pathological T stage		Pathological N stage	
	***p*-value**	**R-value**	***p*-value**	**R-value**	***p*-value**	**R-value**	***p*-value**	**R-value**
ADAM12							0.019	-0.456
CEMIP			0.046	-0.339			0.024	-0.441
DPYSL3							0.024	-0.441
EMILIN1							0.044	-0.398
MOGAT2							0.044	-0.398
NCL					0.034	0.402		
NNMT							0.044	-0.398
NTM							0.033	-0.420
PALD1							0.044	-0.398
PDE4B	0.037	0.349						
PRRX1							0.019	-0.455
RBMS1							0.036	-0.412
ST6GALNAC6							0.044	-0.398

Abbreviations: T stage, tumour stage; N stage, nodal stage.

***Table 6.20*: Significantly downregulated genes in rectal cancer are significantly correlated with patient characteristics, including pathological response to treatment**

	TRS		Clinical T stage		Clinical N stage		Pathological N stage	
	***p*-value**	**R-value**	***p*-value**	**R-value**	***p*-value**	**R-value**	***p*-value**	**R-value**
ANTXR1	0.037	0.494						
CD9	0.037	0.494						
CHGA			0.038	0.347				
INSL5	0.049	0.471						
KIAA1324			0.034	0.354				
MT-TT	0.004	0.643						
SEMA4G							0.036	-0.413
SLC28A2					0.048	0.336		
TGFBI			0.041	0.342				
TPH1			0.032	0.358	0.009	0.438		
TST	0.035	0.499						

Abbreviations: TRS, tumour regression score; T stage, tumour stage; N stage, nodal stage

6.4.17. *Significantly altered genes in rectal cancer tissue permit modest predictive clustering into cancer and non-cancer cohorts*

Given that the transcriptome of rectal cancer is altered, when compared to non-cancer rectal tissue (**Section 6.4.13)**, unsupervised hierarchical clustering analysis was performed on the ten most significantly altered genes between rectal cancer tissue and non-cancer rectal tissue to assess their potential in distinguishing cancer from normal tissue.

Nine non-cancer patients were misclassified into the cancer cohort based on the secreted metabolome (**Fig. 6.17**). Eleven rectal cancer patients were misclassified into the non-cancer cohort based on the secreted metabolome (**Fig. 6.17**). In total, a clustering accuracy of 66% was demonstrated.

These data demonstrate very modest clustering accuracy based on differentially expressed genes in rectal cancer and non-cancer rectal tissue.

6.4.18. *Combination of metabolomic and transcriptomic data permits enhanced predictive clustering into cancer and non-cancer cohorts*

Having demonstrated that the tissue metabolome permits accurate predictive clustering into cancer and rectal cancer cohorts (**section 6.4.8**), the impact of combining the top ten significantly altered metabolites and genes in rectal tumour biopsies on the accuracy of predictive clustering was assessed.

Integration of the top 10 genes and metabolites differentially expressed between rectal cancer and non-cancer rectal tissue resulted in seven non-cancer patients being misclassified into the cancer cohort, and no cancer patients being misclassified into the non-cancer cohort. This led to a clustering accuracy of 85.1% (**Fig. 6.18)**.

These data demonstrate that while the addition of metabolomic data to transcriptomic data results in enhanced clustering accuracy, it is not superior to the clustering provided by metabolomic data alone, highlighting the potential utility of metabolomic data as biomarkers.

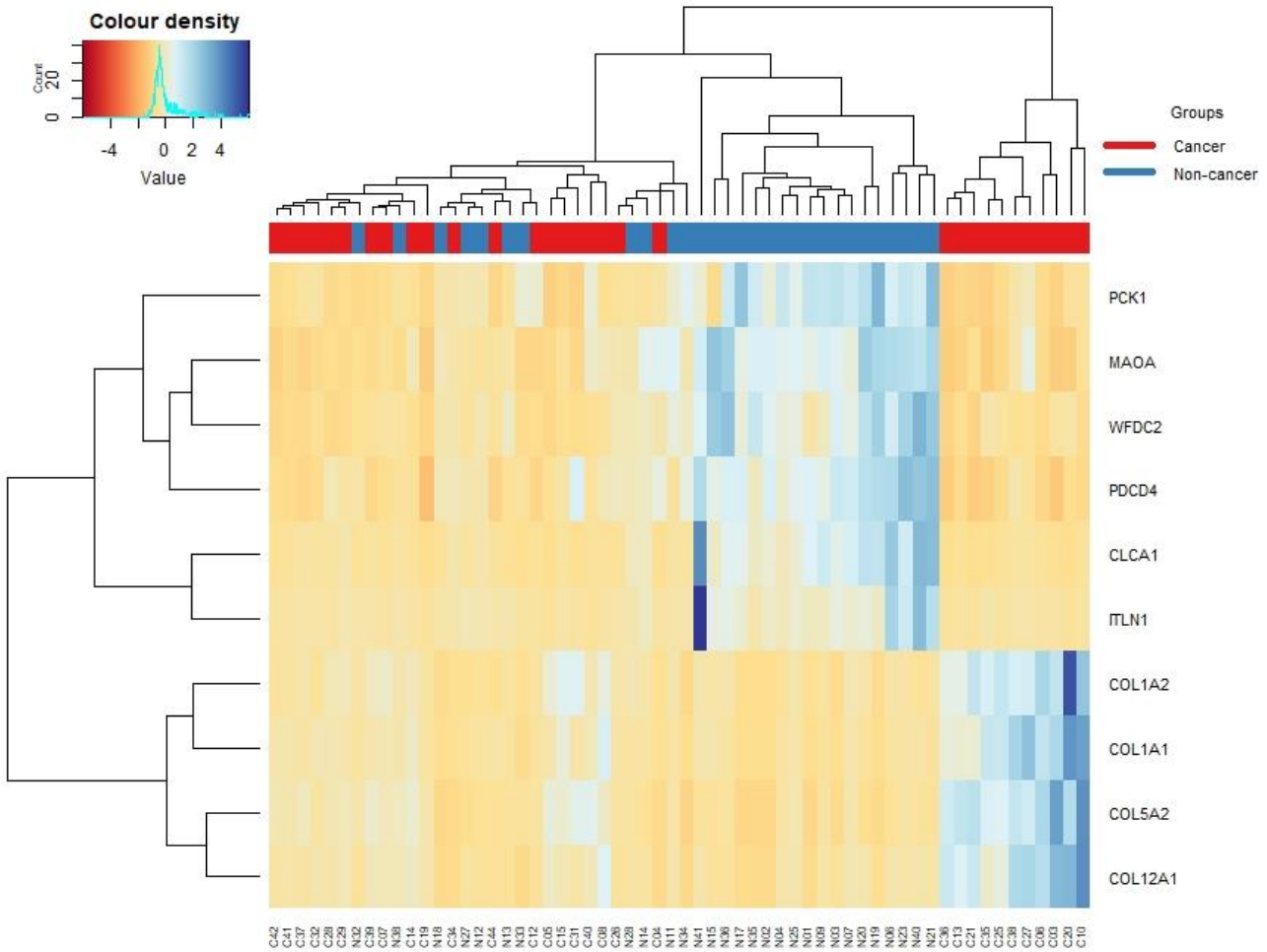

Fig. 6.17: **Hierarchical clustering analysis of genes significantly altered between pre-treatment rectal tumour biopsies and non-cancer rectal tissue biopsies.** Significantly altered genes between rectal tumour biopsies (*n* = 36), and non-cancer rectal tissue biopsies (*n* = 31) were assessed by transcriptomic profiling. Hierarchical clustering analysis was performed using R software to demonstrate the accuracy of clustering into non-cancer and cancer, based on the 10 most significantly altered genes between rectal cancer and non-cancer rectal tissue biopsies. X-axis denotes samples, y-axis denotes significantly altered genes.

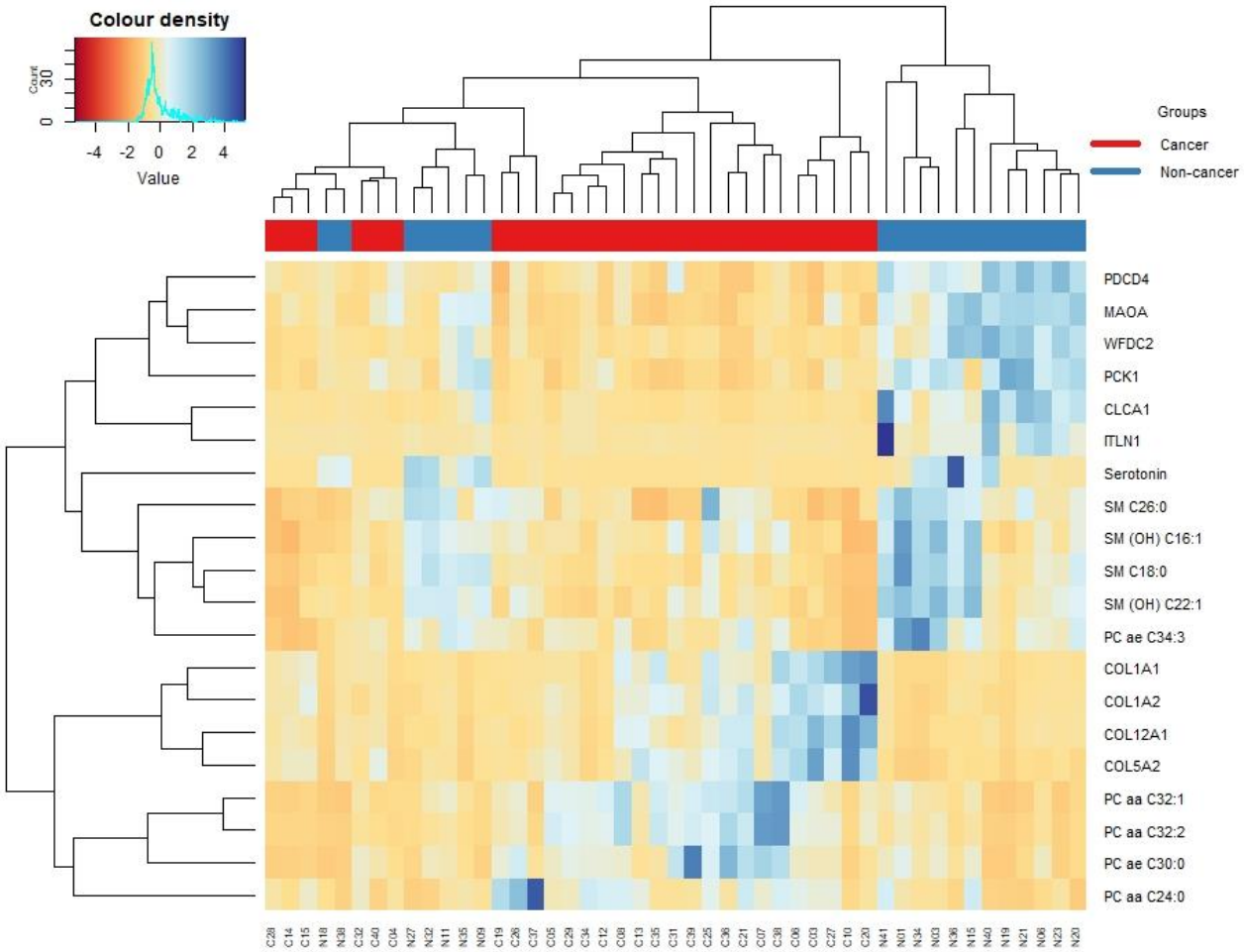

Fig. 6.18: **Hierarchical clustering analysis of top 10 genes and metabolites significantly altered between pre-treatment rectal tumour biopsies and non-cancer rectal tissue biopsies.** Significantly altered metabolites and genes between rectal tumour biopsies (*n* = 31), and non-cancer rectal tissue biopsies (*n* = 20) were assessed by LC-MS and transcriptomic profiling, respectively. Hierarchical clustering analysis was performed using R software to demonstrate the accuracy of clustering into non-cancer and cancer, based on the 10 most significantly altered metabolites and genes between rectal cancer and non-cancer rectal tissue biopsies. X-axis denotes samples, y-axis denotes significantly altered genes.

6.5. Summary of main findings of Chapter 6

- Metabolomic profiling of pre-treatment rectal cancer sera identified 16 metabolites significantly associated with subsequent pathological response to neoCRT.
- Metabolomic profiling of pre-treatment rectal tumour biopsies and TCM demonstrates significant correlations with clinicopathological factors, including tumour response.
- Transcriptomic profiling of pre-treatment rectal tumour biopsies demonstrated significantly altered gene expression in patients having a subsequent poor pathological response (TRS 2) to treatment, when compared to good responders (TRS 0).
- Transcriptomic profiling of pre-treatment rectal tumour biopsies demonstrated significantly altered gene expression in patients who had a pathological T stage T3/4, when compared to those with a pathological T stage T0.
- IPA analysis of the transcriptomic alterations demonstrated significant alterations to cell survival and metabolic pathways in patients with a poor response to therapy (TRS2), and patients with a pathological T stage T3/4.
- Real-time metabolic phenotyping of rectal tumour and non-cancer rectal tissue demonstrated significantly elevated levels of OCR, a marker of oxidative phosphorylation, when compared in ECAR, a marker of glycolysis.
- Real-time metabolic phenotyping demonstrated that non-cancer rectal tissue displays significantly elevated OCR, when compared to rectal cancer tissue.
- Metabolomic profiling of pre-treatment rectal cancer tissue, and non-cancer rectal tissue demonstrated 23 metabolites significantly altered in rectal cancer. These metabolites were primarily phosphatidylcholines.
- Metabolomic profiling of TCM and NCM demonstrated significantly altered secretion of four metabolites from rectal tumour tissue, when compared to non-cancer rectal tissue.
- The protein secretome of rectal tumour tissue was demonstrated to be significantly altered from non-cancer rectal tissue, with the levels of 10 proteins significantly different between TCM and NCM.
- The basal transcriptome of rectal tumour tissue was demonstrated to be significantly altered, when compared to non-cancer rectal tissue.

- IPA analysis revealed significant alterations in pathways commonly associated with tumour development and progression in the transcriptome of rectal cancer.
- IPA analysis predicted alterations in metabolism, including lipid and carbohydrate metabolism in rectal cancer tissue, when compared to non-cancer rectal tissue.
- Hierarchical clustering analysis demonstrated accurate clustering into cancer and non-cancer cohorts using metabolomic data, however the addition of transcriptomic data did not enhance clustering accuracy.

6.6. Discussion

In previous chapters, the role of altered energy metabolism in the radioresponse was assessed in an *in vitro* model of radiosensitive/radioresistant CRC. This chapter aimed to investigate the role of altered metabolism in both the response to therapy and the development of rectal cancer by performing multi-omic profiling of sera and tumour biopsy samples from rectal cancer patients and normal rectal tissue samples from non-cancer controls.

In Chapter 1, altered energy metabolism, specifically reduced reliance on glycolysis and elevated levels of oxidative phosphorylation were demonstrated to be associated with radioresistance in an *in vitro* model of rectal cancer. In addition, in chapter 3, targeting oxidative phosphorylation using the clinically-approved drug metformin, was demonstrated to radiosensitise the *in vitro* model of radiosensitive/radioresistant CRC. To further investigate the potential role of metabolism in the therapeutic response of rectal cancer, the metabolome of pre-treatment sera from rectal cancer patients was assessed, and correlated with subsequent pathological response to neoCRT. GLM analysis demonstrated that 16 metabolites were significantly associated with response to neoCRT. These metabolites were significantly reduced with increasing TRS, using the CAP/AJCC four-point scale, highlighting a potential role for these 16 metabolites as novel circulating minimally-invasive predictive biomarkers of response to neoCRT in rectal cancer. These findings support previous data from Jia *et al*. in which metabolic profiling of pre-treatment sera from rectal cancer identified 15 metabolites predictive of therapeutic response (324). Interestingly, 3 of these 15 altered metabolites were PCs, which was the predominant group of metabolites identified in this study to be associated with therapy response.

PC metabolism has been under investigation for its role in tumourigenesis and therapeutic response in cancer for decades. Catabolism of phosphatidylcholine is mediated by phospholipases (A2, C and D) and produces choline-containing phospholipids and lipid mediators, which have been implicated in pro-tumour signalling (435, 436). These lipid mediators include arachidonic acid, diacylglycerol and platelet-activating factor (PAF), and are deemed as lipid second messengers, associated with resistance to cancer therapy (436). One such PC-derived lipid messenger is lysophosphatidic acid (LPA), which is produced by the action of the phospholipase enzyme autotaxin (ATX) (436). ATX-LPA signalling has been demonstrated to promote chemoresistance in colon cancer (437). In addition, ATX-LPA signalling has been associated with radioresistance in models of breast cancer and glioblastoma, and has been demonstrated to protect against oxidative damage through Nrf2 stabilisation in various cancer types (438-440). Another phosphatidylcholine-derived lipid signalling molecule is phosphatidic acid, which stabilises and activates mTOR signalling on cancer cells, promoting survival (441). In this study, a progressive decrease in circulating PC levels was demonstrated with worsening therapeutic response, which may reflect enhanced catabolism of PC, and therefore the enhanced production of these secondary lipid signalling messengers, associated with poor therapy response.

Having demonstrated significant alterations in the pre-treatment circulating metabolome of rectal cancer patients according to pathological response, the metabolome of rectal cancer was further assessed in relation to clinicopathological factors. The levels of two metabolites in the intracellular metabolome of rectal cancer tissue were demonstrated to be significantly correlated with TRS. Serotonin levels were demonstrated to have a significant negative correlation with TRS. Research has proposed that serotonin may inhibit oxidative stress and DNA damage in cancer, which may support elevated serotonin levels in patients with a good response to treatment (442). In addition, supporting findings of altered PC metabolism associated with TRS in the circulating metabolome of rectal cancer, intracellular PC metabolites were also significantly correlated with clinicopathological factors, including pathological T and N stage. In addition, intracellular PC C16:1 levels displayed a significant positive correlation with TRS in rectal cancer biopsies. As mentioned, alterations in PC metabolism are frequently implicated in relation to pathogenesis and therapeutic response in cancers (443-445), supporting evidence of PC metabolites correlating with clinicopathological factors. Furthermore, significant correlations were demonstrated between intracellular amino

acid levels and BMI in rectal cancer tissue. Metabolism and obesity are intrinsically linked, with the impact of obesity on cancer metabolism having been extensively studied (446). Metabolism of branched chain amino acids, including those demonstrated to be significantly correlated with BMI in our dataset, have been associated with both obesity and cancer (447). A recent study demonstrated that BMI was associated with higher sera levels of valine, isoleucine and glutamate, and higher levels of asparagine, glutamine, glycine and serine, alongside alterations to PC metabolites (448). Furthermore, the metabolic signature of BMI was significantly associated with risk of endometrial cancer in this study (448). The branched-chain amino acid leucine has also been demonstrated to significantly correlate with obesity related cancers (449). These studies support findings of an altered metabolome correlating with BMI.

The secreted metabolome of rectal tumour biopsies was also correlated with clinicopathological data. Many amino acids which were demonstrated to significantly correlate with BMI in the intracellular metabolome, also positively correlated with BMI in the secreted metabolome of rectal cancer. For example, histidine, methionine, tryptophan and valine were demonstrated to have a significant positive correlation with BMI in both the intracellular and secreted metabolome of rectal cancer, supporting evidence of altered metabolome with BMI in cancer (448, 449). In addition, significantly correlations between PC metabolites and clinicopathological factors were demonstrated in the secreted metabolome of rectal tumour tissue. Levels of PC aa C32:3 in the secreted metabolome was demonstrated to be significantly positively correlated with TRS. A closely related diacyl PC metabolite, PC aa C32:0 has been previously demonstrated to be significantly elevated in stage IV CRC patients, when compared to Stage I, supporting the altered PC metabolism in the pathogenesis of CRC (450). Together these data support altered metabolism in therapeutic response, and pathogenesis of rectal cancer.

Transcriptomic profiling of pre-treatment rectal cancer biopsies was also performed to identify genes altered in patients with a poor response to treatment. RNA-Y expression was demonstrated to be significantly downregulated in patients with a poor therapeutic response (TRS 2), when compared to patients with a good response (TRS 0+1, or TRS 0 only). Downregulation of RNA-Y has recently been demonstrated to be significantly associated with poor prognosis in breast cancer (451). In addition, H1-3 gene was demonstrated to be significantly elevated in patient with a poor TRS, when compared to those with a good

response. H1-3 histone has been proposed to act as a prognostic biomarker in pancreatic cancer (452). DUOX2 was also demonstrated to be significantly downregulated in patients with a poor response to treatment (TRS 2), when compared to those with a complete response (TRS 0). In contrast to these findings, evidence in the literature has demonstrated overexpression of DUOX2 to be associated with 5-FU resistance in colon cancer cells (453) and doxorubicin resistance in pancreatic cancer (454). APOE expression was also demonstrated to be significantly downregulated in patients with a poor response to treatment (TRS 2), when compared to complete responders, which is in contrast to evidence in the literature, highlighting APOE upregulation as a potential prognostic and diagnostic biomarker in many cancers, including colorectal and breast cancer (455, 456). However, alterations to APOE supports alterations in lipid metabolites in rectal cancer patients with a poor prognosis demonstrated here.

IPA analysis of genes significantly altered in patients with a poor response to treatment (TRS 2), and those with a more advanced pathological T stage, also demonstrated significant alterations to metabolic pathways associated with worse prognosis. Importantly, in patients with advanced pathological T stage, oxidative phosphorylation was predicted to be significantly activated, with enhanced expression of 6 oxidative phosphorylation related genes. In addition, pathological T stage has been demonstrated to have implications on patient outcome in rectal cancer. In a recent study of over 44,000 rectal cancer patients, it was demonstrated that higher pathological T stage predicted reduced survival in rectal cancer patients having received neoCRT, independent of the pre-therapy clinical stage, demonstrating the importance of pathological T stage in rectal cancer patient outcome (457). Together, these data support findings in Chapters 2-5 of this thesis, and previous research in our laboratory, highlighting the importance of oxidative phosphorylation in therapy response and pathogenesis of rectal cancer (213).

Having demonstrated that the tumour metabolome was significantly associated with therapy response, energy metabolism in rectal cancer was further investigated. Real-time metabolic phenotyping of pre-treatment rectal cancer biopsies demonstrated that OCR, a marker of oxidative phosphorylation, was significantly higher, when compared to ECAR. These findings support *in vitro* data from Chapter 1, highlighting the importance of oxidative energy metabolism in rectal cancer. Furthermore, the real-time metabolic phenotype of non-cancer rectal tissue was also assessed, demonstrating significantly higher rates of OCR in non-cancer

rectal tissue, when compared to ECAR. In addition, OCR rates were demonstrated to be significantly elevated in non-cancer rectal tissue biopsies, when compared to rectal cancer biopsies. Importantly, no significant alterations in ECAR, a marker of glycolysis, were demonstrated between rectal cancer biopsies and non-cancer rectal tissue. These data demonstrate the importance of oxidative phosphorylation in both non-malignant and malignant rectal tissue.

To further investigate altered energy metabolism in the pathogenesis of rectal cancer, metabolomic profiling of pre-treatment rectal cancer biopsies and non-cancer rectal biopsies was assessed. Twenty-three metabolites were demonstrated to be significantly altered in rectal cancer tissue, when compared to non-cancer rectal tissue. PCs were significantly elevated in rectal cancer tissue, when compared to non-cancer tissue. PC functions not only as a structural building block to support cell proliferation, but also acts as an important source of secondary signalling molecules (436). PC levels have been demonstrated to be significantly elevated in multiple cancer types (436, 443). Intermediates of PC metabolism, including choline, glycerophosphocholine (GPC) and phosphocholine have been demonstrated to be significantly elevated in cancer (443, 458). Interestingly, the ratio of phosphocholine/GPC has been proposed as a marker of malignant transformation and tumour progression in breast and ovarian cancer (443, 444, 459). In a study conducted by Kurabe *et al*., PC (16:0/16:1) was demonstrated to be significantly elevated in CRC tissue, when compared to non-neoplastic tissue, highlighting this metabolite as a potential diagnostic biomarker of CRC (460). Decreased levels of sphingomyelin (SM) metabolites were also demonstrated in rectal cancer tissue, when compared to non-cancer rectal tissue. Hydrolysis of SM has been demonstrated in cancer cells, to contribute to elevated phosphatidylcholine generation (436). Together these data suggest extensive alterations to choline, and subsequent lipid metabolism in rectal cancer.

Serotonin and histamine, two biogenic amines, were also significantly downregulated in rectal cancer tissue, when compared to non-cancer rectal tissue. Histamine has been demonstrated to induce both pro and anti-tumour effects, depending on tumour features and type (461). One study demonstrated elevated levels of histamine in colon cancer tissue, when compared to surrounding tissue (462). However, overexpression of a histamine receptor, H4HR, and histamine exposure has been demonstrated to induce growth arrest in CRC cells (463), indicating an incomplete understanding of the role of histamine signalling in CRC.

The majority of serotonin in the body is produced in the intestine, and serotonin signalling is crucial for the maintenance of intestinal function, and proliferation of intestinal crypts (464). It has been proposed that serotonin may act as a protective factor against the development of colorectal tumours (464). Interestingly, this is supported by an observational study conducted by Coogan *et al.,* in which patients using selective serotonin reuptake inhibitor (SSRI) drugs have a reduced risk of developing CRC (465). The mechanism by which serotonin may protect against tumorigenesis is under investigation, however recent evidence suggests that serotonin may counteract oxidative stress and DNA damage (442). In contrast, studies have also demonstrated that serotonin may promote proliferation of CRC cells (466). In addition, serotonin levels have been demonstrated to be elevated in the plasma of CRC patients, when compared to healthy controls, and predicts recurrence and poor prognosis (467). These significant alterations to serotonin in rectal cancer tissue may be reflective of dysbiosis in the microbiome of patients with rectal cancer (468)

Alterations in the secreted metabolome of rectal cancer and non-cancer rectal tissue were also demonstrated, with four metabolites significantly altered in TCM and NCM. One metabolite demonstrated to be significantly increased in TCM was dopamine. In a recent paper conducted by Lee *et al*., elevated expression of the dopamine receptor D2 (DRD2), was demonstrated to be significantly associated with a poor survival rate in CRC patients (469). In addition, inhibition of this receptor *in vitro* and *in vivo* was demonstrated to inhibit CRC cell growth and motility (469). These findings support dopamine activity in CRC pathogenesis.

To further assess the secretome of rectal cancer and non-cancer rectal tissue, TCM and NCM samples were assessed by multiplex ELISA. Ten inflammatory mediators were demonstrated to be significantly altered in the secretome of rectal cancer tissue, when compared to non-cancer rectal tissue. Significant alterations to the concentration of Th-17 related cytokines were demonstrated in rectal cancer. The pro-tumourigenic role of Th-17 cells and cytokines in CRC has been extensively studied (470). A trend towards reduced IL-21 production was demonstrated in TCM, when compared to NCM, and this has been supported in the literature to have potent anti-tumour effects (471).

Angiogenesis related proteins (Flt-1, PlGF and VEGF-C) were also demonstrated to be significantly elevated in TCM, when compared to NCM. The crucial role of angiogenesis in the development and progression of CRC is well established, with an anti-VEGF treatment, bevacizumab, being a mainstay of treatment in advanced CRC (472). Previous studies have

also demonstrated that expression of PlGF gene is elevated in CRC patients, when compared to non-cancer tissues and is associated with tumour progression (473). In addition, sera PlGF levels have been demonstrated to be elevated in CRC patients, and to act as a prognostic indicator of survival and recurrence in these patients (474). In addition, CRC patients with elevated Flt-1 and PlGF expression in their tissue have been demonstrated to have a poor prognosis (475). These findings support the role of angiogenesis in rectal cancer development and progression.

The protein secretome of rectal cancer was also correlated with clinicopathological factors. These data demonstrate significant positive correlations between pathological T stage and two proteins, IL-16 and sVCAM. IL-16 levels have been demonstrated to be significantly elevated in the sera of CRC and gastric cancer patients, when compared to healthy controls, and were also significantly associated with poor prognosis and tumour recurrence in gastric cancer (476, 477). As pathological T stage is associated with worse survival and patient outcome following neoCRT treatment in rectal cancer (457), these data suggest that IL-16 may be contributing to pathogenesis and worse outcomes in rectal cancer patients. In addition, sVCAM, an adhesion molecule, was demonstrated to have a significant positive correlation with pathological T stage and TRS in the rectal cancer secretome. Previous research has demonstrated significant correlations between sera sVCAM levels and TNM stage and lymph node involvement (478). Furthermore, plasma levels of sVCAM have been demonstrated to be associated with progression in CRC (479). In addition, preoperative sVCAM levels in the sera of ovarian cancer patients has been demonstrated to be elevated in patients with early tumour progression or relapse (480). Together these data demonstrate significant correlations between the tumour secretome and the pathogenesis and therapeutic response of rectal cancer.

To further characterise the molecular alterations between rectal cancer and non-cancer rectal tissue, transcriptomic profiling was performed. While a number of previous studies have assessed the transcriptome of CRC, many of these studies utilised colon cancer tissue only, did not specify whether rectal or colon tissue was included, or use matched adjacent 'normal' tissue as a comparator (481-483). Importantly, this study utilised rectal adenocarcinoma tissue only, and compared to rectal tissue from non-cancer patients. Transcriptomic profiling revealed extensive alterations to the transcriptome of rectal cancer, when compared to non-cancer rectal tissue, with 470 genes being differentially expressed. IPA

analysis demonstrated significant alterations to cancer-related molecular pathways. In addition, alterations to carbohydrate and lipid metabolism were identified in rectal cancer tissue, supporting findings from the metabolomic profiling in this study.

Transcriptomic profiling supported alterations demonstrated by metabolome and secretome profiling of rectal cancer. Serotonin was demonstrated to be significantly elevated in rectal cancer tissue by metabolomic profiling. IPA profiling of transcriptomic data predicted significant alterations to serotonin-associated pathways. 'Serotonin receptor signalling' was demonstrated to be altered in rectal cancer tissue, with 4 related genes being significantly differentially expressed (GUCY1A1, GUCY1B1, MAOA, TPH1). In addition, 'serotonin degradation' was a canonical pathway predicted to be significantly inhibited in rectal cancer tissue, when compared to non-cancer tissue, (Z-score = -2), supporting the demonstrated increase in serotonin identified by metabolomic profiling of rectal cancer tissue. In addition, dopamine was significantly elevated in TCM, when compared to NCM. This was supported at the transcriptome level, with multiple dopamine-related genes demonstrated to be significantly altered in rectal cancer tissue. For example, the monoamine oxidase A (MAOA) gene was significantly downregulated in rectal cancer tissue. MAOA is an enzyme which degrades dopamine, and the downregulation of this gene in rectal cancer tissue may contribute to the elevated dopamine demonstrated in TCM.

Multiplex ELISA profiling of the secretome of rectal cancer and non-cancer tissue biopsies revealed significant alterations to cytokine levels in TCM, when compared to NCM. This was supported by transcriptomic profiling, which also demonstrated significant alterations to the gene expression of numerous cytokine and chemokine genes in rectal cancer, including the increased expression of CXCL-1, CXCL5, CXCL8 and CXCL-11 genes. Interestingly, while the gene expression of CXCL8 was demonstrated to be significantly elevated in rectal cancer, the secreted level of CXCL8 (IL-8) was demonstrated to be significantly reduced in TCM, when compared to NCM. IL-8 is a pro-inflammatory cytokine, which has been previously demonstrated to be significantly increased in CRC, and associated with early progression and poor response (484). It would be interesting to investigate intracellular levels of IL-8 to determine if secreted levels are reflective of the intracellular tumour environment. Multiplex profiling of the secretome also significantly altered Th-17 related cytokines. IPA analysis of transcriptomic data supported findings of altered Th-17 signalling in rectal cancer tissue, predicting activation of IL-17 related signalling. In addition,

RUNX1, a transcription factor that regulates the differentiation of Th-17 cells, was demonstrated to be significantly upregulated in rectal cancer tissue, when compared to non-cancer rectal tissue. Together these data highlight congruence between upstream transcriptomic analysis and downstream proteomic and metabolomic analysis in differentiating rectal cancer from non-cancer rectal tissue.

The significantly altered genes in rectal cancer, when compared to non-cancer rectal tissue, were subsequently correlated with clinicopathological factors. Transcriptomic profiling has been utilised to identify predictive biomarkers of therapeutic response in cancer (485-487). In a recent study conducted by Cao *et al.,* transcriptomic profiling was utilised to identify biomarkers predictive of adjuvant therapy response in CRC patients (486) Seventeen genes which were significantly upregulated, and five genes which were significantly downregulated in rectal cancer were also demonstrated to have a significant positive correlation with TRS. Two of these upregulated genes, NCL (nucleolin), and PTPN12 (protein tyrosine phosphatase non-receptor type 12) are involved in the regulation of lipid metabolism, supporting data demonstrating altered lipid metabolism in rectal cancer. Furthermore, lipid metabolism has been demonstrated to be associated with response and resistance to cancer treatment (488).

While transcriptomic profiling is utilised in the identification of biomarkers predictive of response in cancer, very few have been validated in clinical trials (487). Hierarchical clustering analysis using the top 10 genes and top 10 metabolites significantly altered in rectal cancer, when compared to non-cancer rectal tissue was utilised to identify whether these transcripts/metabolites could accurately cluster patients. While the most significantly altered metabolites permitted moderate clustering into non-cancer and cancer cohorts, clustering utilising the top ten significantly altered genes yielded poor clustering accuracy of 65%. Combining the most significant transcriptomic and metabolomic alterations however resulted in enhanced predictive clustering into non-cancer and cancer cohorts. Importantly, combining metabolic and transcriptomic data did not result in any false positive predictions of cancer in non-cancer patients. These data demonstrate the combined utility of metabolomic and transcriptomic data in the identification of the pathogenesis of rectal cancer.

In summary, this chapter demonstrated significant alterations to the metabolome of rectal cancer and identified metabolites predictive of therapeutic response in rectal cancer sera. These data also demonstrated significant correlations between the intracellular and secreted metabolome of rectal cancer and clinicopathological factors, including TRS. In

addition, significant alterations in the transcriptome of rectal cancer were demonstrated based on response to treatment (TRS) and pathological T stage. These data also highlighted significant alterations in the transcriptome, metabolome and protein secretome of rectal cancer, when compared to non-cancer rectal tissue. These data support a role for altered energy metabolism in the pathogenesis and therapeutic response of rectal cancer and supports the combined use of multi-omic platforms for identification of biomarkers in rectal cancer.

Chapter 7: Discussion and Future Directions

7.1. Discussion

CRC is the 3rd most commonly diagnosed cancer in the world, and accounts for an estimated 10% of all cancer diagnoses (1). One in three cases of CRC occur in the rectum (6). Incidence rates of rectal cancer are increasing, in particular in the younger age demographic, who often present at a later, more advanced stage (10-12, 14, 15). The standard of care for locally-advanced rectal cancer is neoCRT, followed by surgery (6). Patients with locally advanced disease typically receive 5-FU/capecitabine based chemotherapy, in combination with either SCRT (5 fractions of 5 Gy radiation) or LCRT (45-50.4 Gy total, in 15-28 fractions of 1.8 Gy radiation) prior to TME surgery (6). However, resistance to treatment is a clinical challenge in the management of rectal cancer, with only an estimated 15-30% of patients achieving a pCR following neoCRT (44-47). Importantly, pCR is associated with favourable prognosis, and improved patient outcomes in rectal cancer (44-47). There are currently no routinely used biomarkers to predict, prior to initiation of treatment, those patients who are likely to have a good response and conversely, those patients who are likely to be resistant to the standard of care.

Consequently, there is an unmet global need to identify predictive biomarkers of response to treatment to improve patient stratification, and to identify novel therapeutic targets to boost response to neoCRT for those majority of patients who are resistant to treatment. This study aimed to investigate mechanisms underpinning radioresistance in rectal cancer using both *in vitro* models and patient tissue and serum samples, to identify potential novel biomarkers predicting response to treatment and to investigate novel radiosensitising drugs to boost radiation efficacy in rectal cancer.

Clinicopathological factors do not predict the response to radiation therapy, suggesting that molecular and cellular alterations are involved in the radioresistance of rectal tumours. *In vitro* models of radioresistant rectal cancer are a key tool to investigate mechanisms underlying radioresistance, however, as there are few characterised rectal cancer cell lines available, the majority of *in vitro* rectal cancer research is performed utilising cell lines of colon cancer origin (35, 36). Not only are colon and rectal cancers anatomically distinct, but it has been demonstrated that there are differing underlying molecular and immunological phenotypes between rectal and colon cancers (32-34), highlighting the importance of utilising models derived from primary rectal cancers in future studies.

In this study, the generation of novel *in vitro* isogenic model of radioresistant colon and rectal cancer was attempted by chronic exposure of colon and rectal cancer cell lines to clinically-relevant fractionated doses of X-ray radiation. However, the three irradiation regimens utilised in this study did not result in a radioresistant phenotype in either HCT116 or SW837 cell lines. Isogenic models of radioresistance are a useful tool in examining underlying mechanisms of radioresistance, as parental and radioresistant lines are derived from the same origin, therefore eliminating genetic variability as a confounding factor in identifying mechanisms of radioresistance. However, this elimination of underlying genetic variability does not accurately portray inherent genetic aberrations between patients. For a biomarker of radioresistance to be reliable, it must emerge despite the huge variability between patients, and not only in its absence. In addition, isogenic models of radioresistance reflect acquired radioresistance, developed as a direct result of exposure to radiation. However, in the development of biomarkers predictive of patient response, resistance should be identified prior to treatment initiation. Isogenic models of acquired radioresistance therefore may not be an accurate representation of the clinical challenge, and so a model of intrinsic radioresistance would be of greater benefit in predictive biomarker identification.

Importantly, this study profiled the inherent radioresistance of 3 rectal and 1 colon cancer cell line to identify an *in vitro* model of inherently radioresistant rectal cancer (SW837 cells) and radiosensitive colon cancer (HCT116 cells). Importantly, this model reflects inherent radioresistance, which may more accurately mimic the clinical challenge in rectal cancer therapeutic resistance and permits the identification of predictive biomarkers of response.

Radioresistant SW837 cells were also demonstrated to be significantly more resistant to 5-FU treatment, when compared to radiosensitive HCT116 cells, demonstrating SW837 cells as a highly treatment resistant cell line, supporting previous findings (355, 356). This inherent model of radiosensitive/radioresistant CRC was then characterised in terms of factors often implicated in radioresistance, including proliferation, cell cycle, DNA damage induction and repair, cell death and energy metabolism to identify underlying mechanisms of radioresistance.

Radiosensitive HCT116 cells were demonstrated to have an elevated proliferative rate, when compared to radioresistant SW837 cells. These data support previous findings suggesting that enhanced proliferation is significantly associated with enhanced sensitivity to

radiation therapy in lung cancer and oral squamous cell carcinoma (357, 358), and may be a potential contributing factor to the radiosensitivity of HCT116 cells.

In addition, cell cycle distribution and progression are commonly implicated in radioresistance, with cells in the S phase being the most radioresistant, while G2/M phase cells being the most radiosensitive cell cycle phase (52). SW837 cells were demonstrated to display a more radioresistant basal cell cycle distribution, when compared to HCT116 cells, with an elevated proportion of cells in the G0/G1 and S phase, and a reduced proportion of G2/M phase cells basally. These data support previous research which demonstrated a low proportion of G2/M phase cells in SW837 cells basally (355). Furthermore, progression through the cell cycle was also demonstrated to be significantly different in SW837 cells following radiation, when compared to HCT116 cells. While extensive alterations to the cell cycle distribution of radiosensitive HCT116 cells was demonstrated following clinically-relevant doses of 1.8 Gy radiation, no significant alterations to SW837 cell cycle phase distribution was demonstrated following 1.8 Gy radiation. Furthermore, transcriptomic profiling also demonstrated significant alterations to cell cycle related genes and canonical pathways in SW837 cells, when compared to HCT116 cells. These data support previous research, highlighting cell cycle checkpoint regulation as a potential mechanism of radioresistance in rectal cancer (344). Together, these data suggest a potential role for altered cell cycle distribution and progression following radiation treatment in the radioresistance of SW837 rectal cancer cells.

Radioresistant SW837 cells also displayed enhanced repair of radiation-induced DNA damage, when compared to HCT116 cells. This was supported by transcriptomic profiling in these cells, which demonstrated altered expression of DNA repair genes, highlighting enhanced DNA damage repair capacity as a mechanism of radioresistance in this *in vitro* model of radioresistant rectal cancer. High DNA damage repair capacity has been previously demonstrated to be a feature of radioresistant cancers (361).

Importantly, both cell cycle and DNA repair require energy and are therefore functionally dependant on energy metabolism. Increasing evidence supports altered metabolism as a contributing factor underlying therapeutic resistance. To investigate this, the *in vitro* model of radiosensitive/radioresistant CRC was assessed by Seahorse™ technology. This demonstrated significantly lower levels of ECAR, a marker of glycolysis, in radioresistant cells, and an elevated OCR:ECAR ratio, indicating enhanced reliance on oxidative

phosphorylation in radioresistant cells. In addition, spare respiratory capacity was significantly elevated in SW837 cells, when compared to HCT116 cells, suggesting that radioresistant SW837 cells have an enhanced ability to respond to energetic demands. Furthermore, transcriptomic profiling and IPA analysis demonstrated significant alterations to many metabolic pathways in SW837 cells, when compared to HCT116 cells. Supporting functional experiments, oxidative phosphorylation was the most significantly activated pathway in SW837 cells, when compared to HCT116, as assessed by IPA analysis. In total, 33 oxidative phosphorylation genes were demonstrated to be significantly upregulated in SW837 cells, when compared to HCT116 cells. These data support previous studies by our department, in which elevated oxidative phosphorylation levels were demonstrated to be associated with radioresistance in oesophageal adenocarcinoma (212, 213, 392) and suggest a common role for altered energy metabolism in the response of gastrointestinal cancers to radiation. Together these data support a potential role of altered tumour energy metabolism in radioresistance of rectal cancer.

Data in chapter 2 identified potential mechanisms underpinning radioresistance in rectal cancer, and highlighted the importance of combining transcriptomic and functional analyses. Data from functional assays was supported by transcriptomic analysis. As transcriptomic technology is becoming more widespread and accessible, these data support the use of transcriptomic analysis in the identification of novel biomarkers, and for the validation of functional *in vitro* assays.

Having characterised the *in vitro* model of inherently radiosensitive or radioresistant CRC and identified potential mechanisms of radioresistance, this model was subsequently assessed under hypoxic conditions (0.5% O_2) in Chapter 3. Hypoxia is not only a common feature of solid malignancies but is also a major contributing factor to tumour radioresistance (231, 363, 364), and therefore, it was important to validate this *in vitro* model in conditions that mimic the *in vivo* tumour microenvironment.

Hypoxia was demonstrated to enhance the radioresistance of radiosensitive HCT116 cells and importantly, SW837 cells remained significantly more resistant to radiation treatment under hypoxia, when compared to HCT116, demonstrating the robustness of this model of inherent radioresistance/radiosensitivity. These data are supported by the literature, demonstrating enhanced clonogenic survival in HCT116 cells, when irradiated under hypoxic conditions (489).

HCT116 and SW837 cells were also characterised in terms of hallmarks of radioresistance, under hypoxic conditions. Hypoxia induced significant cell death in radiosensitive HCT116 cells, and not in SW837 cells, suggesting that SW837 cells are more resilient to hypoxia exposure, which is potentially due in part to the elevated spare respiratory capacity demonstrated in these cells in Chapter 2. In addition, hypoxia altered the basal cell cycle distribution and progression following radiation exposure in both HCT116 and SW837 cells and may contribute to the enhanced radioresistance demonstrated in both cell lines under hypoxic conditions. In HCT116 cells, the increased proportion of S phase cells in hypoxia, when compared to normoxia, is supported by the literature as being a potential mechanism of enhanced radioresistance (376, 379). Furthermore, radiation-induced DNA damage was demonstrated to be efficiently and rapidly repaired under hypoxia in both HCT116 and SW837 cells. Hypoxia has previously been demonstrated to be associated with enhanced DNA damage repair pathways, including HRR and NHEJ, and enhanced resolution of DNA damage, supporting these data (376, 380-382).

The metabolism of HCT116 and SW837 cells was also demonstrated to be significantly altered under hypoxic conditions, with significantly inhibited OCR rates, and a shift in OCR:ECAR, supporting elevated glycolysis under hypoxia. In addition, hypoxic exposure was demonstrated to induce mitochondrial dysfunction in these cell lines. These data are supported by previous studies, which demonstrate that a metabolic shift under hypoxia from oxidative phosphorylation, which is limited by low oxygen availability, to enhanced glycolysis, which is HIF1-α regulated, occurs in cells under hypoxic conditions (226, 371). In addition, it has been demonstrated that under hypoxia, mitochondrial biogenesis and growth occurs, and is proposed to act as a mechanism to prime cells to resist cell death and induce radioresistance (373-376).

Having demonstrated that this model of radioresistant and radiosensitive CRC is robust under both normoxic and hypoxic conditions and that energy metabolism is associated with radioresistance in this model, the impact of targeting metabolism on radiosensitivity was assessed in chapter 4.

P3 is a small molecule inhibitor drug, which has been demonstrated to display anti-angiogenic and anti-metabolic effects in oesophageal adenocarcinoma *in vitro* and *ex vivo* (212). Importantly, P3 has also been demonstrated to inhibit oxidative phosphorylation, the metabolic pathway associated with radioresistance in this cancer type, and glycolysis both *in*

vitro and *ex vivo* in oesophageal cancer (212, 392). In chapter 4, P3 treatment was demonstrated to significantly inhibit both OCR and ECAR in radioresistant SW837 cells and alter mitochondrial function. However, P3 treatment, at any dose examined, did not significantly sensitise HCT116 or SW837 cells to clinically-relevant doses of radiation, under normoxic or hypoxic conditions. One potential explanation for this is that the molecular target and mechanism underlying P3-mediated radiosensitisation is not currently known. As P3 displayed similar anti-metabolic effects in CRC cells as it did in oesophageal cancer cells, but did not radiosensitise CRC cells, it is possible that the molecular target of P3 that results in P3-mediated radiosensitisation of oesophageal cancer cells may not be expressed in HCT116 or SW837 cells.

To further investigate the potential of metabolic inhibitors as radiosensitising drugs in rectal cancer, the clinically-approved drug metformin was investigated. Metformin is used in the management of diabetes, but in recent years has been associated with enhanced therapeutic response in various cancer types (231, 300-302, 305). In addition, metformin is a demonstrated inhibitor of complex I of the electron transport chain, and subsequently inhibits oxidative phosphorylation (279, 386). Metformin treatment was demonstrated to significantly inhibit oxidative phosphorylation under both normoxic and hypoxic conditions in both HCT116 and SW837 cells. In addition, metformin treatment was demonstrated to increase glycolysis rates in both cell lines, potentially as a compensatory mechanism. Furthermore, metformin treatment was demonstrated to significantly induce mitochondrial dysfunction, by increasing mitochondrial mass, mitochondrial membrane potential and ROS production, which are supported by previous studies in many cancers, including CRC, lung, prostate, endometrial cancer (396-400). In addition, enhancing mitochondrial targeting of metformin, through the development of novel metformin analogues, including mito-metformin$_{10}$, has been demonstrated to enhance metformin-mediated inhibition of mitochondrial respiration, and enhance radiosensitivity in models of prostate cancer (490). This demonstrates the importance of metformin targeted inhibition of mitochondrial respiration in its radiosensitising capacity.

Importantly, metformin treatment was demonstrated to significantly sensitise both HCT116 and SW837 cells to clinically relevant doses of 1.8 Gy radiation. Metformin-induced radiosensitisation of HCT116 cells is supported by previous studies (232, 305, 404), however, this study is the first to demonstrate metformin-mediated radiosensitisation in radioresistant

SW837 cells. Importantly, metformin-mediated radiosensitisation was demonstrated to be superior to that induced by clinical standard radiosensitiser 5-FU.

The precise mechanisms of action of metformin are largely unknown, but are believed to be centrally mediated through its effects on energy metabolism (275). Chapter 5 investigated the potential underlying mechanisms of metformin-induced radiosensitivity in this *in vitro* model of radiosensitive and radioresistant CRC. Metformin treatment was demonstrated to significantly alter both basal cell cycle distribution, and cell cycle progression following radiation in HCT116 and SW837 cells. Importantly, metformin treatment was demonstrated to significantly decrease the proportion of cells in the G2/M phase, and overcome radiation-induced G2/M blockade. This reduction in the proportion of G2/M phase cells in HCT116 cells following Metformin treatment has been supported by previous studies (491). Elimination of the G2/M blockade induced by radiation has been proposed as an effective strategy to overcome radioresistance (97, 407), which suggests that this may contribute to the metformin-mediated radiosensitisation demonstrated in these cells. Furthermore, transcriptomic profiling of SW837 cells treated with metformin demonstrated altered expression of cell cycle related genes following metformin treatment, supporting functional studies.

In addition, metformin treatment was demonstrated to impair radiation-induced DNA damage repair in HCT116 cells. Transcriptomic analysis also confirmed inhibition of DNA-damage repair pathways in metformin treated SW837 cells, which supports previous studies investigating metformin treatment in other cancer types, including nasopharyngeal and pancreatic cancer (306, 307). In addition, metformin treatment was also demonstrated to induce oxidative stress in HCT116 and SW837 cells, with an imbalance of ROS production and antioxidant capacity demonstrated. Together, these data suggest that metformin-induced radiosensitisation in this *in vitro* CRC model may be mediated by alterations in cell cycle, DNA damage repair, and oxidative stress.

Importantly, these mechanisms of radioresistance are intrinsically linked with metabolism and metabolic flux. Having demonstrated that oxidative phosphorylation was significantly inhibited in metformin treated SW837 and HCT116 cells and given that transcriptomic data also supported inhibition of oxidative phosphorylation in metformin treated SW837 cells, the impact of metformin on the metabolic phenotype of rectal cancer tissue biopsies was investigated.

While 2D cell line *in vitro* models have great utility in basic cancer research, they do not reflect the tumour microenvironment. Tumour explant models offer a number of advantages in cancer research as they more accurately mimic the 3D architecture and diverse tumour microenvironment, which contains tumour, stromal and immune cells. Importantly, these cancer and stromal cells form a diverse signalling network and crosstalk, which has implications for the development, progression and therapeutic response of cancer (416). Importantly, these *ex vivo* explant models are also a more accurate representation of inherent patient variability, when compared to cell lines, and thus are an important research model in biomarker development and drug discovery.

Supporting *in vitro* data, metformin was demonstrated to significantly inhibit OCR, a marker of oxidative phosphorylation, in fresh rectal cancer biopsies. In addition, metformin treatment was demonstrated to significantly inhibit ECAR, a marker of glycolysis in rectal cancer tissue biopsies. Furthermore, metformin significantly altered the protein secretome of rectal cancer tissue biopsies, with significant alterations to 7 proteins, five of which were cytokines, demonstrated. These data support recent findings in the literature, proposing metformin as an immune modulator in ovarian cancer, in which metformin promoted an immunoreactive microenvironment (492). Furthermore, the importance of the immunomodulatory effects of metformin in the context of its radiosensitising effects were recently demonstrated in a study by Tojo *et al.* (493). This study demonstrated, in a murine model of LARC, that metformin treatment enhanced not only local effects of radiation therapy, but also induced abscopal effects (493). Interestingly, this enhanced effect of radiation by combination metformin treatment was mediated through the activation of immune cells, namely enhanced T cells and NK cell activation (493). Our research demonstrated that metformin treatment in rectal cancer tissue induced increased secretion of IL-15, a known mediator of CD8+ T cell and NK cell activation (419, 420), supporting this potential mechanism of metformin-mediated immune cell activation.

An important factor to consider in the development of radiosensitising drugs is the therapeutic index. The ultimate aim of an effective radiosensitiser is to enhance tumour radiosensitivity, while sparing normal tissue (418). Therefore, it is important to assess the radiosensitising effects of any novel radiosensitising drugs on non-cancer normal cells. However, there is limited availability of non-cancer rectal cell lines. The effects of metformin on the radiosensitivity of CRL-1831 cells, which are non-malignant 'normal' embryonic cells

and are reported in the literature as being of either 'colon' or 'rectal' origin was investigated using the gold standard clonogenic assay. However, no colonies formed, despite optimisation of conditions and therefore the effects of metformin on the radiosensitivity of these 'normal' cells could not be assessed. A recent study conducted by Warkad *et al.* demonstrated that while metformin treatment significantly induced DNA damage, cell death and ROS production in an *in vitro* model of pancreatic cancer, minimal effects on normal human primary dermal fibroblasts were demonstrated (399). This study indicates that the anti-cancer effects of metformin may spare normal cells.

As a proxy to 'normal' cell lines, the effect of metformin on rectal tissue biopsies, from patients who did not have cancer was investigated. While metabolic inhibition was demonstrated in rectal cancer biopsies following metformin treatment, no significant alteration in the real-time metabolic phenotype of non-cancer rectal tissue biopsies was demonstrated. In addition, the secretome of non-cancer rectal tissue biopsies demonstrated significant alterations to only three inflammatory proteins, in comparison to the 7 proteins altered in the rectal cancer secretome following metformin treatment. These data suggest that metformin has differential effects on energy metabolism and the inflammatory secretome of normal non-cancer rectal tissue and rectal cancer tissue, further supporting its potential utility as a radiosensitiser in rectal cancer.

Having demonstrated that altered metabolism is associated with radioresistance in rectal cancer *in vitro*, and that targeting metabolism using metformin can enhance radiosensitivity, the role of altered metabolism in the therapeutic response of rectal cancer patients was assessed by multi-omic profiling of blood and tumour biopsy samples. Metabolomic profiling of pre-treatment sera from rectal cancer patients identified 16 metabolites which were significantly associated with subsequent pathological TRS. These metabolites were primarily PCs, which have been previously demonstrated to be significantly associated with tumourigenesis and therapeutic resistance in many cancer types (435, 436). In a study conducted by Jia *et al.*, a panel of 15 metabolic markers, which included three PCs, were identified as predictive of response to neoCRT in the sera of rectal cancer patients, supporting their potential as predictive biomarkers in rectal cancer (424).

Correlation analysis of the intracellular and secreted metabolome of rectal cancer was also performed on a second independent cohort of rectal cancer patient samples. Although limited by sample size, these data demonstrated significant correlations between metabolites

and clinical parameters in rectal cancer, including those related to therapeutic response (TRS, pathological N stage, pathological T stage). Previous research has supported the capacity of metabolomic profiling to characterise CRC according to different clinicopathological features (494). These findings support previous research demonstrating the identification of metabolites significantly associated with therapy response in rectal cancer (324, 423). Although further validation of these metabolomic alterations is required in an independent cohort to further assess their utility as biomarkers, these data support the potential use of metabolomic profiling for the identification of biomarkers. Importantly, an advantage to this study is the profiling of the intracellular, secreted and circulating metabolome of rectal cancer, to comprehensively assess tumour metabolism. However, traditional metabolomic profiling methodologies, including LC-MS are not easily accessible in the clinic, limiting the applicability of metabolomic derived biomarkers. To counteract this, promising novel metabolomic profiling methods, which are more user friendly, and therefore easier to integrate into the clinic, are currently in development (495, 496).

To further investigate the role of altered metabolism in rectal cancer, real-time metabolic phenotyping of fresh *ex vivo* rectal cancer biopsies and non-cancer rectal biopsies was investigated. These data demonstrated a significant dependence on oxidative phosphorylation in both rectal cancer and non-cancer rectal tissue, supporting previous findings in our department in oesophageal adenocarcinoma (392). This is the first time in which real-time metabolic phenotyping has been performed on both rectal cancer tissue and non-cancer tissue. Importantly, these data highlight the complexity of tumour metabolism, and suggest that the traditional viewpoint of the Warburg effect being a predominant feature of cancer tissue may not accurately reflect tumour metabolism. In addition, these data again highlight the importance of oxidative phosphorylation in cancer metabolism (178).

It is important to understand metabolism of non-cancer tissue in addition to cancer tissue, to interrogate altered metabolism in rectal cancer pathogenesis, and also to investigate the impact targeting metabolism in the tumour may have in normal tissue. Therefore, the metabolome of pre-treatment rectal cancer and non-cancer rectal cancer tissue was profiled. Twenty-three metabolites were demonstrated to be significantly altered between cancer and non-cancer tissue. In addition, the secreted levels of four metabolites were demonstrated to be significantly altered in cancer, when compared to non-cancer. Again, elevation of PC levels in cancer tissue was demonstrated, which is supported in a number of cancer types (436, 443).

A recent study profiling the tissue metabolome of CRC tissue, when compared to that of normal adjacent mucosa demonstrated lipid metabolism as being associated with tumour development and progression in CRC (494). Profiling of the secreted metabolome of rectal cancer and non-cancer rectal tissue also demonstrated 4 metabolites significantly altered in rectal cancer. Together these data suggest an important role of altered metabolism in the pathogenesis of rectal cancer.

In addition, the inflammatory secretome of rectal cancer demonstrated significant alterations to inflammatory mediators, Th-17 related cytokines, and angiogenic factors, when compared to non-cancer tissue. Th-17 cells have been demonstrated to be significantly associated with tumourigenesis in CRC studies (470). To further characterise the inflammatory secretome in rectal cancer, secreted protein levels were correlated with clinicopathological factors. Two proteins, sVCAM and IL-16 were demonstrated to be significantly associated with response to therapy (TRS). Each of these proteins have been previously demonstrated to be significantly associated with poor prognosis in cancer (476, 477, 479, 480). Together, these data demonstrate significant alterations to the protein secretome associated with rectal cancer pathogenesis and therapeutic response.

Transcriptomic profiling of non-cancer rectal tissue and rectal cancer tissue demonstrated 470 genes that were significantly altered in rectal cancer. IPA analysis supported many of the metabolomic and inflammatory findings from previous studies. Serotonin was demonstrated to be significantly downregulated in the metabolome of rectal cancer, when compared to non-cancer tissue. Transcriptomic analysis also identified alterations to serotonin degradation and signalling pathways in rectal cancer tissue, supporting the combined use of omic platforms. While the use of single-omic methods is commonly utilised in biomarker research, very few biomarkers have been reliably identified using these approaches (331). By combining upstream and downstream omic platforms, a more comprehensive and dynamic understanding of the biology of disease can be obtained (331, 497). Indeed, the combined use of multi-omic methodology have identified reliable biomarkers of disease in cancer (497), highlighting the importance of combined omic profiling in the identification and development of cancer biomarkers.

Importantly, genes associated with metabolic pathways, including carbohydrate metabolism and lipid metabolism were demonstrated to be significantly altered in the transcriptome of rectal cancer, when compared to non-cancer rectal tissue. Furthermore,

correlation analysis of significantly altered genes in rectal cancer, when compared to non-cancer rectal tissue demonstrated significant correlations with clinicopathological factors, including TRS. Importantly, two genes involved in lipid metabolism regulation were demonstrated to significantly correlate with TRS in rectal cancer. These findings further highlight the importance of altered metabolism in rectal cancer.

This study importantly utilised non-cancer rectal biopsy explant models. The majority of research comparing cancer tissue to non-cancer tissue includes the use of normal adjacent tissue. However, growing evidence demonstrates that normal adjacent tissue is not in fact normal, but actually may represent an intermediate state between healthy and cancer tissue (498). Normal adjacent tissue has been demonstrated to display an inflammatory response to the tumour, and is therefore not an accurate 'healthy' control (498).

Together this thesis demonstrates that altered energy metabolism is a major factor in both the development and therapeutic response of rectal cancer, highlighting the potential role of metabolic markers as both diagnostic and predictive biomarkers of treatment response in rectal cancer. Importantly, while the identification of predictive biomarkers will improve patient stratification, there are no alternative treatments available for those patients predicted to be resistant to the standard of care. Therefore, it is crucial that a two-armed theranostic approach is utilised, in order to boost response in patients predicted to have a poor response to existing treatment. The potential utility of metformin, as a novel anti-metabolic radiosensitiser in rectal cancer is also demonstrated for the first time, with alterations to cell cycle, DNA damage repair, and oxidative stress demonstrated as potential mechanisms underlying metformin-mediated radiosensitisation in rectal cancer.

7.2. Future directions

The results of this thesis have highlighted a number of further research directions.

1. We have profiled the transcriptome and metabolome of rectal cancer and non-cancer tissue. Further interrogation of this multi-omic data generated from assessing rectal cancer and non-cancer tissue is required to identify an integrated multi-omic metabolic diagnostic signature. This multi-omic signature may have superior diagnostic ability to that obtained using a single omic method alone. In addition, combining the upstream transcriptomic data with downstream metabolomic data will provide more information on the precise metabolic pathways altered in rectal cancer. Through a collaboration with the Amber Centre, TCD, we will perform this analysis combining the data obtained from both metabolomic and transcriptomic analyses with their biostatistical support and expertise. In addition, these data will need to be validated in independent cohorts.
2. Furthermore, multiple analyses of the metabolome, transcriptome and secretome of both rectal cancer and non-cancer rectal samples have been performed in this study. However, due to the prospective manner of patient sample collection employed throughout this study, only a limited number of matched samples were assessed by multiple analytical approaches. We therefore aim to increase the power of the matched samples assessed. Assessing the intracellular, secreted and circulating metabolome of matched samples from rectal cancer patients, and non-cancer patients, would permit a more comprehensive understanding of the precise metabolic alterations in rectal cancer, when compared to non-cancer. The Lower GI Biobank, established through this study in the Dept. of Surgery, is continuing patient recruitment and sample collection of both rectal cancer and non-cancer samples, which will aid increasing the power of matched samples available for further analysis.
3. Due to the prospective collection method of rectal cancer patient samples, the number of patients receiving neoCRT, and given a subsequent TRS was limited. Further investigation of the metabolome and transcriptome in relation to therapy response in a larger patient cohort is warranted. In addition, the 16 metabolites identified in pre-treatment patient sera as being predictive of patient response will be validated in independent multi-centred cohorts of rectal cancer patients, which are currently being collected.

4. Having identified metabolites involved in the pathogenesis and therapeutic response of rectal cancer patient samples, it would be interesting to mechanistically interrogate these metabolic pathways to further elucidate their role in radioresponse. For example, utilising inhibitors/activators of PC metabolism *in vitro*, to investigate the impact on cellular radioresponse.
5. Further investigation of the therapeutic index of metformin is required. While the effects of metformin treatment on the metabolic phenotype and secretome of non-cancer rectal tissue was assessed, further examination of the effects of metformin treatment on the radiosensitivity of normal rectal tissue should be determined.
6. Having identified various potential mechanisms of metformin-mediated radiosensitisation in this study using *in vitro* models, it would be necessary to validate these findings using other methodologies. A limitation to this study is the small number of methodologies utilised to assess each potential mechanism. For example, this study utilised only annexin-V/PI flow cytometry to measure apoptosis. To strengthen these data, other methodologies, such as western blot and caspase assays should be investigated.
7. Further investigation of the safety and efficacy of metformin as a radiosensitising drug in rectal cancer *in vivo* (using animal models) is required.
8. Having demonstrated metformin induced alterations to the inflammatory secretome of both rectal cancer and non-cancer rectal tissue, it would be important to assess the impact of metformin treatment on immune cells, to ensure that metformin treatment does not promote pro-tumour immunity. Furthermore, given recent evidence in the literature highlighting the radiosensitising effects of metformin being partially mediated through its impact on effector CD8+ T cells and NK cells, these cells could be assessed in rectal cancer tissue treated with metformin.
9. To further investigate altered metabolism in rectal cancer, the use of Carbon-13 metabolic flux analysis would be of great benefit. This method is a powerful tool, allowing for the identification and tracking of specific alterations to metabolic pathways in cancer cells, and would be of great benefit to further elucidate the specific metabolic pathways activated in rectal cancer. Furthermore, this method would be of interest to further investigate how metformin treatment alters metabolic flux in rectal cancer.

10. In addition, the Lower GI Biobank in the Dept. of Surgery has recently initiated the collection of post-treatment surgical specimens from rectal cancer patients. These samples are an invaluable resource, which will allow for further assessment of metabolic alterations in rectal cancer, but also assessment of the predictive biomarker panel identified in this study.

8. Bibliography

1. Sung H, Ferlay J, Siegel RL, Laversanne M, Soerjomataram I, Jemal A, et al. Global Cancer Statistics 2020: GLOBOCAN Estimates of Incidence and Mortality Worldwide for 36 Cancers in 185 Countries. 2021;71(3):209-49.

2. National Cancer Registry Ireland. Cancer in Ireland 1994-2018 with estimates for 2018-2020: Annual report of the National Cancer Registry. NCRI, Cork, Ireland. 2020.

3. Arnold M, Sierra MS, Laversanne M, Soerjomataram I, Jemal A, Bray F. Global patterns and trends in colorectal cancer incidence and mortality. Gut. 2017;66(4):683-91.

4. Xi Y, Xu P. Global colorectal cancer burden in 2020 and projections to 2040. Translational oncology. 2021;14(10):101174-.

5. World Health Organisation. International Classification of Diseases for Oncology. Third Edition. First Revision. 2013.

6. Glynne-Jones R, Wyrwicz L, Tiret E, Brown G, Rödel C, Cervantes A, et al. Rectal cancer: ESMO Clinical Practice Guidelines for diagnosis, treatment and follow-up. Ann Oncol. 2017;28(suppl_4):iv22-iv40.

7. National Cancer Registry Ireland (NCRI). Cancer Incidence Projections for Ireland 2020-2045. National Cancer Registry, Cork, Ireland. 2019.

8. Favoriti P, Carbone G, Greco M, Pirozzi F, Pirozzi RE, Corcione F. Worldwide burden of colorectal cancer: a review. Updates Surg. 2016;68(1):7-11.

9. Levin TR, Corley DA, Jensen CD, Schottinger JE, Quinn VP, Zauber AG, et al. Effects of Organized Colorectal Cancer Screening on Cancer Incidence and Mortality in a Large Community-Based Population. Gastroenterology. 2018;155(5):1383-91.e5.

10. Araghi M, Soerjomataram I, Bardot A, Ferlay J, Cabasag CJ, Morrison DS, et al. Changes in colorectal cancer incidence in seven high-income countries: a population-based study. Lancet Gastroenterol Hepatol. 2019;4(7):511-8.

11. Vuik FE, Nieuwenburg SA, Bardou M, Lansdorp-Vogelaar I, Dinis-Ribeiro M, Bento MJ, et al. Increasing incidence of colorectal cancer in young adults in Europe over the last 25 years. Gut. 2019;68(10):1820-6.

12. Ullah MF, Fleming CA, Mealy K. Changing trends in age and stage of colorectal cancer presentation in Ireland - From the nineties to noughties and beyond. Surgeon. 2018;16(6):350-4.

13. Saad El Din K, Loree JM, Sayre EC, Gill S, Brown CJ, Dau H, et al. Trends in the epidemiology of young-onset colorectal cancer: a worldwide systematic review. BMC cancer. 2020;20(1):288.

14. Campos FG. Colorectal cancer in young adults: A difficult challenge. World J Gastroenterol. 2017;23(28):5041-4.

15. Chou CL, Chang SC, Lin TC, Chen WS, Jiang JK, Wang HS, et al. Differences in clinicopathological characteristics of colorectal cancer between younger and elderly patients: an analysis of 322 patients from a single institution. American journal of surgery. 2011;202(5):574-82.

16. Al-Barrak J, Gill S. Presentation and outcomes of patients aged 30 years and younger with colorectal cancer: a 20-year retrospective review. Med Oncol. 2011;28(4):1058-61.

17. Fancher TT, Palesty JA, Rashidi L, Dudrick SJ. Is gender related to the stage of colorectal cancer at initial presentation in young patients? J Surg Res. 2011;165(1):15-8.

18. Siegel RL, Fedewa SA, Anderson WF, Miller KD, Ma J, Rosenberg PS, et al. Colorectal Cancer Incidence Patterns in the United States, 1974-2013. J Natl Cancer Inst. 2017;109(8).

19. Nguyen HT, Duong HQ. The molecular characteristics of colorectal cancer: Implications for diagnosis and therapy (Review). Oncol Lett. 2018;16(1):9-18.

20. Amersi F, Agustin M, Ko CY. Colorectal cancer: epidemiology, risk factors, and health services. Clinics in colon and rectal surgery. 2005;18(3):133-40.

21. Nguyen LH, Goel A, Chung DC. Pathways of Colorectal Carcinogenesis. Gastroenterology. 2020;158(2):291-302.

22. Sievers CK, Grady WM, Halberg RB, Pickhardt PJ. New insights into the earliest stages of colorectal tumorigenesis. Expert review of gastroenterology & hepatology. 2017;11(8):723-9.

23. Sottoriva A, Kang H, Ma Z, Graham TA, Salomon MP, Zhao J, et al. A Big Bang model of human colorectal tumor growth. Nat Genet. 2015;47(3):209-16.

24. Lynch HT, Smyrk T. Hereditary nonpolyposis colorectal cancer (Lynch syndrome). An updated review. Cancer. 1996;78(6):1149-67.

25. Aleksandrova K, Pischon T, Jenab M, Bueno-de-Mesquita HB, Fedirko V, Norat T, et al. Combined impact of healthy lifestyle factors on colorectal cancer: a large European cohort study. BMC Medicine. 2014;12(1):168.

26. O'Donoghue D, Sheahan K, MacMathuna P, Stephens RB, Fenlon H, Morrin M, et al. A National Bowel Cancer Screening Programme using FIT: Achievements and Challenges. Cancer Prev Res. 2019;12(2):89-94.

27. Simon K. Colorectal cancer development and advances in screening. Clin Interv Aging. 2016;11:967-76.

28. Vital signs: colorectal cancer screening test use--United States, 2012. MMWR Morbidity and mortality weekly report. 2013;62(44):881-8.

29. National Cancer Registry Ireland. Cancer in Irelant 1994-2017 with estimates for 2017-2019: Annual report of the national cancer registry 2019. National Cancer Registry Ireland, Cork, Ireland. . 2019.

30. Department of Health, Ireland. Diagnosis, staging and treatment of patients with rectal cancer. National Clinical Guidelines No. 25. 2020.

31. Brierley J.D GMK, Wittekind C. Union for International Cancer Control. TNM Classification of Malignant Tumours. 8th Edition. . 2016.

32. Lee GH, Malietzis G, Askari A, Bernardo D, Al-Hassi HO, Clark SK. Is right-sided colon cancer different to left-sided colorectal cancer? - a systematic review. Eur J Surg Oncol. 2015;41(3):300-8.

33. Stintzing S, Tejpar S, Gibbs P, Thiebach L, Lenz HJ. Understanding the role of primary tumour localisation in colorectal cancer treatment and outcomes. Eur J Cancer. 2017;84:69-80.

34. Yang SY, Cho MS, Kim NK. Difference between right-sided and left-sided colorectal cancers: from embryology to molecular subtype. Expert review of anticancer therapy. 2018;18(4):351-8.

35. Ganesh K, Wu C, O'Rourke KP, Adileh M, Szeglin BC, Wasserman I, et al. A rectal cancer model establishes a platform to study individual responses to chemoradiation. 2019:640193.

36. Janakiraman H, Zhu Y, Becker SA, Wang C, Cross A, Curl E, et al. Modeling rectal cancer to advance neoadjuvant precision therapy. 2020;147(5):1405-18.

37. Guinney J, Dienstmann R, Wang X, de Reyniès A, Schlicker A, Soneson C, et al. The consensus molecular subtypes of colorectal cancer. Nature medicine. 2015;21(11):1350-6.

38. Paschke S, Jafarov S, Staib L, Kreuser E-D, Maulbecker-Armstrong C, Roitman M, et al. Are Colon and Rectal Cancer Two Different Tumor Entities? A Proposal to Abandon the Term Colorectal Cancer. International journal of molecular sciences. 2018;19(9):2577.

39. Slattery ML, Curtin K, Wolff RK, Boucher KM, Sweeney C, Edwards S, et al. A comparison of colon and rectal somatic DNA alterations. Dis Colon Rectum. 2009;52(7):1304-11.

40. Kapiteijn E, Liefers GJ, Los LC, Klein Kranenbarg E, Hermans J, Tollenaar RAEM, et al. Mechanisms of oncogenesis in colon versus rectal cancer. 2001;195(2):171-8.

41. Li M, Li JY, Zhao AL, Gu J. Colorectal cancer or colon and rectal cancer? Clinicopathological comparison between colonic and rectal carcinomas. Oncology. 2007;73(1-2):52-7.

42. Riihimäki M, Hemminki A, Sundquist J, Hemminki K. Patterns of metastasis in colon and rectal cancer. Scientific Reports. 2016;6(1):29765.

43. Ryan R, Gibbons D, Hyland JM, Treanor D, White A, Mulcahy HE, et al. Pathological response following long-course neoadjuvant chemoradiotherapy for locally advanced rectal cancer. Histopathology. 2005;47(2):141-6.

44. Ferrari L, Fichera A. Neoadjuvant chemoradiation therapy and pathological complete response in rectal cancer. Gastroenterol Rep (Oxf). 2015;3(4):277-88.

45. Park IJ, You YN, Agarwal A, Skibber JM, Rodriguez-Bigas MA, Eng C, et al. Neoadjuvant treatment response as an early response indicator for patients with rectal cancer. J Clin Oncol. 2012;30(15):1770-6.

46. Glimelius B. Neo-adjuvant radiotherapy in rectal cancer. World J Gastroenterol. 2013;19(46):8489-501.

47. Janjan NA, Khoo VS, Abbruzzese J, Pazdur R, Dubrow R, Cleary KR, et al. Tumor downstaging and sphincter preservation with preoperative chemoradiation in locally advanced rectal cancer: the M. D. Anderson Cancer Center experience. Int J Radiat Oncol Biol Phys. 1999;44(5):1027-38.

48. Liu S, Jiang T, Xiao L, Yang S, Liu Q, Gao Y, et al. Total Neoadjuvant Therapy (TNT) versus Standard Neoadjuvant Chemoradiotherapy for Locally Advanced Rectal Cancer: A Systematic Review and Meta-Analysis. Oncologist. 2021;26(9):e1555-e66.

49. Baskar R, Lee KA, Yeo R, Yeoh K-W. Cancer and radiation therapy: current advances and future directions. International journal of medical sciences. 2012;9(3):193-9.

50. Withers HR. The Four R's of Radiotherapy. In: Lett JT, Adler H, editors. Advances in Radiation Biology. 5: Elsevier; 1975. p. 241-71.

51. Sinclair WK, Morton RA. X-RAY AND ULTRAVIOLET SENSITIVITY OF SYNCHRONIZED CHINESE HAMSTER CELLS AT VARIOUS STAGES OF THE CELL CYCLE. Biophysical journal. 1965;5(1):1-25.

52. Sinclair WK, Morton RA. X-Ray Sensitivity during the Cell Generation Cycle of Cultured Chinese Hamster Cells. Radiation Research. 1966;29(3):450-74.

53. Yang J, Yue JB, Liu J, Yu JM. Repopulation of tumor cells during fractionated radiotherapy and detection methods (Review). Oncol Lett. 2014;7(6):1755-60.

54. Wang K, Tepper JE. Radiation therapy-associated toxicity: Etiology, management, and prevention.n/a(n/a).

55. Habr-Gama A, Lynn PB, Jorge JM, São Julião GP, Proscurshim I, Gama-Rodrigues J, et al. Impact of Organ-Preserving Strategies on Anorectal Function in Patients with Distal Rectal Cancer Following Neoadjuvant Chemoradiation. Dis Colon Rectum. 2016;59(4):264-9.

56. Quezada-Diaz FF, Smith JJ, Jimenez-Rodriguez RM, Wasserman I, Pappou EP, Patil S, et al. Patient-Reported Bowel Function in Patients With Rectal Cancer Managed by a Watch-and-Wait Strategy After Neoadjuvant Therapy: A Case-Control Study. Dis Colon Rectum. 2020;63(7):897-902.

57. Radford IR. The Level of Induced DNA Double-strand Breakage Correlates with Cell Killing after X-irradiation. International Journal of Radiation Biology and Related Studies in Physics, Chemistry and Medicine. 1985;48(1):45-54.

58. Desouky O, Ding N, Zhou G. Targeted and non-targeted effects of ionizing radiation. Journal of Radiation Research and Applied Sciences. 2015;8(2):247-54.

59. Meyn RE, Stephens C, Milas L. Programmed cell death and radioresistance. Cancer and Metastasis Reviews. 1996;15(1):119-31.

60. Sia J, Szmyd R, Hau E, Gee HE. Molecular Mechanisms of Radiation-Induced Cancer Cell Death: A Primer. 2020;8(41).

61. Longley DB, Harkin DP, Johnston PG. 5-Fluorouracil: mechanisms of action and clinical strategies. Nat Rev Cancer. 2003;3(5):330-8.

62. Rich TA, Shepard RC, Mosley ST. Four Decades of Continuing Innovation With Fluorouracil: Current and Future Approaches to Fluorouracil Chemoradiation Therapy. 2004;22(11):2214-32.

63. Lawrence TS, Blackstock AW, McGinn C. The mechanism of action of radiosensitization of conventional chemotherapeutic agents. Semin Radiat Oncol. 2003;13(1):13-21.

64. Lee BJ, Chon KM, Kim YS, An WG, Roh HJ, Goh EK, et al. Effects of cisplatin, 5-fluorouracil, and radiation on cell cycle regulation and apoptosis in the hypopharyngeal carcinoma cell line. Chemotherapy. 2005;51(2-3):103-10.

65. Ojima E, Inoue Y, Watanabe H, Hiro J, Toiyama Y, Miki C, et al. The optimal schedule for 5-fluorouracil radiosensitization in colon cancer cell lines. Oncology reports. 2006;16(5):1085-91.

66. Pawlik TM, Keyomarsi K. Role of cell cycle in mediating sensitivity to radiotherapy. Int J Radiat Oncol Biol Phys. 2004;59(4):928-42.

67. Biau J, Chautard E, Verrelle P, Dutreix M. Altering DNA Repair to Improve Radiation Therapy: Specific and Multiple Pathway Targeting. 2019;9(1009).

68. Sharda N, Yang C-R, Kinsella T, Boothman D. Radiation Resistance. In: Bertino JR, editor. Encyclopedia of Cancer (Second Edition). New York: Academic Press; 2002. p. 1-11.

69. Krokan HE, Bjørås M. Base excision repair. Cold Spring Harbor perspectives in biology. 2013;5(4):a012583.

70. Begg K, Tavassoli M. Inside the hypoxic tumour: reprogramming of the DDR and radioresistance. Cell Death Discovery. 2020;6(1):77.

71. Vens C, Begg AC. Targeting Base Excision Repair as a Sensitization Strategy in Radiotherapy. Seminars in Radiation Oncology. 2010;20(4):241-9.

72. Kim J-S, Kim J-M, Liang ZL, Jang JY, Kim S, Huh GJ, et al. Prognostic Significance of Human Apurinic/Apyrimidinic Endonuclease (APE/Ref-1) Expression in Rectal Cancer Treated With Preoperative Radiochemotherapy. International Journal of Radiation Oncology, Biology, Physics. 2012;82(1):130-7.

73. Huang MY, Huang JJ, Huang CM, Lin CH, Tsai HL, Huang CW, et al. Relationship Between Expression of Proteins ERCC1, ERCC2, and XRCC1 and Clinical Outcomes in Patients with Rectal Cancer Treated with FOLFOX-Based Preoperative Chemoradiotherapy. World journal of surgery. 2017;41(11):2884-97.

74. Czito BG, Deming DA, Jameson GS, Mulcahy MF, Vaghefi H, Dudley MW, et al. Safety and tolerability of veliparib combined with capecitabine plus radiotherapy in patients with locally advanced rectal cancer: a phase 1b study. Lancet Gastroenterol Hepatol. 2017;2(6):418-26.

75. Glynne-Jones R, Hall M. PARP inhibitors and chemoradiation for rectal cancer. Lancet Gastroenterol Hepatol. 2017;2(6):389-90.

76. George TJ, Yothers G, Hong TS, Russell MM, You YN, Parker W, et al. NRG-GI002: A phase II clinical trial platform using total neoadjuvant therapy (TNT) in locally advanced rectal cancer (LARC)—First experimental arm (EA) initial results. 2019;37(15_suppl):3505-.

77. Pannunzio NR, Watanabe G, Lieber MR. Nonhomologous DNA end-joining for repair of DNA double-strand breaks. Journal of Biological Chemistry. 2018;293(27):10512-23.

78. Sishc BJ, Davis AJ. The Role of the Core Non-Homologous End Joining Factors in Carcinogenesis and Cancer. Cancers. 2017;9(7):81.

79. Schaue D, McBride WH. Counteracting tumor radioresistance by targeting DNA repair. 2005;4(10):1548-50.

80. Komuro Y, Watanabe T, Hosoi Y, Matsumoto Y, Nakagawa K, Tsuno N, et al. The expression pattern of Ku correlates with tumor radiosensitivity and disease free survival in patients with rectal carcinoma. Cancer. 2002;95(6):1199-205.

81. Shintani S, Mihara M, Li C, Nakahara Y, Hino S, Nakashiro K, et al. Up-regulation of DNA-dependent protein kinase correlates with radiation resistance in oral squamous cell carcinoma. Cancer Sci. 2003;94(10):894-900.

82. Yang L, Yang X, Tang Y, Zhang D, Zhu L, Wang S, et al. Inhibition of DNA-PK activity sensitizes A549 cells to X-ray irradiation by inducing the ATM-dependent DNA damage response. Mol Med Rep. 2018;17(6):7545-52.

83. Li Y, Li H, Peng W, He XY, Huang M, Qiu D, et al. DNA-dependent protein kinase catalytic subunit inhibitor reverses acquired radioresistance in lung adenocarcinoma by suppressing DNA repair. Mol Med Rep. 2015;12(1):1328-34.

84. Wen Y, Dai G, Wang L, Fu K, Zuo S. Silencing of XRCC4 increases radiosensitivity of triple-negative breast cancer cells. Biosci Rep. 2019;39(3):BSR20180893.

85. Wright WD, Shah SS, Heyer W-D. Homologous recombination and the repair of DNA double-strand breaks. Journal of Biological Chemistry. 2018;293(27):10524-35.

86. Balbous A, Cortes U, Guilloteau K, Rivet P, Pinel B, Duchesne M, et al. A radiosensitizing effect of RAD51 inhibition in glioblastoma stem-like cells. BMC cancer. 2016;16(1):604.

87. Xu K, Song X, Chen Z, Qin C, He Y, Zhan W. XRCC2 promotes colorectal cancer cell growth, regulates cell cycle progression, and apoptosis. Medicine (Baltimore). 2014;93(28):e294.

88. Xu K, Song X, Chen Z, Qin C, He Y. XRCC2 rs3218536 polymorphism decreases the sensitivity of colorectal cancer cells to poly(ADP-ribose) polymerase 1 inhibitor. Oncol Lett. 2014;8(3):1222-8.

89. Qin C-J, Song X-M, Chen Z-H, Ren X-Q, Xu K-W, Jing H, et al. XRCC2 as a predictive biomarker for radioresistance in locally advanced rectal cancer patients undergoing preoperative radiotherapy. Oncotarget. 2015;6(31):32193-204.

90. Barnum KJ, O'Connell MJ. Cell cycle regulation by checkpoints. Methods in molecular biology (Clifton, NJ). 2014;1170:29-40.

91. Hartwell LH, Kastan MB. Cell cycle control and cancer. Science. 1994;266(5192):1821-8.

92. Iliakis G, Wang Y, Guan J, Wang H. DNA damage checkpoint control in cells exposed to ionizing radiation. Oncogene. 2003;22(37):5834-47.

93. Hickman ES, Moroni MC, Helin K. The role of p53 and pRB in apoptosis and cancer. Curr Opin Genet Dev. 2002;12(1):60-6.

94. Dillon MT, Good JS, Harrington KJ. Selective targeting of the G2/M cell cycle checkpoint to improve the therapeutic index of radiotherapy. Clinical oncology (Royal College of Radiologists (Great Britain)). 2014;26(5):257-65.

95. Xu B, Kim S-T, Lim D-S, Kastan MB. Two Molecularly Distinct G₂/M Checkpoints Are Induced by Ionizing Irradiation. 2002;22(4):1049-59.

96. Strunz AM, Peschke P, Waldeck W, Ehemann V, Kissel M, Debus J. Preferential radiosensitization in p53-mutated human tumour cell lines by pentoxifylline-mediated disruption of the G2/M checkpoint control. International Journal of Radiation Biology. 2002;78(8):721-32.

97. Anastasov N, Höfig I, Vasconcellos IG, Rappl K, Braselmann H, Ludyga N, et al. Radiation resistance due to high expression of miR-21 and G2/M checkpoint arrest in breast cancer cells. Radiation Oncology. 2012;7(1):206.

98. Qiu Z, Oleinick NL, Zhang J. ATR/CHK1 inhibitors and cancer therapy. Radiotherapy and oncology : journal of the European Society for Therapeutic Radiology and Oncology. 2018;126(3):450-64.

99. Lin S, Shen Z, Yang Y, Qiu Y, Wang Y, Wang X. Expression profiles of radio-resistant genes in colorectal cancer cells. Radiation Medicine and Protection. 2021;2(2):48-54.

100. Lee J, Kwon J, Kim D, Park M, Kim K, Bae I, et al. Gene Expression Profiles Associated with Radio-Responsiveness in Locally Advanced Rectal Cancer. Biology. 2021;10(6).

101. Xiao C, Wang Y, Zheng M, Chen J, Song G, Zhou Z, et al. RBBP6 increases radioresistance and serves as a therapeutic target for preoperative radiotherapy in colorectal cancer. Cancer Sci. 2018;109(4):1075-87.

102. Wang Q, Sun Z, Du L, Xu C, Wang Y, Yang B, et al. Melatonin Sensitizes Human Colorectal Cancer Cells to γ-ray Ionizing Radiation In Vitro and In Vivo. Int J Mol Sci. 2018;19(12).

103. Carter R, Westhorpe A, Romero MJ, Habtemariam A, Gallevo CR, Bark Y, et al. Radiosensitisation of human colorectal cancer cells by ruthenium(II) arene anticancer complexes. Sci Rep. 2016;6:20596.

104. Vakifahmetoglu H, Olsson M, Zhivotovsky B. Death through a tragedy: mitotic catastrophe. Cell Death & Differentiation. 2008;15(7):1153-62.

105. Kuwahara Y, Tomita K, Urushihara Y, Sato T, Kurimasa A, Fukumoto M. Association between radiation-induced cell death and clinically relevant radioresistance. Histochemistry and cell biology. 2018;150(6):649-59.

106. Elmore S. Apoptosis: a review of programmed cell death. Toxicol Pathol. 2007;35(4):495-516.

107. Bao Q, Shi Y. Apoptosome: a platform for the activation of initiator caspases. Cell Death & Differentiation. 2007;14(1):56-65.

108. Cory S, Adams JM. The Bcl2 family: regulators of the cellular life-or-death switch. Nat Rev Cancer. 2002;2(9):647-56.

109. Hsu H, Xiong J, Goeddel DV. The TNF receptor 1-associated protein TRADD signals cell death and NF-kappa B activation. Cell. 1995;81(4):495-504.

110. Wajant H. The Fas signaling pathway: more than a paradigm. Science. 2002;296(5573):1635-6.

111. Kischkel FC, Hellbardt S, Behrmann I, Germer M, Pawlita M, Krammer PH, et al. Cytotoxicity-dependent APO-1 (Fas/CD95)-associated proteins form a death-inducing signaling complex (DISC) with the receptor. The EMBO journal. 1995;14(22):5579-88.

112. Meyn RE, Stephens LC, Milas L. Programmed cell death and radioresistance. Cancer Metastasis Rev. 1996;15(1):119-31.

113. Ramesh P, Medema JP. BCL-2 family deregulation in colorectal cancer: potential for BH3 mimetics in therapy. Apoptosis. 2020;25(5-6):305-20.

114. Scopa CD, Vagianos C, Kardamakis D, Kourelis TG, Kalofonos HP, Tsamandas AC. bcl-2/bax ratio as a predictive marker for therapeutic response to radiotherapy in patients with rectal cancer. Applied immunohistochemistry & molecular morphology : AIMM. 2001;9(4):329-34.

115. Chang HJ, Jung KH, Kim DY, Jeong SY, Choi HS, Kim YH, et al. Bax, a predictive marker for therapeutic response to preoperative chemoradiotherapy in patients with rectal carcinoma. Human pathology. 2005;36(4):364-71.

116. Geng L, Wang J. Molecular effectors of radiation resistance in colorectal cancer. 2017;1(1):27-33.

117. Rödel F, Hoffmann J, Distel L, Herrmann M, Noisternig T, Papadopoulos T, et al. Survivin as a radioresistance factor, and prognostic and therapeutic target for radiotherapy in rectal cancer. Cancer Res. 2005;65(11):4881-7.

118. Moussata D, Amara S, Siddeek B, Decaussin M, Hehlgans S, Paul-Bellon R, et al. XIAP as a Radioresistance Factor and Prognostic Marker for Radiotherapy in Human Rectal Adenocarcinoma. The American Journal of Pathology. 2012;181(4):1271-8.

119. Flanagan L, Kehoe J, Fay J, Bacon O, Lindner AU, Kay EW, et al. High levels of X-linked Inhibitor-of-Apoptosis Protein (XIAP) are indicative of radio chemotherapy resistance in rectal cancer. Radiation Oncology. 2015;10(1):131.

120. Huerta S, Gao X, Livingston EH, Kapur P, Sun H, Anthony T. In vitro and in vivo radiosensitization of colorectal cancer HT-29 cells by the smac mimetic JP-1201. Surgery. 2010;148(2):346-53.

121. Liang Q-l, Li Z-y, Chen G-q, Lai Z-n, Wang B-r, Huang J. Prognostic value of serum soluble Fas in patients with locally advanced unresectable rectal cancer receiving concurrent chemoradiotherapy. J Zhejiang Univ Sci B. 2010;11(12):912-7.

122. Asaduzzaman Khan M, Tania M, Zhang D-z, Chen H-c. Antioxidant enzymes and cancer. Chinese Journal of Cancer Research. 2010;22(2):87-92.

123. Lee HC, Kim DW, Jung KY, Park IC, Park MJ, Kim MS, et al. Increased expression of antioxidant enzymes in radioresistant variant from U251 human glioblastoma cell line. International journal of molecular medicine. 2004;13(6):883-7.

124. Qu Y, Zhang H, Zhao S, Hong J, Tang C. The effect on radioresistance of manganese superoxide dismutase in nasopharyngeal carcinoma. Oncology reports. 2010;23(4):1005-11.

125. Kalen AL, Sarsour EH, Venkataraman S, Goswami PC. Mn-Superoxide Dismutase Overexpression Enhances G2 Accumulation and Radioresistance in Human Oral Squamous Carcinoma Cells. Antioxidants & Redox Signaling. 2006;8(7-8):1273-81.

126. Du J, Carroll RS, Steers GJ, Wagner BA, O'Leary BR, Jensen CS, et al. Catalase Modulates the Radio-Sensitization of Pancreatic Cancer Cells by Pharmacological Ascorbate. Antioxidants (Basel, Switzerland). 2021;10(4).

127. Epperly MW, Melendez JA, Zhang X, Nie S, Pearce L, Peterson J, et al. Mitochondrial Targeting of a Catalase Transgene Product by Plasmid Liposomes Increases Radioresistance in vitro and in Vivo. Radiation Research. 2009;171(5):588-95.

128. Pizzorno J. Glutathione! Integr Med (Encinitas). 2014;13(1):8-12.

129. Ketterer B, Coles B, Meyer DJ. The role of glutathione in detoxication. Environ Health Perspect. 1983;49:59-69.

130. Wang H, Wang L, Zhang H, Deng P, Chen J, Zhou B, et al. (1)H NMR-based metabolic profiling of human rectal cancer tissue. Molecular cancer. 2013;12(1):121.

131. Moreno A, Arús C. Quantitative and Qualitative Characterization of 1H NMR Spectra of Colon Tumors, Normal Mucosa and their Perchloric Acid Extracts: Decreased Levels of Myo-inositol in Tumours can be Detected in Intact Biopsies. NMR in Biomedicine. 1996;9(1):33-45.

132. Barranco SC, Perry RR, Durm ME, Quraishi M, Werner AL, Gregorcyk SG, et al. Relationship between colorectal cancer glutathione levels and patient survival: early results. Dis Colon Rectum. 2000;43(8):1133-40.

133. Miura M, Sasaki T. Role of glutathione in the intrinsic radioresistance of cell lines from a mouse squamous cell carcinoma. Radiat Res. 1991;126(2):229-36.

134. Gamcsik MP, Kasibhatla MS, Teeter SD, Colvin OM. Glutathione levels in human tumors. Biomarkers : biochemical indicators of exposure, response, and susceptibility to chemicals. 2012;17(8):671-91.

135. Seiwert TY, Salama JK, Vokes EE. The concurrent chemoradiation paradigm--general principles. Nat Clin Pract Oncol. 2007;4(2):86-100.

136. Greijer AE, van der Wall E. The role of hypoxia inducible factor 1 (HIF-1) in hypoxia induced apoptosis. J Clin Pathol. 2004;57(10):1009-14.

137. Ioannou M, Paraskeva E, Baxevanidou K, Simos G, Papamichali R, Papacharalambous C, et al. HIF-1alpha in colorectal carcinoma: review of the literature. J BUON. 2015;20(3):680-9.

138. Simiantonaki N, Taxeidis M, Jayasinghe C, Kurzik-Dumke U, Kirkpatrick CJ. Hypoxia-inducible factor 1 alpha expression increases during colorectal carcinogenesis and tumor progression. BMC cancer. 2008;8:320.

139. Greijer AE, Delis-van Diemen PM, Fijneman RJ, Giles RH, Voest EE, van Hinsbergh VW, et al. Presence of HIF-1 and related genes in normal mucosa, adenomas and carcinomas of the colorectum. Virchows Arch. 2008;452(5):535-44.

140. Jiang YA, Fan LF, Jiang CQ, Zhang YY, Luo HS, Tang ZJ, et al. Expression and significance of PTEN, hypoxia-inducible factor-1 alpha in colorectal adenoma and adenocarcinoma. World J Gastroenterol. 2003;9(3):491-4.

141. Krishnamachary B, Berg-Dixon S, Kelly B, Agani F, Feldser D, Ferreira G, et al. Regulation of colon carcinoma cell invasion by hypoxia-inducible factor 1. Cancer Res. 2003;63(5):1138-43.

142. Baltaziak M, Wincewicz A, Kanczuga-Koda L, Lotowska JM, Koda M, Sulkowska U, et al. The relationships between hypoxia-dependent markers: HIF-1alpha, EPO and EPOR in colorectal cancer. Folia Histochem Cytobiol. 2013;51(4):320-5.

143. Baba Y, Nosho K, Shima K, Irahara N, Chan AT, Meyerhardt JA, et al. HIF1A overexpression is associated with poor prognosis in a cohort of 731 colorectal cancers. Am J Pathol. 2010;176(5):2292-301.

144. Fan LF, Dong WG, Jiang CQ, Qian Q, Yu QF. Role of Hypoxia-inducible factor-1 alpha and Survivin in colorectal carcinoma progression. Int J Colorectal Dis. 2008;23(11):1057-64.

145. Griffiths EA, Pritchard SA, Valentine HR, Whitchelo N, Bishop PW, Ebert MP, et al. Hypoxia-inducible factor-1alpha expression in the gastric carcinogenesis sequence and its prognostic role in gastric and gastro-oesophageal adenocarcinomas. British journal of cancer. 2007;96(1):95-103.

146. Wang JS, Jing CQ, Shan KS, Chen YZ, Guo XB, Cao ZX, et al. Semaphorin 4D and hypoxia-inducible factor-1alpha overexpression is related to prognosis in colorectal carcinoma. World J Gastroenterol. 2015;21(7):2191-8.

147. Kimura S, Kitadai Y, Tanaka S, Kuwai T, Hihara J, Yoshida K, et al. Expression of hypoxia-inducible factor (HIF)-1alpha is associated with vascular endothelial growth factor expression and tumour angiogenesis in human oesophageal squamous cell carcinoma. Eur J Cancer. 2004;40(12):1904-12.

148. Kurokawa T, Miyamoto M, Kato K, Cho Y, Kawarada Y, Hida Y, et al. Overexpression of hypoxia-inducible-factor 1alpha(HIF-1alpha) in oesophageal squamous cell carcinoma correlates with lymph node metastasis and pathologic stage. British journal of cancer. 2003;89(6):1042-7.

149. Shioya M, Takahashi T, Ishikawa H, Sakurai H, Ebara T, Suzuki Y, et al. Expression of hypoxia-inducible factor 1alpha predicts clinical outcome after preoperative hyperthermo-chemoradiotherapy for locally advanced rectal cancer. J Radiat Res. 2011;52(6):821-7.

150. Nardinocchi L, Puca R, Sacchi A, D'Orazi G. Inhibition of HIF-1alpha activity by homeodomain-interacting protein kinase-2 correlates with sensitization of chemoresistant cells to undergo apoptosis. Molecular cancer. 2009;8:1.

151. Barker HE, Paget JT, Khan AA, Harrington KJ. The tumour microenvironment after radiotherapy: mechanisms of resistance and recurrence. Nat Rev Cancer. 2015;15(7):409-25.

152. Hanahan D, Weinberg RA. Hallmarks of cancer: the next generation. Cell. 2011;144(5):646-74.

153. Hanahan D, Weinberg RA. The hallmarks of cancer. Cell. 2000;100(1):57-70.

154. DeBerardinis RJ, Chandel NS. Fundamentals of cancer metabolism. Sci Adv. 2016;2(5):e1600200.

155. Hirschey MD, DeBerardinis RJ, Diehl AME, Drew JE, Frezza C, Green MF, et al. Dysregulated metabolism contributes to oncogenesis. Semin Cancer Biol. 2015;35 Suppl:S129-S50.

156. Pavlova NN, Thompson CB. The Emerging Hallmarks of Cancer Metabolism. Cell Metab. 2016;23(1):27-47.

157. Tennant DA, Duran RV, Boulahbel H, Gottlieb E. Metabolic transformation in cancer. Carcinogenesis. 2009;30(8):1269-80.

158. Cairns RA, Harris I, McCracken S, Mak TW. Cancer cell metabolism. Cold Spring Harb Symp Quant Biol. 2011;76:299-311.

159. Warburg O. On the origin of cancer cells. Science. 1956;123(3191):309-14.

160. Warburg O. On respiratory impairment in cancer cells. Science. 1956;124(3215):269-70.

161. Hagland HR, Berg M, Jolma IW, Carlsen A, Soreide K. Molecular pathways and cellular metabolism in colorectal cancer. Dig Surg. 2013;30(1):12-25.

162. Mason EF, Rathmell JC. Cell metabolism: an essential link between cell growth and apoptosis. Biochim Biophys Acta. 2011;1813(4):645-54.

163. Qiu Y, Cai G, Su M, Chen T, Zheng X, Xu Y, et al. Serum metabolite profiling of human colorectal cancer using GC-TOFMS and UPLC-QTOFMS. J Proteome Res. 2009;8(10):4844-50.

164. Chae YK, Kang WY, Kim SH, Joo JE, Han JK, Hong BW. Combining Information of Common Metabolites Reveals Global Differences between Colorectal Cancerous and Normal Tissues. B Korean Chem Soc. 2010;31(2):379-83.

165. Piotto M, Moussallieh FM, Dillmann B, Imperiale A, Neuville A, Brigand C, et al. Metabolic characterization of primary human colorectal cancers using high resolution magic angle spinning H-1 magnetic resonance spectroscopy. Metabolomics. 2009;5(3):292-301.

166. Righi V, Durante C, Cocchi M, Calabrese C, Di Febo G, Lecce F, et al. Discrimination of Healthy and Neoplastic Human Colon Tissues by ex Vivo HR-MAS NMR Spectroscopy and Chemometric Analyses. Journal of Proteome Research. 2009;8(4):1859-69.

167. Tessem MB, Selnaes KM, Sjursen W, Trano G, Giskeodegard GF, Bathen TF, et al. Discrimination of patients with microsatellite instability colon cancer using 1H HR MAS MR spectroscopy and chemometric analysis. J Proteome Res. 2010;9(7):3664-70.

168. Zhang X, Xu L, Shen J, Cao B, Cheng T, Zhao T, et al. Metabolic signatures of esophageal cancer: NMR-based metabolomics and UHPLC-based focused metabolomics of blood serum. Biochimica et Biophysica Acta (BBA) - Molecular Basis of Disease. 2013;1832(8):1207-16.

169. Zhang J, Liu L, Wei S, Nagana Gowda GA, Hammoud Z, Kesler KA, et al. Metabolomics study of esophageal adenocarcinoma. J Thorac Cardiovasc Surg. 2011;141(2):469-75, 75 e1-4.

170. Zhang J, Bowers J, Liu L, Wei S, Gowda GA, Hammoud Z, et al. Esophageal cancer metabolite biomarkers detected by LC-MS and NMR methods. PLoS One. 2012;7(1):e30181.

171. Mun CW, Cho JY, Shin WJ, Choi KS, Eun CK, Cha SS, et al. Ex vivo proton MR spectroscopy (1H-MRS) for evaluation of human gastric carcinoma. Magn Reson Imaging. 2004;22(6):861-70.

172. Cai Z, Zhao JS, Li JJ, Peng DN, Wang XY, Chen TL, et al. A combined proteomics and metabolomics profiling of gastric cardia cancer reveals characteristic dysregulations in glucose metabolism. Mol Cell Proteomics. 2010;9(12):2617-28.

173. Faubert B, Solmonson A, DeBerardinis RJ. Metabolic reprogramming and cancer progression. Science. 2020;368(6487).

174. Graziano F, Ruzzo A, Giacomini E, Ricciardi T, Aprile G, Loupakis F, et al. Glycolysis gene expression analysis and selective metabolic advantage in the clinical progression of colorectal cancer. The pharmacogenomics journal. 2017;17(3):258-64.

175. Sciacovelli M, Frezza C. Metabolic reprogramming and epithelial-to-mesenchymal transition in cancer. The FEBS journal. 2017;284(19):3132-44.

176. Sun Y, Daemen A, Hatzivassiliou G, Arnott D, Wilson C, Zhuang G, et al. Metabolic and transcriptional profiling reveals pyruvate dehydrogenase kinase 4 as a mediator of epithelial-mesenchymal transition and drug resistance in tumor cells. Cancer & Metabolism. 2014;2:20.

177. Tang L, Wei F, Wu Y, He Y, Shi L, Xiong F, et al. Role of metabolism in cancer cell radioresistance and radiosensitization methods. Journal of Experimental & Clinical Cancer Research. 2018;37(1):87.

178. Sica V, Bravo-San Pedro JM, Stoll G, Kroemer G. Oxidative phosphorylation as a potential therapeutic target for cancer therapy. Int J Cancer. 2020;146(1):10-7.

179. Sandulache VC, Chen Y, Feng L, William WN, Skinner HD, Myers JN, et al. Metabolic interrogation as a tool to optimize chemotherapeutic regimens. Oncotarget. 2017;8(11):18154-65.

180. Obrist F, Michels J, Durand S, Chery A, Pol J, Levesque S, et al. Metabolic vulnerability of cisplatin-resistant cancers. The EMBO journal. 2018;37(14).

181. Morandi A, Indraccolo S. Linking metabolic reprogramming to therapy resistance in cancer. Biochimica et Biophysica Acta (BBA) - Reviews on Cancer. 2017;1868(1):1-6.

182. Bhattacharya B, Low SH, Soh C, Kamal Mustapa N, Beloueche-Babari M, Koh KX, et al. Increased drug resistance is associated with reduced glucose levels and an enhanced glycolysis phenotype. Br J Pharmacol. 2014;171(13):3255-67.

183. Shukla SK, Purohit V, Mehla K, Gunda V, Chaika NV, Vernucci E, et al. MUC1 and HIF-1alpha Signaling Crosstalk Induces Anabolic Glucose Metabolism to Impart Gemcitabine Resistance to Pancreatic Cancer. Cancer Cell. 2017;32(1):71-87.e7.

184. Mungo E, Bergandi L, Salaroglio IC, Doublier S. Pyruvate Treatment Restores the Effectiveness of Chemotherapeutic Agents in Human Colon Adenocarcinoma and Pleural Mesothelioma Cells. Int J Mol Sci. 2018;19(11).

185. Zhao Z-X, Lu L-W, Qiu J, Li Q-P, Xu F, Liu B-J, et al. Glucose transporter-1 as an independent prognostic marker for cancer: a meta-analysis. Oncotarget. 2017;9(2):2728-38.

186. Brophy S, Sheehan KM, McNamara DA, Deasy J, Bouchier-Hayes DJ, Kay EW. GLUT-1 expression and response to chemoradiotherapy in rectal cancer. Int J Cancer. 2009;125(12):2778-82.

187. Korkeila E, Jaakkola PM, Syrjanen K, Pyrhonen S, Sundstrom J. Pronounced tumour regression after radiotherapy is associated with negative/weak glucose transporter-1 expression in rectal cancer. Anticancer Res. 2011;31(1):311-5.

188. Saigusa S, Toiyama Y, Tanaka K, Okugawa Y, Fujikawa H, Matsushita K, et al. Prognostic significance of glucose transporter-1 (GLUT1) gene expression in rectal cancer after preoperative chemoradiotherapy. Surgery today. 2012;42(5):460-9.

189. Sawayama H, Ogata Y, Ishimoto T, Mima K, Hiyoshi Y, Iwatsuki M, et al. Glucose transporter 1 regulates the proliferation and cisplatin sensitivity of esophageal cancer. Cancer science. 2019;110(5):1705-14.

190. Chiba I, Ogawa K, Morioka T, Shimoji H, Sunagawa N, Iraha S, et al. Clinical significance of GLUT-1 expression in patients with esophageal cancer treated with concurrent chemoradiotherapy. Oncology letters. 2011;2(1):21-8.

191. Tozzi F, Zhou Y, Chen J, Bose D, Fan F, Wang J, et al. Evaluation of glycolytic activity and HIF-1α expression in chemoresistant colorectal cancer cells. Journal of Clinical Oncology. 2011;29(4_suppl):415-.

192. Shi T, Ma Y, Cao L, Zhan S, Xu Y, Fu F, et al. B7-H3 promotes aerobic glycolysis and chemoresistance in colorectal cancer cells by regulating HK2. Cell death & disease. 2019;10(4):308-.

193. Jiang JX, Gao S, Pan YZ, Yu C, Sun CY. Overexpression of microRNA-125b sensitizes human hepatocellular carcinoma cells to 5-fluorouracil through inhibition of glycolysis by targeting hexokinase II. Mol Med Rep. 2014;10(2):995-1002.

194. Guo C, Li G, Hou J, Deng X, Ao S, Li Z, et al. Tumor pyruvate kinase M2: A promising molecular target of gastrointestinal cancer. Chinese journal of cancer research = Chung-kuo yen cheng yen chiu. 2018;30(6):669-76.

195. Taniguchi K, Sakai M, Sugito N, Kuranaga Y, Kumazaki M, Shinohara H, et al. PKM1 is involved in resistance to anti-cancer drugs. Biochem Biophys Res Commun. 2016;473(1):174-80.

196. Denise C, Paoli P, Calvani M, Taddei ML, Giannoni E, Kopetz S, et al. 5-fluorouracil resistant colon cancer cells are addicted to OXPHOS to survive and enhance stem-like traits. Oncotarget. 2015;6(39):41706-21.

197. Okazaki M, Fushida S, Tsukada T, Kinoshita J, Oyama K, Miyashita T, et al. The effect of HIF-1alpha and PKM1 expression on acquisition of chemoresistance. Cancer management and research. 2018;10:1865-74.

198. Kim DJ, Park YS, Kang MG, You YM, Jung Y, Koo H, et al. Pyruvate kinase isoenzyme M2 is a therapeutic target of gemcitabine-resistant pancreatic cancer cells. Exp Cell Res. 2015;336(1):119-29.

199. He J, Xie G, Tong J, Peng Y, Huang H, Li J, et al. Overexpression of microRNA-122 re-sensitizes 5-FU-resistant colon cancer cells to 5-FU through the inhibition of PKM2 in vitro and in vivo. Cell biochemistry and biophysics. 2014;70(2):1343-50.

200. Fukuda S, Miyata H, Miyazaki Y, Makino T, Takahashi T, Kurokawa Y, et al. Pyruvate Kinase M2 Modulates Esophageal Squamous Cell Carcinoma Chemotherapy Response by Regulating the Pentose Phosphate Pathway. Annals of Surgical Oncology. 2015;22(3):1461-8.

201. Yoo BC, Ku JL, Hong SH, Shin YK, Park SY, Kim HK, et al. Decreased pyruvate kinase M2 activity linked to cisplatin resistance in human gastric carcinoma cell lines. Int J Cancer. 2004;108(4):532-9.

202. Pan C, Wang X, Shi K, Zheng Y, Li J, Chen Y, et al. MiR-122 Reverses the Doxorubicin-Resistance in Hepatocellular Carcinoma Cells through Regulating the Tumor Metabolism. PLoS One. 2016;11(5):e0152090.

203. Yu M, Chen S, Hong W, Gu Y, Huang B, Lin Y, et al. Prognostic role of glycolysis for cancer outcome: evidence from 86 studies. J Cancer Res Clin Oncol. 2019;145(4):967-99.

204. Lee HC, Yin PH, Lin JC, Wu CC, Chen CY, Wu CW, et al. Mitochondrial genome instability and mtDNA depletion in human cancers. Ann N Y Acad Sci. 2005;1042:109-22.

205. Feng S, Xiong L, Ji Z, Cheng W, Yang H. Correlation between increased copy number of mitochondrial DNA and clinicopathological stage in colorectal cancer. Oncol Lett. 2011;2(5):899-903.

206. Guerra F, Arbini AA, Moro L. Mitochondria and cancer chemoresistance. Biochim Biophys Acta Bioenerg. 2017;1858(8):686-99.

207. Cui H, Huang P, Wang Z, Zhang Y, Zhang Z, Xu W, et al. Association of decreased mitochondrial DNA content with the progression of colorectal cancer. BMC cancer. 2013;13:110.

208. Bol V, Bol A, Bouzin C, Labar D, Lee JA, Janssens G, et al. Reprogramming of tumor metabolism by targeting mitochondria improves tumor response to irradiation. Acta Oncol. 2015;54(2):266-74.

209. Mizutani S, Miyato Y, Shidara Y, Asoh S, Tokunaga A, Tajiri T, et al. Mutations in the mitochondrial genome confer resistance of cancer cells to anticancer drugs. Cancer Sci. 2009;100(9):1680-7.

210. Guaragnella N, Giannattasio S, Moro L. Mitochondrial dysfunction in cancer chemoresistance. Biochem Pharmacol. 2014;92(1):62-72.

211. Fulda S, Galluzzi L, Kroemer G. Targeting mitochondria for cancer therapy. Nat Rev Drug Discov. 2010;9(6):447-64.

212. Buckley AM, Dunne MR, Lynam-Lennon N, Kennedy SA, Cannon A, Reynolds AL, et al. Pyrazinib (P3), [(E)-2-(2-Pyrazin-2-yl-vinyl)-phenol], a small molecule pyrazine compound enhances radiosensitivity in oesophageal adenocarcinoma. Cancer Lett. 2019.

213. Lynam-Lennon N, Maher SG, Maguire A, Phelan J, Muldoon C, Reynolds JV, et al. Altered mitochondrial function and energy metabolism is associated with a radioresistant phenotype in oesophageal adenocarcinoma. PLoS One. 2014;9(6):e100738.

214. Lu CL, Qin L, Liu HC, Candas D, Fan M, Li JJ. Tumor cells switch to mitochondrial oxidative phosphorylation under radiation via mTOR-mediated hexokinase II inhibition--a Warburg-reversing effect. PLoS One. 2015;10(3):e0121046.

215. Rao M, Gao C, Guo M, Law BYK, Xu Y. Effects of metformin treatment on radiotherapy efficacy in patients with cancer and diabetes: a systematic review and meta-analysis. Cancer management and research. 2018;10:4881-90.

216. Samsuri NAB, Leech M, Marignol L. Metformin and improved treatment outcomes in radiation therapy – A review. Cancer Treatment Reviews. 2017;55:150-62.

217. Lin A, Maity A. Molecular Pathways: A Novel Approach to Targeting Hypoxia and Improving Radiotherapy Efficacy via Reduction in Oxygen Demand. Clinical cancer research : an official journal of the American Association for Cancer Research. 2015;21(9):1995-2000.

218. Mortezaee K, Shabeeb D, Musa AE, Najafi M, Farhood B. Metformin as a Radiation Modifier; Implications to Normal Tissue Protection and Tumor Sensitization. Curr Clin Pharmacol. 2019;14(1):41-53.

219. Buckley AM, Bibby BA, Dunne MR, Kennedy SA, Davern MB, Kennedy BN, et al. Characterisation of an Isogenic Model of Cisplatin Resistance in Oesophageal Adenocarcinoma Cells. Pharmaceuticals (Basel, Switzerland). 2019;12(1).

220. Aichler M, Elsner M, Ludyga N, Feuchtinger A, Zangen V, Maier SK, et al. Clinical response to chemotherapy in oesophageal adenocarcinoma patients is linked to defects in mitochondria. J Pathol. 2013;230(4):410-9.

221. Alistar A, Morris BB, Desnoyer R, Klepin HD, Hosseinzadeh K, Clark C, et al. Safety and tolerability of the first-in-class agent CPI-613 in combination with modified FOLFIRINOX in patients with metastatic pancreatic cancer: a single-centre, open-label, dose-escalation, phase 1 trial. Lancet Oncol. 2017;18(6):770-8.

222. Vaziri-Gohar A, Zarei M, Brody JR, Winter JM. Metabolic Dependencies in Pancreatic Cancer. 2018;8(617).

223. Semenza GL. HIF-1: upstream and downstream of cancer metabolism. Curr Opin Genet Dev. 2010;20(1):51-6.

224. Semenza GL. HIF-1 mediates metabolic responses to intratumoral hypoxia and oncogenic mutations. J Clin Invest. 2013;123(9):3664-71.

225. Meijer TW, Kaanders JH, Span PN, Bussink J. Targeting hypoxia, HIF-1, and tumor glucose metabolism to improve radiotherapy efficacy. Clin Cancer Res. 2012;18(20):5585-94.

226. Gillies RJ, Gatenby RA. Hypoxia and adaptive landscapes in the evolution of carcinogenesis. Cancer Metastasis Rev. 2007;26(2):311-7.

227. Semenza GL. HIF-1 inhibitors for cancer therapy: from gene expression to drug discovery. Curr Pharm Des. 2009;15(33):3839-43.

228. Lu H, Forbes RA, Verma A. Hypoxia-inducible factor 1 activation by aerobic glycolysis implicates the Warburg effect in carcinogenesis. J Biol Chem. 2002;277(26):23111-5.

229. McFate T, Mohyeldin A, Lu H, Thakar J, Henriques J, Halim ND, et al. Pyruvate dehydrogenase complex activity controls metabolic and malignant phenotype in cancer cells. J Biol Chem. 2008;283(33):22700-8.

230. Xiang L, Mou J, Shao B, Wei Y, Liang H, Takano N, et al. Glutaminase 1 expression in colorectal cancer cells is induced by hypoxia and required for tumor growth, invasion, and metastatic colonization. Cell Death Dis. 2019;10(2):40.

231. Zannella VE, Dal Pra A, Muaddi H, McKee TD, Stapleton S, Sykes J, et al. Reprogramming metabolism with metformin improves tumor oxygenation and radiotherapy response. Clin Cancer Res. 2013;19(24):6741-50.

232. de Mey S, Jiang H, Corbet C, Wang H, Dufait I, Law K, et al. Antidiabetic Biguanides Radiosensitize Hypoxic Colorectal Cancer Cells Through a Decrease in Oxygen Consumption. Frontiers in pharmacology. 2018;9:1073.

233. Sattler UG, Mueller-Klieser W. The anti-oxidant capacity of tumour glycolysis. Int J Radiat Biol. 2009;85(11):963-71.

234. Jin L, Zhou Y. Crucial role of the pentose phosphate pathway in malignant tumors. Oncol Lett. 2019;17(5):4213-21.

235. Li J, Ward KM, Zhang D, Dayanandam E, Denittis AS, Prendergast GC, et al. A bioactive probe of the oxidative pentose phosphate cycle: novel strategy to reverse radioresistance in glucose deprived human colon cancer cells. Toxicol In Vitro. 2013;27(1):367-77.

236. Rashmi R, Huang X, Floberg JM, Elhammali AE, McCormick ML, Patti GJ, et al. Radioresistant Cervical Cancers Are Sensitive to Inhibition of Glycolysis and Redox Metabolism. Cancer Res. 2018;78(6):1392-403.

237. Hasim A, Ma H, Mamtimin B, Abudula A, Niyaz M, Zhang LW, et al. Revealing the metabonomic variation of EC using (1)H-NMR spectroscopy and its association with the clinicopathological characteristics. Mol Biol Rep. 2012;39(9):8955-64.

238. Groussard C, Morel I, Chevanne M, Monnier M, Cillard J, Delamarche A. Free radical scavenging and antioxidant effects of lactate ion: an in vitro study. J Appl Physiol (1985). 2000;89(1):169-75.

239. Hirayama A, Kami K, Sugimoto M, Sugawara M, Toki N, Onozuka H, et al. Quantitative metabolome profiling of colon and stomach cancer microenvironment by capillary electrophoresis time-of-flight mass spectrometry. Cancer Res. 2009;69(11):4918-25.

240. Colen CB, Seraji-Bozorgzad N, Marples B, Galloway MP, Sloan AE, Mathupala SP. Metabolic remodeling of malignant gliomas for enhanced sensitization during radiotherapy: an in vitro study. Neurosurgery. 2006;59(6):1313-23; discussion 23-4.

241. Chandra D, Liu JW, Tang DG. Early mitochondrial activation and cytochrome c up-regulation during apoptosis. J Biol Chem. 2002;277(52):50842-54.

242. Lee MS, Kim JY, Park SY. Resistance of rho(0) cells against apoptosis. Ann N Y Acad Sci. 2004;1011:146-53.

243. Scherr A-L, Gdynia G, Salou M, Radhakrishnan P, Duglova K, Heller A, et al. Bcl-x(L) is an oncogenic driver in colorectal cancer. Cell Death & Disease. 2016;7(8):e2342.

244. Al-Khayal K, Abdulla M, Al-Obeed O, Al Kattan W, Zubaidi A, Vaali-Mohammed MA, et al. Identification of the TP53-induced glycolysis and apoptosis regulator in various stages of colorectal cancer patients. Oncology reports. 2016;35(3):1281-6.

245. Tomiyama A, Serizawa S, Tachibana K, Sakurada K, Samejima H, Kuchino Y, et al. Critical Role for Mitochondrial Oxidative Phosphorylation in the Activation of Tumor Suppressors Bax and Bak. JNCI: Journal of the National Cancer Institute. 2006;98(20):1462-73.

246. Schwarz CS, Evert BO, Seyfried J, Schaupp M, Kunz WS, Vielhaber S, et al. Overexpression of bcl-2 results in reduction of cytochrome c content and inhibition of complex I activity. Biochem Biophys Res Commun. 2001;280(4):1021-7.

247. Vrbacký M, Krijt J, Drahota Z, Mělková Z. Inhibitory effects of Bcl-2 on mitochondrial respiration. Physiological research. 2003;52(5):545-54.

248. Wang K, Fan H, Chen Q, Ma G, Zhu M, Zhang X, et al. Curcumin inhibits aerobic glycolysis and induces mitochondrial-mediated apoptosis through hexokinase II in human colorectal cancer cells in vitro. Anticancer Drugs. 2015;26(1):15-24.

249. Yan XL, Zhang XB, Ao R, Guan L. Effects of shRNA-Mediated Silencing of PKM2 Gene on Aerobic Glycolysis, Cell Migration, Cell Invasion, and Apoptosis in Colorectal Cancer Cells. J Cell Biochem. 2017;118(12):4792-803.

250. Madhok BM, Yeluri S, Perry SL, Hughes TA, Jayne DG. Dichloroacetate induces apoptosis and cell-cycle arrest in colorectal cancer cells. British journal of cancer. 2010;102(12):1746-52.

251. Guo X, Zhang X, Wang T, Xian S, Lu Y. 3-Bromopyruvate and sodium citrate induce apoptosis in human gastric cancer cell line MGC-803 by inhibiting glycolysis and promoting mitochondria-regulated apoptosis pathway. Biochem Biophys Res Commun. 2016;475(1):37-43.

252. Wang TA, Zhang XD, Guo XY, Xian SL, Lu YF. 3-bromopyruvate and sodium citrate target glycolysis, suppress survivin, and induce mitochondrial-mediated apoptosis in gastric cancer cells and inhibit gastric orthotopic transplantation tumor growth. Oncology reports. 2016;35(3):1287-96.

253. Kalucka J, Missiaen R, Georgiadou M, Schoors S, Lange C, De Bock K, et al. Metabolic control of the cell cycle. Cell cycle (Georgetown, Tex). 2015;14(21):3379-88.

254. Buchakjian MR, Kornbluth S. The engine driving the ship: metabolic steering of cell proliferation and death. Nature reviews Molecular cell biology. 2010;11(10):715-27.

255. Foster DA, Yellen P, Xu L, Saqcena M. Regulation of G1 Cell Cycle Progression: Distinguishing the Restriction Point from a Nutrient-Sensing Cell Growth Checkpoint(s). Genes & cancer. 2010;1(11):1124-31.

256. Tudzarova S, Colombo SL, Stoeber K, Carcamo S, Williams GH, Moncada S. Two ubiquitin ligases, APC/C-Cdh1 and SKP1-CUL1-F (SCF)-beta-TrCP, sequentially regulate glycolysis during the cell cycle. Proceedings of the National Academy of Sciences of the United States of America. 2011;108(13):5278-83.

257. Almeida A, Bolaños JP, Moncada S. E3 ubiquitin ligase APC/C-Cdh1 accounts for the Warburg effect by linking glycolysis to cell proliferation. Proceedings of the National Academy of Sciences of the United States of America. 2010;107(2):738-41.

258. Zhang XD, Deslandes E, Villedieu M, Poulain L, Duval M, Gauduchon P, et al. Effect of 2-deoxy-D-glucose on various malignant cell lines in vitro. Anticancer Res. 2006;26(5A):3561-6.

259. Wang Q, Huang C, Hu Y, Yan W, Gong L. Preliminary screening and correlation analysis for lncRNAs related to radiosensitivity in melanoma cells by inhibiting glycolysis. Zhong nan da xue xue bao Yi xue ban = Journal of Central South University Medical sciences. 2021;46(6):565-74.

260. Muley P, Olinger A, Tummala H. 2-Deoxyglucose induces cell cycle arrest and apoptosisin colorectal cancer cells independent of its glycolysis inhibition. Nutr Cancer. 2015;67(3):514-22.

261. Adhikari JS, Dwarakanath BS, Mathur R, Ravindranath T. Alterations in radiation induced cell cycle perturbations by 2-deoxy-D-glucose in human tumor cell lines. Indian J Exp Biol. 2003;41(12):1392-9.

262. Sakamaki T, Casimiro MC, Ju X, Quong AA, Katiyar S, Liu M, et al. Cyclin D1 determines mitochondrial function in vivo. Mol Cell Biol. 2006;26(14):5449-69.

263. Xie B, Wang S, Jiang N, Li JJ. Cyclin B1/CDK1-regulated mitochondrial bioenergetics in cell cycle progression and tumor resistance. Cancer Lett. 2019;443:56-66.

264. Turgeon MO, Perry NJS, Poulogiannis G. DNA Damage, Repair, and Cancer Metabolism. Front Oncol. 2018;8:15.

265. Rao X, Duan X, Mao W, Li X, Li Z, Li Q, et al. O-GlcNAcylation of G6PD promotes the pentose phosphate pathway and tumor growth. Nature communications. 2015;6(1):8468.

266. Bhatt AN, Chauhan A, Khanna S, Rai Y, Singh S, Soni R, et al. Transient elevation of glycolysis confers radio-resistance by facilitating DNA repair in cells. BMC cancer. 2015;15:335.

267. Dwarkanath BS, Jain VK. Energy linked modifications of the radiation response in a human cerebral glioma cell line. Int J Radiat Oncol Biol Phys. 1989;17(5):1033-40.

268. Shimura T, Noma N, Sano Y, Ochiai Y, Oikawa T, Fukumoto M, et al. AKT-mediated enhanced aerobic glycolysis causes acquired radioresistance by human tumor cells. Radiother Oncol. 2014;112(2):302-7.

269. Hao J, Graham P, Chang L, Ni J, Wasinger V, Beretov J, et al. Proteomic identification of the lactate dehydrogenase A in a radioresistant prostate cancer xenograft mouse model for improving radiotherapy. Oncotarget. 2016;7(45):74269-85.

270. Nadalutti CA, Stefanick DF, Zhao M-L, Horton JK, Prasad R, Brooks AM, et al. Mitochondrial dysfunction and DNA damage accompany enhanced levels of formaldehyde in cultured primary human fibroblasts. Scientific Reports. 2020;10(1):5575.

271. Shimura T, Sasatani M, Kawai H, Kamiya K, Kobayashi J, Komatsu K, et al. ATM-mediated mitochondrial damage response triggered by nuclear DNA damage in normal human lung fibroblasts. Cell Cycle. 2017;16(24):2345-54.

272. Bai P, Cantó C, Oudart H, Brunyánszki A, Cen Y, Thomas C, et al. PARP-1 inhibition increases mitochondrial metabolism through SIRT1 activation. Cell metabolism. 2011;13(4):461-8.

273. Andrabi SA, Umanah GK, Chang C, Stevens DA, Karuppagounder SS, Gagné JP, et al. Poly(ADP-ribose) polymerase-dependent energy depletion occurs through inhibition of glycolysis. Proc Natl Acad Sci U S A. 2014;111(28):10209-14.

274. Andrzejewski S, Siegel PM, St-Pierre J. Metabolic Profiles Associated With Metformin Efficacy in Cancer. Front Endocrinol (Lausanne). 2018;9:372.

275. Pernicova I, Korbonits M. Metformin—mode of action and clinical implications for diabetes and cancer. Nature Reviews Endocrinology. 2014;10(3):143-56.

276. White JR, Jr. A Brief History of the Development of Diabetes Medications. Diabetes Spectr. 2014;27(2):82-6.

277. Cicero AFG, Tartagni E, Ertek S. Metformin and its clinical use: new insights for an old drug in clinical practice. Arch Med Sci. 2012;8(5):907-17.

278. Saraei P, Asadi I, Kakar MA, Moradi-Kor N. The beneficial effects of metformin on cancer prevention and therapy: a comprehensive review of recent advances. Cancer management and research. 2019;11:3295-313.

279. Foretz M, Guigas B, Bertrand L, Pollak M, Viollet B. Metformin: from mechanisms of action to therapies. Cell Metab. 2014;20(6):953-66.

280. Gunton JE, Delhanty PJ, Takahashi S, Baxter RC. Metformin rapidly increases insulin receptor activation in human liver and signals preferentially through insulin-receptor substrate-2. The Journal of clinical endocrinology and metabolism. 2003;88(3):1323-32.

281. Giovannucci E, Harlan DM, Archer MC, Bergenstal RM, Gapstur SM, Habel LA, et al. Diabetes and cancer: a consensus report. Diabetes care. 2010;33(7):1674-85.

282. Evans JM, Donnelly LA, Emslie-Smith AM, Alessi DR, Morris AD. Metformin and reduced risk of cancer in diabetic patients. BMJ (Clinical research ed). 2005;330(7503):1304-5.

283. Shuai Y, Li C, Zhou X. The effect of metformin on gastric cancer in patients with type 2 diabetes: a systematic review and meta-analysis. Clin Transl Oncol. 2020;22(9):1580-90.

284. Col NF, Ochs L, Springmann V, Aragaki AK, Chlebowski RT. Metformin and breast cancer risk: a meta-analysis and critical literature review. Breast Cancer Res Treat. 2012;135(3):639-46.

285. Cunha V, Cotrim HP, Rocha R, Carvalho K, Lins-Kusterer L. Metformin in the prevention of hepatocellular carcinoma in diabetic patients: A systematic review. Annals of Hepatology. 2020;19(3):232-7.

286. Zhang J, Ma J, Guo L, Yuan B, Jiao Z, Li Y. Survival Benefit of Metformin Use for Pancreatic Cancer Patients Who Underwent Pancreatectomy: Results From a Meta-Analysis. 2020;7(282).

287. Zeng S, Gan HX, Xu JX, Liu JY. Metformin improves survival in lung cancer patients with type 2 diabetes mellitus: A meta-analysis. Medicina clinica. 2019;152(8):291-7.

288. Ma SJ, Zheng YX, Zhou PC, Xiao YN, Tan HZ. Metformin use improves survival of diabetic liver cancer patients: systematic review and meta-analysis. Oncotarget. 2016;7(40):66202-11.

289. Tang GH, Satkunam M, Pond GR, Steinberg GR, Blandino G, Schünemann HJ, et al. Association of Metformin with Breast Cancer Incidence and Mortality in Patients with Type II Diabetes: A GRADE-Assessed Systematic Review and Meta-analysis. 2018;27(6):627-35.

290. DeCensi A, Puntoni M, Goodwin P, Cazzaniga M, Gennari A, Bonanni B, et al. Metformin and Cancer Risk in Diabetic Patients: A Systematic Review and Meta-analysis. 2010;3(11):1451-61.

291. Noto H, Goto A, Tsujimoto T, Noda M. Cancer Risk in Diabetic Patients Treated with Metformin: A Systematic Review and Meta-analysis. PLOS ONE. 2012;7(3):e33411.

292. Zhang Z-J, Zheng Z-J, Kan H, Song Y, Cui W, Zhao G, et al. Reduced Risk of Colorectal Cancer With Metformin Therapy in Patients With Type 2 Diabetes. A meta-analysis. 2011;34(10):2323-8.

293. Cardel M, Jensen SM, Pottegård A, Jørgensen TL, Hallas J. Long-term use of metformin and colorectal cancer risk in type II diabetics: a population-based case-control study. Cancer medicine. 2014;3(5):1458-66.

294. Nie Z, Zhu H, Gu M. Reduced colorectal cancer incidence in type 2 diabetic patients treated with metformin: a meta-analysis. Pharmaceutical biology. 2016;54(11):2636-42.

295. Mei Z-B, Zhang Z-J, Liu C-Y, Liu Y, Cui A, Liang Z-L, et al. Survival benefits of metformin for colorectal cancer patients with diabetes: a systematic review and meta-analysis. PloS one. 2014;9(3):e91818-e.

296. Kamarudin MNA, Sarker MMR, Zhou J-R, Parhar I. Metformin in colorectal cancer: molecular mechanism, preclinical and clinical aspects. Journal of Experimental & Clinical Cancer Research. 2019;38(1):491.

297. Hosono K, Endo H, Takahashi H, Sugiyama M, Sakai E, Uchiyama T, et al. Metformin Suppresses Colorectal Aberrant Crypt Foci in a Short-term Clinical Trial. 2010;3(9):1077-83.

298. Higurashi T, Hosono K, Takahashi H, Komiya Y, Umezawa S, Sakai E, et al. Metformin for chemoprevention of metachronous colorectal adenoma or polyps in post-polypectomy patients without diabetes: a multicentre double-blind, placebo-controlled, randomised phase 3 trial. The Lancet Oncology. 2016;17(4):475-83.

299. Kourelis TV, Siegel RD. Metformin and cancer: new applications for an old drug. Med Oncol. 2012;29(2):1314-27.

300. Skinner HD, Crane CH, Garrett CR, Eng C, Chang GJ, Skibber JM, et al. Metformin use and improved response to therapy in rectal cancer. Cancer Med. 2013;2(1):99-107.

301. Skinner HD, McCurdy MR, Echeverria AE, Lin SH, Welsh JW, O'Reilly MS, et al. Metformin use and improved response to therapy in esophageal adenocarcinoma. Acta Oncol. 2013;52(5):1002-9.

302. Van De Voorde L, Janssen L, Larue R, Houben R, Buijsen J, Sosef M, et al. Can metformin improve 'the tomorrow' of patients treated for oesophageal cancer? Eur J Surg Oncol. 2015;41(10):1333-9.

303. Jiralerspong S, Palla SL, Giordano SH, Meric-Bernstam F, Liedtke C, Barnett CM, et al. Metformin and pathologic complete responses to neoadjuvant chemotherapy in diabetic patients with breast cancer. Journal of clinical oncology : official journal of the American Society of Clinical Oncology. 2009;27(20):3297-302.

304. Wong CS, Chu W, Ashamalla S, Fenech D, Berry S, Kiss A, et al. Metformin with neoadjuvant chemoradiation to improve pathologic response in rectal cancer: A pilot phase I/II trial. Clinical and Translational Radiation Oncology. 2021;30:60-4.

305. Jeong YK, Kim MS, Lee JY, Kim EH, Ha H. Metformin Radiosensitizes p53-Deficient Colorectal Cancer Cells through Induction of G2/M Arrest and Inhibition of DNA Repair Proteins. PLoS One. 2015;10(11):e0143596.

306. Li H, Chen X, Yu Y, Wang Z, Zuo Y, Li S, et al. Metformin inhibits the growth of nasopharyngeal carcinoma cells and sensitizes the cells to radiation via inhibition of the DNA damage repair pathway. Oncology reports. 2014;32(6):2596-604.

307. Wang Z, Lai ST, Ma NY, Deng Y, Liu Y, Wei DP, et al. Radiosensitization of metformin in pancreatic cancer cells via abrogating the G2 checkpoint and inhibiting DNA damage repair. Cancer Lett. 2015;369(1):192-201.

308. Jin DH, Kim Y, Lee BB, Han J, Kim HK, Shim YM, et al. Metformin induces cell cycle arrest at the G1 phase through E2F8 suppression in lung cancer cells. 2017;8(60).

309. Wang Y, Xu W, Yan Z, Zhao W, Mi J, Li J, et al. Metformin induces autophagy and G0/G1 phase cell cycle arrest in myeloma by targeting the AMPK/mTORC1 and mTORC2 pathways. J Exp Clin Cancer Res. 2018;37(1):63.

310. Zhao L, Wen Z-H, Jia C-H, Li M, Luo S-Q, Bai X-C. Metformin Induces G1 Cell Cycle Arrest and Inhibits Cell Proliferation in Nasopharyngeal Carcinoma Cells. 2011;294(8):1337-43.

311. Vial G, Detaille D, Guigas B. Role of Mitochondria in the Mechanism(s) of Action of Metformin. 2019;10(294).

312. Sena P, Mancini S, Benincasa M, Mariani F, Palumbo C, Roncucci L. Metformin Induces Apoptosis and Alters Cellular Responses to Oxidative Stress in Ht29 Colon Cancer Cells: Preliminary Findings. International journal of molecular sciences. 2018;19(5):1478.

313. Marinello PC, da Silva TN, Panis C, Neves AF, Machado KL, Borges FH, et al. Mechanism of metformin action in MCF-7 and MDA-MB-231 human breast cancer cells involves oxidative stress generation, DNA damage, and transforming growth factor β1 induction. Tumour biology : the journal of the International Society for Oncodevelopmental Biology and Medicine. 2016;37(4):5337-46.

314. Srivastava A, Creek DJ. Discovery and Validation of Clinical Biomarkers of Cancer: A Review Combining Metabolomics and Proteomics. Proteomics. 2019;19(10):e1700448.

315. Goossens N, Nakagawa S, Sun X, Hoshida Y. Cancer biomarker discovery and validation. Transl Cancer Res. 2015;4(3):256-69.

316. Hu Z-Z, Huang H, Wu CH, Jung M, Dritschilo A, Riegel AT, et al. Omics-based molecular target and biomarker identification. Methods in molecular biology (Clifton, NJ). 2011;719:547-71.

317. Olivier M, Asmis R, Hawkins GA, Howard TD, Cox LA. The Need for Multi-Omics Biomarker Signatures in Precision Medicine. International journal of molecular sciences. 2019;20(19):4781.

318. Jiang Z, Zhou X, Li R, Michal JJ, Zhang S, Dodson MV, et al. Whole transcriptome analysis with sequencing: methods, challenges and potential solutions. Cell Mol Life Sci. 2015;72(18):3425-39.

319. Mini E, Lapucci A, Perrone G, D'Aurizio R, Napoli C, Brugia M, et al. RNA sequencing reveals PNN and KCNQ1OT1 as predictive biomarkers of clinical outcome in stage III colorectal cancer patients treated with adjuvant chemotherapy. Int J Cancer. 2019;145(9):2580-93.

320. Canto LMd, Cury SS, Barros-Filho MC, Kupper BEC, Begnami MDFdS, Scapulatempo-Neto C, et al. Locally advanced rectal cancer transcriptomic-based secretome analysis reveals novel biomarkers useful to identify patients according to neoadjuvant chemoradiotherapy response. Scientific Reports. 2019;9(1):8702.

321. Gonçalves-Ribeiro S, Sanz-Pamplona R, Vidal A, Sanjuan X, Guillen Díaz-Maroto N, Soriano A, et al. Prediction of pathological response to neoadjuvant treatment in rectal cancer with a two-protein immunohistochemical score derived from stromal gene-profiling. Annals of Oncology. 2017;28(9):2160-8.

322. Cheasley D, Jorissen RN, Liu S, Tan CW, Love C, Palmieri M, et al. Genomic approach to translational studies in colorectal cancer. 2015. 2015;4(3):235-55.

323. Akiyoshi T, Kobunai T, Watanabe T. Predicting the response to preoperative radiation or chemoradiation by a microarray analysis of the gene expression profiles in rectal cancer. Surgery today. 2012;42(8):713-9.

324. Jia H, Shen X, Guan Y, Xu M, Tu J, Mo M, et al. Predicting the pathological response to neoadjuvant chemoradiation using untargeted metabolomics in locally advanced rectal cancer. Radiotherapy and Oncology. 2018;128(3):548-56.

325. Gowda GA, Zhang S, Gu H, Asiago V, Shanaiah N, Raftery D. Metabolomics-based methods for early disease diagnostics. Expert Rev Mol Diagn. 2008;8(5):617-33.

326. Gunther UL. Metabolomics Biomarkers for Breast Cancer. Pathobiology. 2015;82(3-4):153-65.

327. Serkova NJ, Glunde K. Metabolomics of cancer. Methods in molecular biology (Clifton, NJ). 2009;520:273-95.

328. Qiu Y, Cai G, Zhou B, Li D, Zhao A, Xie G, et al. A distinct metabolic signature of human colorectal cancer with prognostic potential. Clin Cancer Res. 2014;20(8):2136-46.

329. Chan ECY, Koh PK, Mal M, Cheah PY, Eu KW, Backshall A, et al. Metabolic Profiling of Human Colorectal Cancer Using High-Resolution Magic Angle Spinning Nuclear Magnetic Resonance (HR-MAS NMR) Spectroscopy and Gas Chromatography Mass Spectrometry (GC/MS). Journal of Proteome Research. 2009;8(1):352-61.

330. Erben V, Bhardwaj M, Schrotz-King P, Brenner H. Metabolomics biomarkers for detection of colorectal neoplasms: A systematic review. Cancers. 2018;10(8).

331. Turanli B, Karagoz K, Gulfidan G, Sinha R, Mardinoglu A, Arga KY. A Network-Based Cancer Drug Discovery: From Integrated Multi-Omics Approaches to Precision Medicine. Curr Pharm Des. 2018;24(32):3778-90.

332. Liu N, Wu Y, Cheng W, Wu Y, Wang L, Zhuang L. Identification of novel prognostic biomarkers by integrating multi-omics data in gastric cancer. BMC cancer. 2021;21(1):460.

333. Wang TH, Lee CY, Lee TY, Huang HD, Hsu JB, Chang TH. Biomarker Identification through Multiomics Data Analysis of Prostate Cancer Prognostication Using a Deep Learning Model and Similarity Network Fusion. Cancers (Basel). 2021;13(11).

334. Jones RT, Zuiverloon TCM, Vekony H, Goodspeed A, Laajala TD, Joshi M, et al. Abstract B11: Multi-omic interrogation of gemcitabine and cisplatin-resistant bladder cancer cell lines identifies unique and shared mediators of chemosensitivity and resistance. 2020;26(15 Supplement):B11-B.

335. McCarthy K, Pearson K, Fulton R, Hewitt J. Pre-operative chemoradiation for non-metastatic locally advanced rectal cancer. Cochrane Database Syst Rev. 2012;12:Cd008368.

336. Roeder F, Meldolesi E, Gerum S, Valentini V, Rödel C. Recent advances in (chemo-)radiation therapy for rectal cancer: a comprehensive review. Radiation Oncology. 2020;15(1):262.

337. TAoCoGBaI. Guidelines for the management of Colorectal cancer. 3rd ed.

338. McDermott N, Meunier A, Lynch TH, Hollywood D, Marignol L. Isogenic radiation resistant cell lines: development and validation strategies. Int J Radiat Biol. 2014;90(2):115-26.

339. Lynam-Lennon N, Reynolds JV, Pidgeon GP, Lysaght J, Marignol L, Maher SG. Alterations in DNA repair efficiency are involved in the radioresistance of esophageal adenocarcinoma. Radiat Res. 2010;174(6):703-11.

340. McDermott N, Meunier A, Mooney B, Nortey G, Hernandez C, Hurley S, et al. Fractionated radiation exposure amplifies the radioresistant nature of prostate cancer cells. Sci Rep. 2016;6:34796.

341. Emons G, Spitzner M, Reineke S, Möller J, Auslander N, Kramer F, et al. Chemoradiotherapy Resistance in Colorectal Cancer Cells is Mediated by Wnt/β-catenin Signaling. Molecular cancer research : MCR. 2017;15(11):1481-90.

342. Shang Y, Wang L, Zhu Z, Gao W, Li D, Zhou Z, et al. Downregulation of miR-423-5p Contributes to the Radioresistance in Colorectal Cancer Cells. Frontiers in oncology. 2021;10:582239-.

343. Oike T, Ohno T. Molecular mechanisms underlying radioresistance: data compiled from isogenic cell experiments. Annals of translational medicine. 2020;8(6):273-.

344. Huerta S, Gao X, Saha D. Mechanisms of resistance to ionizing radiation in rectal cancer. Expert Rev Mol Diagn. 2009;9(5):469-80.

345. Bansal A, Simon MC. Glutathione metabolism in cancer progression and treatment resistance. Journal of Cell Biology. 2018;217(7):2291-8.

346. Conklin KA. Cancer chemotherapy and antioxidants. J Nutr. 2004;134(11):3201S-4S.

347. Mitchell JB, Russo A. The role of glutathione in radiation and drug induced cytotoxicity. The British journal of cancer Supplement. 1987;8:96-104.

348. Avantaggiati ML. Cancer metabolism as a therapeutic target: finding the right target(s) in the context of tumor heterogeneity, evolution, and metabolic plasticity. Oncology (Williston Park). 2013;27(5):474, 6-7.

349. Liu Y, Bodmer WF. Analysis of P53 mutations and their expression in 56 colorectal cancer cell lines. Proc Natl Acad Sci U S A. 2006;103(4):976-81.

350. van Erk MJ, Krul CA, Caldenhoven E, Stierum RH, Peters WH, Woutersen RA, et al. Expression profiling of colon cancer cell lines and colon biopsies: towards a screening system for potential cancer-preventive compounds. European journal of cancer prevention : the official journal of the European Cancer Prevention Organisation (ECP). 2005;14(5):439-57.

351. Franken NA, Rodermond HM, Stap J, Haveman J, van Bree C. Clonogenic assay of cells in vitro. Nat Protoc. 2006;1(5):2315-9.

352. Mah LJ, El-Osta A, Karagiannis TC. γH2AX: a sensitive molecular marker of DNA damage and repair. Leukemia. 2010;24(4):679-86.

353. Zhang J, Nuebel E, Wisidagama DRR, Setoguchi K, Hong JS, Van Horn CM, et al. Measuring energy metabolism in cultured cells, including human pluripotent stem cells and differentiated cells. Nature protocols. 2012;7(6):1068-85.

354. Mookerjee SA, Nicholls DG, Brand MD. Determining Maximum Glycolytic Capacity Using Extracellular Flux Measurements. PLOS ONE. 2016;11(3):e0152016.

355. Kendziorra E, Ahlborn K, Spitzner M, Rave-Fränk M, Emons G, Gaedcke J, et al. Silencing of the Wnt transcription factor TCF4 sensitizes colorectal cancer cells to (chemo-) radiotherapy. Carcinogenesis. 2011;32(12):1824-31.

356. Koerdel K, Spitzner M, Meyer T, Engels N, Krause F, Gaedcke J, et al. NOTCH Activation via gp130/STAT3 Signaling Confers Resistance to Chemoradiotherapy. Cancers. 2021;13(3):455.

357. Ishibashi N, Maebayashi T, Aizawa T, Sakaguchi M, Nishimaki H, Masuda S. Correlation between the Ki-67 proliferation index and response to radiation therapy in small cell lung cancer. Radiation Oncology. 2017;12(1):16.

358. Freudlsperger C, Freier K, Hoffmann J, Engel M. Ki-67 expression predicts radiosensitivity in oral squamous cell carcinoma. International journal of oral and maxillofacial surgery. 2012;41(8):965-9.

359. Liu C, Nie J, Wang R, Mao W. The Cell Cycle G2/M Block Is an Indicator of Cellular Radiosensitivity. Dose-response : a publication of International Hormesis Society. 2019;17(4):1559325819891008-.

360. Visconti R, Della Monica R, Grieco D. Cell cycle checkpoint in cancer: a therapeutically targetable double-edged sword. J Exp Clin Cancer Res. 2016;35(1):153.

361. Raleigh DR, Haas-Kogan DA. Molecular targets and mechanisms of radiosensitization using DNA damage response pathways. Future Oncol. 2013;9(2):219-33.

362. Wu T, Dai Y. Tumor microenvironment and therapeutic response. Cancer Lett. 2017;387:61-8.

363. Wilson WR, Hay MP. Targeting hypoxia in cancer therapy. Nat Rev Cancer. 2011;11(6):393-410.

364. Jing X, Yang F, Shao C, Wei K, Xie M, Shen H, et al. Role of hypoxia in cancer therapy by regulating the tumor microenvironment. Molecular cancer. 2019;18(1):157.

365. Sendoel A, Kohler I, Fellmann C, Lowe SW, Hengartner MO. HIF-1 antagonizes p53-mediated apoptosis through a secreted neuronal tyrosinase. Nature. 2010;465(7298):577-83.

366. Eales KL, Hollinshead KER, Tennant DA. Hypoxia and metabolic adaptation of cancer cells. Oncogenesis. 2016;5(1):e190-e.

367. Sendoel A, Hengartner MO. Apoptotic Cell Death Under Hypoxia. 2014;29(3):168-76.

368. Nicholls DG. Spare respiratory capacity, oxidative stress and excitotoxicity. Biochem Soc Trans. 2009;37(Pt 6):1385-8.

369. Marchetti P, Fovez Q, Germain N, Khamari R, Kluza J. Mitochondrial spare respiratory capacity: Mechanisms, regulation, and significance in non-transformed and cancer cells. 2020;34(10):13106-24.

370. Nagao A, Kobayashi M, Koyasu S, Chow CCT, Harada H. HIF-1-Dependent Reprogramming of Glucose Metabolic Pathway of Cancer Cells and Its Therapeutic Significance. Int J Mol Sci. 2019;20(2).

371. Pfleger J, He M, Abdellatif M. Mitochondrial complex II is a source of the reserve respiratory capacity that is regulated by metabolic sensors and promotes cell survival. Cell Death & Disease. 2015;6(7):e1835-e.

372. Jiang J, Jiang Y, Zhang Y-G, Zhang T, Li J-H, Huang D-L, et al. The effects of hypoxia on mitochondrial function and metabolism in gastric cancer cells. 2021. 2021;10(2):817-26.

373. Tohme S, Yazdani HO, Liu Y, Loughran P, van der Windt DJ, Huang H, et al. Hypoxia mediates mitochondrial biogenesis in hepatocellular carcinoma to promote tumor growth through HMGB1 and TLR9 interaction. 2017;66(1):182-97.

374. Chiche J, Rouleau M, Gounon P, Brahimi-Horn MC, Pouysségur J, Mazure NM. Hypoxic enlarged mitochondria protect cancer cells from apoptotic stimuli. 2010;222(3):648-57.

375. Grosso S, Doyen J, Parks SK, Bertero T, Paye A, Cardinaud B, et al. MiR-210 promotes a hypoxic phenotype and increases radioresistance in human lung cancer cell lines. Cell Death Dis. 2013;4(3):e544.

376. Rakotomalala A, Escande A, Furlan A, Meignan S, Lartigau E. Hypoxia in Solid Tumors: How Low Oxygenation Impacts the "Six Rs" of Radiotherapy. 2021;12.

377. Wang H, Jiang H, Van De Gucht M, De Ridder M. Hypoxic Radioresistance: Can ROS Be the Key to Overcome It? Cancers (Basel). 2019;11(1).

378. Carcereri de Prati A, Butturini E, Rigo A, Oppici E, Rossin M, Boriero D, et al. Metastatic Breast Cancer Cells Enter Into Dormant State and Express Cancer Stem Cells Phenotype Under Chronic Hypoxia. J Cell Biochem. 2017;118(10):3237-48.

379. Yao K, Gietema JA, Shida S, Selvakumaran M, Fonrose X, Haas NB, et al. In vitro hypoxia-conditioned colon cancer cell lines derived from HCT116 and HT29 exhibit altered apoptosis susceptibility and a more angiogenic profile in vivo. British journal of cancer. 2005;93(12):1356-63.

380. Wozny AS, Alphonse G, Cassard A, Malésys C, Louati S, Beuve M, et al. Impact of hypoxia on the double-strand break repair after photon and carbon ion irradiation of radioresistant HNSCC cells. Sci Rep. 2020;10(1):21357.

381. Bouquet F, Ousset M, Biard D, Fallone F, Dauvillier S, Frit P, et al. A DNA-dependent stress response involving DNA-PK occurs in hypoxic cells and contributes to cellular adaptation to hypoxia. Journal of cell science. 2011;124(Pt 11):1943-51.

382. Macedo-Silva C, Miranda-Gonçalves V, Lameirinhas A, Lencart J, Pereira A, Lobo J, et al. JmjC-KDMs KDM3A and KDM6B modulate radioresistance under hypoxic conditions in esophageal squamous cell carcinoma. Cell Death Dis. 2020;11(12):1068.

383. Scanlon SE, Glazer PM. Multifaceted control of DNA repair pathways by the hypoxic tumor microenvironment. DNA Repair (Amst). 2015;32:180-9.

384. Buckley AM, Lynam-Lennon N, O'Neill H, O'Sullivan J. Targeting hallmarks of cancer to enhance radiosensitivity in gastrointestinal cancers. Nature Reviews Gastroenterology & Hepatology. 2020;17(5):298-313.

385. Fontaine E. Metformin-Induced Mitochondrial Complex I Inhibition: Facts, Uncertainties, and Consequences. Front Endocrinol (Lausanne). 2018;9:753.

386. Yu X, Mao W, Zhai Y, Tong C, Liu M, Ma L, et al. Anti-tumor activity of metformin: from metabolic and epigenetic perspectives. Oncotarget. 2017;8(3):5619-28.

387. Leung E, Cairns RA, Chaudary N, Vellanki RN, Kalliomaki T, Moriyama EH, et al. Metabolic targeting of HIF-dependent glycolysis reduces lactate, increases oxygen consumption and enhances response to high-dose single-fraction radiotherapy in hypoxic solid tumors. BMC cancer. 2017;17(1):418.

388. Yang Y, Su D, Zhao L, Zhang D, Xu J, Wan J, et al. Different effects of LDH-A inhibition by oxamate in non-small cell lung cancer cells. Oncotarget. 2014;5(23):11886-96.

389. Hunter AJ, Hendrikse AS, Renan MJ. Can radiation-induced apoptosis be modulated by inhibitors of energy metabolism? Int J Radiat Biol. 2007;83(2):105-14.

390. Miller TW, Soto-Pantoja DR, Schwartz AL, Sipes JM, DeGraff WG, Ridnour LA, et al. CD47 Receptor Globally Regulates Metabolic Pathways That Control Resistance to Ionizing Radiation. J Biol Chem. 2015;290(41):24858-74.

391. McCann E, O'Sullivan J, Marcone S. Targeting cancer-cell mitochondria and metabolism to improve radiotherapy response. Translational oncology. 2021;14(1):100905.

392. Buckley AM, Dunne MR, Morrissey ME, Kennedy SA, Nolan A, Davern M, et al. Real-time metabolic profiling of oesophageal tumours reveals an altered metabolic phenotype to different oxygen tensions and to treatment with Pyrazinib. Sci Rep. 2020;10(1):12105.

393. Kojima S, Ohshima Y, Nakatsukasa H, Tsukimoto M. Role of ATP as a Key Signaling Molecule Mediating Radiation-Induced Biological Effects. Dose-response : a publication of International Hormesis Society. 2017;15(1):1559325817690638-.

394. Byfield JE. 5-Fluorouracil radiation sensitization — A brief review. Investigational New Drugs. 1989;7(1):111-6.

395. Cheng G, Zielonka J, Ouari O, Lopez M, McAllister D, Boyle K, et al. Mitochondria-Targeted Analogues of Metformin Exhibit Enhanced Antiproliferative and Radiosensitizing Effects in Pancreatic Cancer Cells. Cancer Research. 2016;76(13):3904.

396. Loubiere C, Clavel S, Gilleron J, Harisseh R, Fauconnier J, Ben-Sahra I, et al. The energy disruptor metformin targets mitochondrial integrity via modification of calcium flux in cancer cells. Scientific Reports. 2017;7(1):5040.

397. Sivalingam VN, Latif A, Kitson S, McVey R, Finegan KG, Marshall K, et al. Hypoxia and hyperglycaemia determine why some endometrial tumours fail to respond to metformin. British journal of cancer. 2020;122(1):62-71.

398. Huttemann M, Lee I, Pecinova A, Pecina P, Przyklenk K, Doan JW. Regulation of oxidative phosphorylation, the mitochondrial membrane potential, and their role in human disease. Journal of bioenergetics and biomembranes. 2008;40(5):445-56.

399. Warkad MS, Kim C-H, Kang B-G, Park S-H, Jung J-S, Feng J-H, et al. Metformin-induced ROS upregulation as amplified by apigenin causes profound anticancer activity while sparing normal cells. Scientific Reports. 2021;11(1):14002.

400. Brown SL, Kolozsvary A, Isrow DM, Al Feghali K, Lapanowski K, Jenrow KA, et al. A Novel Mechanism of High Dose Radiation Sensitization by Metformin. 2019;9.

401. Mogavero A, Maiorana MV, Zanutto S, Varinelli L, Bozzi F, Belfiore A, et al. Metformin transiently inhibits colorectal cancer cell proliferation as a result of either AMPK activation or increased ROS production. Scientific Reports. 2017;7(1):15992.

402. Fasih A, Elbaz HA, Hüttemann M, Konski AA, Zielske SP. Radiosensitization of pancreatic cancer cells by metformin through the AMPK pathway. Radiat Res. 2014;182(1):50-9.

403. Song CW, Lee H, Dings RPM, Williams B, Powers J, Santos TD, et al. Metformin kills and radiosensitizes cancer cells and preferentially kills cancer stem cells. Scientific Reports. 2012;2(1):362.

404. Fernandes JM, Jandrey EHF, Koyama FC, Leite KRM, Camargo AA, Costa É T, et al. Metformin as an Alternative Radiosensitizing Agent to 5-Fluorouracil During Neoadjuvant Treatment for Rectal Cancer. Dis Colon Rectum. 2020;63(7):918-26.

405. Park J-H, Kim Y-H, Park EH, Lee S-J, Kim H, Kim A, et al. Effects of metformin and phenformin on apoptosis and epithelial-mesenchymal transition in chemoresistant rectal cancer. Cancer science. 2019;110(9):2834-45.

406. Benej M, Hong X, Vibhute S, Scott S, Wu J, Graves E, et al. Papaverine and its derivatives radiosensitize solid tumors by inhibiting mitochondrial metabolism. Proc Natl Acad Sci U S A. 2018;115(42):10756-61.

407. Bucher N, Britten CD. G2 checkpoint abrogation and checkpoint kinase-1 targeting in the treatment of cancer. British journal of cancer. 2008;98(3):523-8.

408. Wang LW, Li ZS, Zou DW, Jin ZD, Gao J, Xu GM. Metformin induces apoptosis of pancreatic cancer cells. World J Gastroenterol. 2008;14(47):7192-8.

409. Weir CB, Jan A. BMI Classification Percentile And Cut Off Points. StatPearls. Treasure Island (FL)2022.

410. Kumari R, Jat P. Mechanisms of Cellular Senescence: Cell Cycle Arrest and Senescence Associated Secretory Phenotype. 2021;9(485).

411. Vitale I, Galluzzi L, Castedo M, Kroemer G. Mitotic catastrophe: a mechanism for avoiding genomic instability. Nature reviews Molecular cell biology. 2011;12(6):385-92.

412. Chen T, Stephens PA, Middleton FK, Curtin NJ. Targeting the S and G2 checkpoint to treat cancer. Drug discovery today. 2012;17(5-6):194-202.

413. Liu C, Liu Q, Yan A, Chang H, Ding Y, Tao J, et al. Metformin revert insulin-induced oxaliplatin resistance by activating mitochondrial apoptosis pathway in human colon cancer HCT116 cells. Cancer Med. 2020;9(11):3875-84.

414. Correia S, Carvalho C, Santos MS, Proença T, Nunes E, Duarte AI, et al. Metformin protects the brain against the oxidative imbalance promoted by type 2 diabetes. Medicinal chemistry (Shariqah (United Arab Emirates)). 2008;4(4):358-64.

415. He J, Wang K, Zheng N, Qiu Y, Xie G, Su M, et al. Metformin suppressed the proliferation of LoVo cells and induced a time-dependent metabolic and transcriptional alteration. Scientific reports. 2015;5:17423-.

416. Suwa T, Kobayashi M, Nam J-M, Harada H. Tumor microenvironment and radioresistance. Experimental & Molecular Medicine. 2021;53(6):1029-35.

417. Salani B, Rio AD, Marini C, Sambuceti G, Cordera R, Maggi D. Metformin, cancer and glucose metabolism. Endocrine-Related Cancer. 2014;21(6):R461-R71.

418. Khan MK, Nasti TH, Buchwald ZS, Weichselbaum RR, Kron SJ. Repurposing Drugs for Cancer Radiotherapy: Early Successes and Emerging Opportunities. Cancer journal (Sudbury, Mass). 2019;25(2):106-15.

419. Isvoranu G, Surcel M, Munteanu AN, Bratu OG, Ionita-Radu F, Neagu MT, et al. Therapeutic potential of interleukin-15 in cancer (Review). Exp Ther Med. 2021;22(1):675.

420. Pilones K, Aryankalayil J, Formenti S, Demaria S. Intratumoral IL-15 potentiates radiation-induced anti-tumor immunity. Journal for ImmunoTherapy of Cancer. 2015;3(2):P239.

421. Zak KP, Furmanova, O.V, Popova, V.V, Sayenko, Y.A. The content of pro-inflammatory cytokines IL-1β, IL-6, IL-17A and TNFα in the blood of patients with type 2 diabetes after therapy with metformin

K. P. Zak*, O. V. Furmanova, V. V. Popova, Ya. A. Sayenko. The Ukranian Biochemical Journal. 2020;92(6):105-12.

422. Gong L, Zhang Y, Liu C, Zhang M, Han S. Application of Radiosensitizers in Cancer Radiotherapy. Int J Nanomedicine. 2021;16:1083-102.

423. Rodríguez-Tomàs E, Arenas M, Gómez J, Acosta J, Trilla J, López Y, et al. Identification of potential metabolic biomarkers of rectal cancer and of the effect of neoadjuvant radiochemotherapy. PLOS ONE. 2021;16(4):e0250453.

424. Jia H, Shen X, Guan Y, Xu M, Tu J, Mo M, et al. Predicting the pathological response to neoadjuvant chemoradiation using untargeted metabolomics in locally advanced rectal cancer. Radiother Oncol. 2018;128(3):548-56.

425. Dayde D, Tanaka I, Jain R, Tai MC, Taguchi A. Predictive and Prognostic Molecular Biomarkers for Response to Neoadjuvant Chemoradiation in Rectal Cancer. Int J Mol Sci. 2017;18(3).

426. Reuben A, Gopalakrishnan V, Wagner HE, Spencer CN, Austin-Breneman J, Jiang H, et al. Working with Human Tissues for Translational Cancer Research. J Vis Exp. 2015(105):53189.

427. Madhavan S, Gusev Y, Natarajan T, Song L, Bhuvaneshwar K, Gauba R, et al. Genome-wide multi-omics profiling of colorectal cancer identifies immune determinants strongly associated with relapse. 2013;4.

428. Sardo E, Napolitano S, Della Corte CM, Ciardiello D, Raucci A, Arrichiello G, et al. Multi-Omic Approaches in Colorectal Cancer beyond Genomic Data. 2022;12(2):128.

429. Xu X, Gong C, Wang Y, Hu Y, Liu H, Fang Z. Multi-omics analysis to identify driving factors in colorectal cancer. 2020;12(18):1633-50.

430. Chen H-Y, Feng L-L, Li M, Ju H-Q, Ding Y, Lan M, et al. College of American Pathologists Tumor Regression Grading System for Long-Term Outcome in Patients with Locally Advanced Rectal Cancer. 2021;26(5):e780-e93.

431. Zukunft S, Prehn C, Röhring C, Möller G, Hrabě de Angelis M, Adamski J, et al. High-throughput extraction and quantification method for targeted metabolomics in murine tissues. Metabolomics. 2018;14(1):18.

432. Team RC. A language and environment for statistical computing. R Foundation for Statistical Computing, Vienna, Austria. Available online at https://www.Rproject.org/ 2019.

433. Frank E Harrell Jr wcfCDamo. Hmisc: Harrell Miscellaneous. R package version 4.4-0. Available from: https://CRAN.R-project.org/package=Hmisc. 2020.

434. Wei T SV. R package “corrplot”: Visualization of a Correlation Matrix (Version 0.84). 2017. Available from: https://github.com/taiyun/corrplot. 2017.

435. Sulciner ML, Gartung A, Gilligan MM, Serhan CN, Panigrahy D. Targeting lipid mediators in cancer biology. Cancer Metastasis Rev. 2018;37(2-3):557-72.

436. Saito RdF, Andrade LNdS, Bustos SO, Chammas R. Phosphatidylcholine-Derived Lipid Mediators: The Crosstalk Between Cancer Cells and Immune Cells. 2022;13.

437. Sun H, Ren J, Zhu Q, Kong FZ, Wu L, Pan BR. Effects of lysophosphatidic acid on human colon cancer cells and its mechanisms of action. World J Gastroenterol. 2009;15(36):4547-55.

438. Tang X, Wuest M, Benesch MGK, Dufour J, Zhao Y, Curtis JM, et al. Inhibition of Autotaxin with GLPG1690 Increases the Efficacy of Radiotherapy and Chemotherapy in a Mouse Model of Breast Cancer. Molecular cancer therapeutics. 2020;19(1):63-74.

439. Bhave SR, Dadey DY, Karvas RM, Ferraro DJ, Kotipatruni RP, Jaboin JJ, et al. Autotaxin Inhibition with PF-8380 Enhances the Radiosensitivity of Human and Murine Glioblastoma Cell Lines. Front Oncol. 2013;3:236.

440. Venkatraman G, Benesch MG, Tang X, Dewald J, McMullen TP, Brindley DN. Lysophosphatidate signaling stabilizes Nrf2 and increases the expression of genes involved in drug resistance and oxidative stress responses: implications for cancer treatment. Faseb j. 2015;29(3):772-85.

441. Foster DA. Phosphatidic acid and lipid-sensing by mTOR. Trends Endocrinol Metab. 2013;24(6):272-8.

442. Alam RT, Imam TS, Abo-Elmaaty AMA, Arisha AH. Amelioration of fenitrothion induced oxidative DNA damage and inactivation of caspase-3 in the brain and spleen tissues of male rats by N-acetylcysteine. Life Sciences. 2019;231:116534.

443. Cheng M, Bhujwalla ZM, Glunde K. Targeting Phospholipid Metabolism in Cancer. Frontiers in oncology. 2016;6:266-.

444. Iorio E, Mezzanzanica D, Alberti P, Spadaro F, Ramoni C, D'Ascenzo S, et al. Alterations of choline phospholipid metabolism in ovarian tumor progression. Cancer Res. 2005;65(20):9369-76.

445. Zhang H, Wang L, Hou Z, Ma H, Mamtimin B, Hasim A, et al. Metabolomic profiling reveals potential biomarkers in esophageal cancer progression using liquid chromatography-mass spectrometry platform. Biochem Biophys Res Commun. 2017;491(1):119-25.

446. Doerstling SS, O'Flanagan CH, Hursting SD. Obesity and Cancer Metabolism: A Perspective on Interacting Tumor-Intrinsic and Extrinsic Factors. Frontiers in oncology. 2017;7:216-.

447. Sivanand S, Vander Heiden MG. Emerging Roles for Branched-Chain Amino Acid Metabolism in Cancer. Cancer Cell. 2020;37(2):147-56.

448. Kliemann N, Viallon V, Murphy N, Beeken RJ, Rothwell JA, Rinaldi S, et al. Metabolic signatures of greater body size and their associations with risk of colorectal and endometrial cancers in the European Prospective Investigation into Cancer and Nutrition. BMC Medicine. 2021;19(1):101.

449. Tobias DK, Hazra A, Lawler PR, Chandler PD, Chasman DI, Buring JE, et al. Circulating branched-chain amino acids and long-term risk of obesity-related cancers in women. Scientific Reports. 2020;10(1):16534.

450. Geijsen AJMR, van Roekel EH, van Duijnhoven FJB, Achaintre D, Bachleitner-Hofmann T, Baierl A, et al. Plasma metabolites associated with colorectal cancer stage: Findings from an international consortium. International journal of cancer. 2020;146(12):3256-66.

451. Tolkach Y, Stahl AF, Niehoff E-M, Zhao C, Kristiansen G, Müller SC, et al. YRNA expression predicts survival in bladder cancer patients. BMC cancer. 2017;17(1):749.

452. Bauden M, Kristl T, Sasor A, Andersson B, Marko-Varga G, Andersson R, et al. Histone profiling reveals the H1.3 histone variant as a prognostic biomarker for pancreatic ductal adenocarcinoma. BMC cancer. 2017;17(1):810.

453. Kang KA, Ryu YS, Piao MJ, Shilnikova K, Kang HK, Yi JM, et al. DUOX2-mediated production of reactive oxygen species induces epithelial mesenchymal transition in 5-fluorouracil resistant human colon cancer cells. Redox biology. 2018;17:224-35.

454. Lyu P-W, Xu X-D, Zong K, Qiu X-GJGS. Overexpression of DUOX2 mediates doxorubicin resistance and predicts prognosis of pancreatic cancer. 2022. 2022;11(1):115-24.

455. Martin P, Noonan S, Mullen MP, Scaife C, Tosetto M, Nolan B, et al. Predicting response to vascular endothelial growth factor inhibitor and chemotherapy in metastatic colorectal cancer. BMC cancer. 2014;14:887-.

456. Xu X, Wan J, Yuan L, Ba J, Feng P, Long W, et al. Serum levels of apolipoprotein E correlates with disease progression and poor prognosis in breast cancer. Tumour biology : the journal of the International Society for Oncodevelopmental Biology and Medicine. 2016.

457. Delitto D, George TJ, Jr., Loftus TJ, Qiu P, Chang GJ, Allegra CJ, et al. Prognostic Value of Clinical vs Pathologic Stage in Rectal Cancer Patients Receiving Neoadjuvant Therapy. Journal of the National Cancer Institute. 2018;110(5):460-6.

458. Glunde K, Bhujwalla ZM, Ronen SM. Choline metabolism in malignant transformation. Nat Rev Cancer. 2011;11(12):835-48.

459. Aboagye EO, Bhujwalla ZM. Malignant transformation alters membrane choline phospholipid metabolism of human mammary epithelial cells. Cancer Res. 1999;59(1):80-4.

460. Kurabe N, Hayasaka T, Ogawa M, Masaki N, Ide Y, Waki M, et al. Accumulated phosphatidylcholine (16:0/16:1) in human colorectal cancer; possible involvement of LPCAT4. 2013;104(10):1295-302.

461. Kennedy L, Hodges K, Meng F, Alpini G, Francis H. Histamine and histamine receptor regulation of gastrointestinal cancers. Transl Gastrointest Cancer. 2012;1(3):215-27.

462. Coruzzi G, Adami M, Pozzoli C. Role of histamine H4 receptors in the gastrointestinal tract. Frontiers in bioscience (Scholar edition). 2012;4(1):226-39.

463. Fang Z, Yao W, Xiong Y, Li J, Liu L, Shi L, et al. Attenuated expression of HRH4 in colorectal carcinomas: a potential influence on tumor growth and progression. BMC cancer. 2011;11:195:1-11.

464. Kannen V, Bader M, Sakita JY, Uyemura SA, Squire JA. The Dual Role of Serotonin in Colorectal Cancer. Trends in Endocrinology & Metabolism. 2020;31(8):611-25.

465. Coogan PF, Strom BL, Rosenberg L. Antidepressant use and colorectal cancer risk. 2009;18(11):1111-4.

466. Tutton PJM, Barkla DH. THE INFLUENCE OF SEROTONIN ON THE MITOTIC RATE IN THE COLONIC CRYPT EPITHELIUM AND IN COLONIC ADENOCARCINOMA IN RATS. 1978;5(1):91-4.

467. Xia Y, Wang D, Zhang N, Wang Z, Pang L. Plasma serotonin level is a predictor for recurrence and poor prognosis in colorectal cancer patients. 2018;32(2):e22263.

468. Ge Y, Wang X, Guo Y, Yan J, Abuduwaili A, Aximujiang K, et al. Gut microbiota influence tumor development and Alter interactions with the human immune system. Journal of Experimental & Clinical Cancer Research. 2021;40(1):42.

469. Lee H, Shim S, Kong JS, Kim MJ, Park S, Lee SS, et al. Overexpression of dopamine receptor D2 promotes colorectal cancer progression by activating the β-catenin/ZEB1 axis. Cancer Sci. 2021;112(9):3732-43.

470. De Simone V, Pallone F, Monteleone G, Stolfi C. Role of T(H)17 cytokines in the control of colorectal cancer. Oncoimmunology. 2013;2(12):e26617-e.

471. Søndergaard H, Skak K. IL-21: roles in immunopathology and cancer therapy. Tissue antigens. 2009;74(6):467-79.

472. Mousa L, Salem ME, Mikhail S. Biomarkers of Angiogenesis in Colorectal Cancer. Biomark Cancer. 2015;7(Suppl 1):13-9.

473. Wei SC, Tsao PN, Yu SC, Shun CT, Tsai-Wu JJ, Wu CH, et al. Placenta growth factor expression is correlated with survival of patients with colorectal cancer. Gut. 2005;54(5):666-72.

474. Wei SC, Liang JT, Tsao PN, Hsieh FJ, Yu SC, Wong JM. Preoperative serum placenta growth factor level is a prognostic biomarker in colorectal cancer. Dis Colon Rectum. 2009;52(9):1630-6.

475. Wei S-C, Tsao P-N, Weng M-T, Cao Z, Wong J-M. Flt-1 in colorectal cancer cells is required for the tumor invasive effect of placental growth factor through a p38-MMP9 pathway. Journal of Biomedical Science. 2013;20(1):39.

476. Yang H, Han Y, Wu L, Wu C. Diagnostic and prognostic value of serum interleukin-16 in patients with gastric cancer. Mol Med Rep. 2017;16(6):9143-8.

477. Gao L-B, Rao L, Wang Y-Y, Liang W-B, Li C, Xue H, et al. The association of interleukin-16 polymorphisms with IL-16 serum levels and risk of colorectal and gastric cancer. Carcinogenesis. 2008;30(2):295-9.

478. Mantur M, Snarska J, Koper O, Dziecioł J, Płonski A, Lemancewicz D. Serum sICAM, sVCAM and sE-selectin levels in colorectal cancer patients. Folia Histochem Cytobiol. 2009;47(4):621-5.

479. Dymicka-Piekarska V, Guzinska-Ustymowicz K, Kuklinski A, Kemona H. Prognostic significance of adhesion molecules (sICAM-1, sVCAM-1) and VEGF in colorectal cancer patients. Thrombosis Research. 2012;129(4):e47-e50.

480. Jakimovska M, Černe K, Verdenik I, Kobal B. High preoperative serum sVCAM-1 concentration as a predictor of early ovarian cancer recurrence. Journal of Ovarian Research. 2020;13(1):107.

481. Xu L, Wang R, Ziegelbauer J, Wu WW, Shen R-F, Juhl H, et al. Transcriptome analysis of human colorectal cancer biopsies reveals extensive expression correlations among genes related to cell proliferation, lipid metabolism, immune response and collagen catabolism. Oncotarget. 2017;8(43):74703-19.

482. Wu S-M, Tsai W-S, Chiang S-F, Lai Y-H, Ma C-P, Wang J-H, et al. Comprehensive transcriptome profiling of Taiwanese colorectal cancer implicates an ethnic basis for pathogenesis. Scientific Reports. 2020;10(1):4526.

483. Huo T, Canepa R, Sura A, Modave F, Gong Y. Colorectal cancer stages transcriptome analysis. PLOS ONE. 2017;12(11):e0188697.

484. Najdaghi S, Razi S, Rezaei N. An overview of the role of interleukin-8 in colorectal cancer. Cytokine. 2020;135:155205.

485. Bertucci F, Ueno NT, Finetti P, Vermeulen P, Lucci A, Robertson FM, et al. Gene expression profiles of inflammatory breast cancer: correlation with response to neoadjuvant chemotherapy and metastasis-free survival. Annals of Oncology. 2014;25(2):358-65.

486. Cao B, Luo L, Feng L, Ma S, Chen T, Ren Y, et al. A network-based predictive gene-expression signature for adjuvant chemotherapy benefit in stage II colorectal cancer. BMC cancer. 2017;17(1):844.

487. Tsimberidou AM, Fountzilas E, Bleris L, Kurzrock R. Transcriptomics and solid tumors: The next frontier in precision cancer medicine. Seminars in Cancer Biology. 2020.

488. Bacci M, Lorito N, Smiriglia A, Morandi A. Fat and Furious: Lipid Metabolism in Antitumoral Therapy Response and Resistance. Trends in cancer. 2021;7(3):198-213.

489. Ritter V, Krautter F, Klein D, Jendrossek V, Rudner J. Bcl-2/Bcl-xL inhibitor ABT-263 overcomes hypoxia-driven radioresistence and improves radiotherapy. Cell Death & Disease. 2021;12(7):694.

490. Kalyanaraman B, Cheng G, Hardy M, Ouari O, Sikora A, Zielonka J, et al. Mitochondria-targeted metformins: anti-tumour and redox signalling mechanisms. Interface Focus. 2017;7(2):20160109-.

491. Khader EaI, Ismail WW, Mhaidat NM, Alqudah MA. Effect of metformin on irinotecan-induced cell cycle arrest in colorectal cancer cell lines HCT116 and SW480. Int J Health Sci (Qassim). 2021;15(5):34-41.

492. Tsogas FK, Majerczyk D, Hart PC. Possible Role of Metformin as an Immune Modulator in the Tumor Microenvironment of Ovarian Cancer. International journal of molecular sciences. 2021;22(2):867.

493. Tojo M, Miyato H, Koinuma K, Horie H, Tsukui H, Kimura Y, et al. Metformin combined with local irradiation provokes abscopal effects in a murine rectal cancer model. Sci Rep. 2022;12(1):7290.

494. Long Z, Zhou J, Xie K, Wu Z, Yin H, Daria V, et al. Metabolomic Markers of Colorectal Tumor With Different Clinicopathological Features. 2020;10.

495. Kennedy AD, Wittmann BM, Evans AM, Miller LAD, Toal DR, Lonergan S, et al. Metabolomics in the clinic: A review of the shared and unique features of untargeted metabolomics for clinical research and clinical testing. Journal of mass spectrometry : JMS. 2018;53(11):1143-54.

496. Odom JD, Sutton VR. Metabolomics in Clinical Practice: Improving Diagnosis and Informing Management. Clinical Chemistry. 2021;67(12):1606-17.

497. Lu M, Zhan X. The crucial role of multiomic approach in cancer research and clinically relevant outcomes. EPMA J. 2018;9(1):77-102.

498. Aran D, Camarda R, Odegaard J, Paik H, Oskotsky B, Krings G, et al. Comprehensive analysis of normal adjacent to tumor transcriptomes. Nature communications. 2017;8(1):1077.

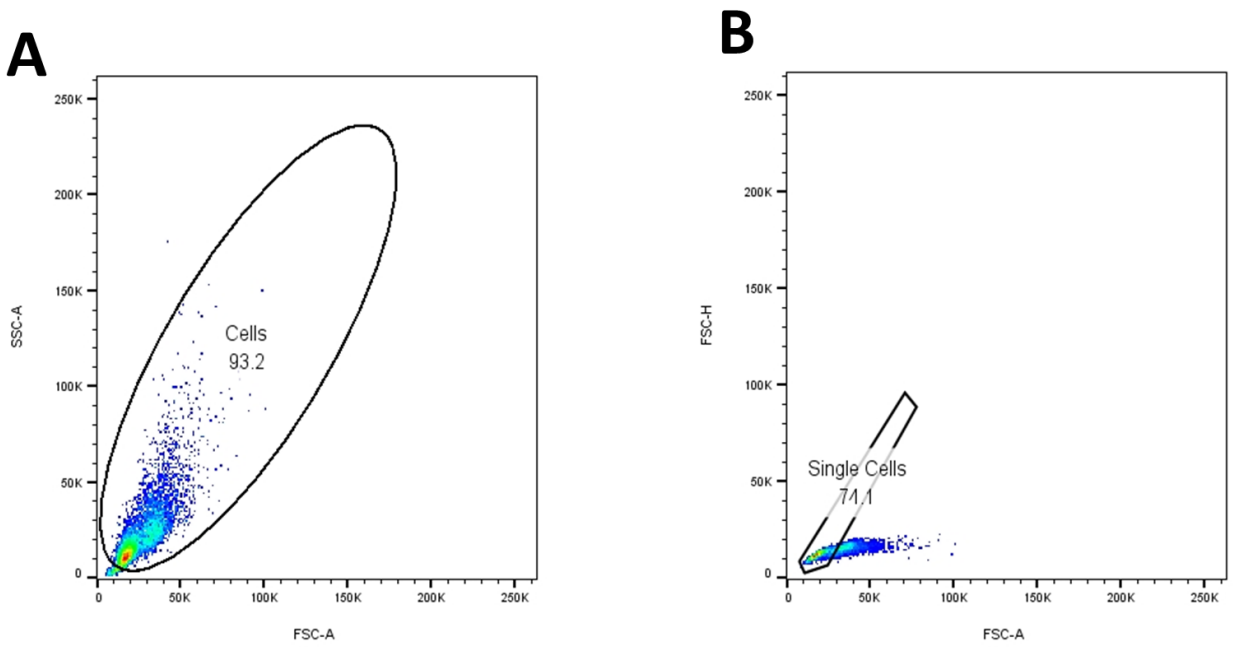

Appendix 1: Representative images of gating strategy employed for flow cytometry experiments. A) Gating on cells to exclude debris. B) Gating on single cells, to exclude doublets.

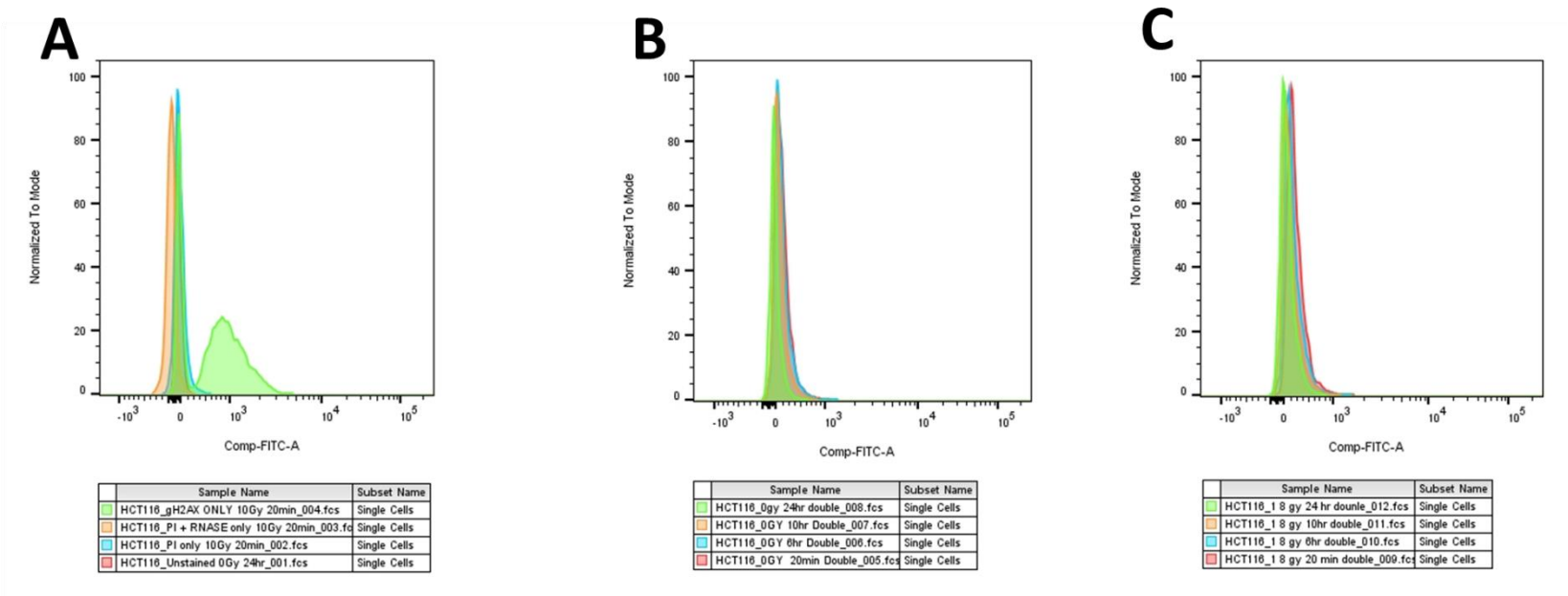

Appendix 2: Representative images of γH2AX flow cytometry histograms. A) Representative image of controls. B) Representative image of γH2AX MFI of unirradiated HCT116 cells at 20 min, 6 h, 10 h and 24 h post mock-irradiation, stained with γH2AX-Alexa 488 antibody, assessed using FITC channel. C) Representative image of γH2AX MFI of HCT116 cells irradiated with 1.8 Gy at 20 min, 6 h, 10 h and 24 h post radiation, stained with γH2AX-Alexa 488 antibody, assessed using FITC channel.

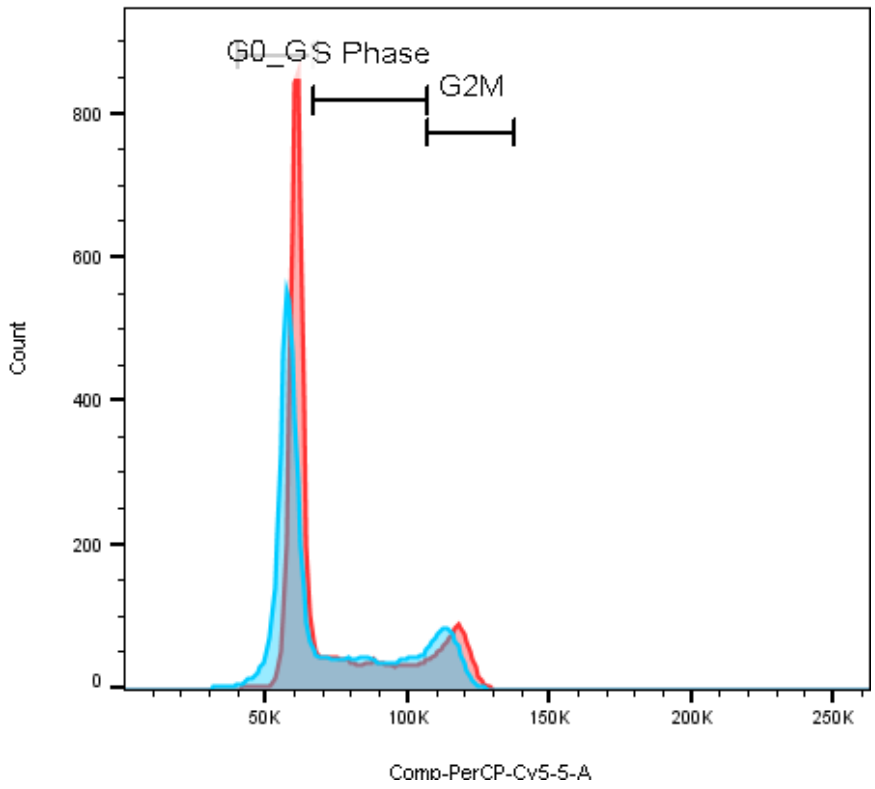

Appendix 3: Representative image of cell cycle flow cytometry histogram. Cell cycle distribution was assessed by PI staining. Image demonstrating the proportion of cells in each cell cycle phase following H_2O treatment (Blue) or metformin (10 mM) treatment (red), at 48 h post treatment in SW837 cells.

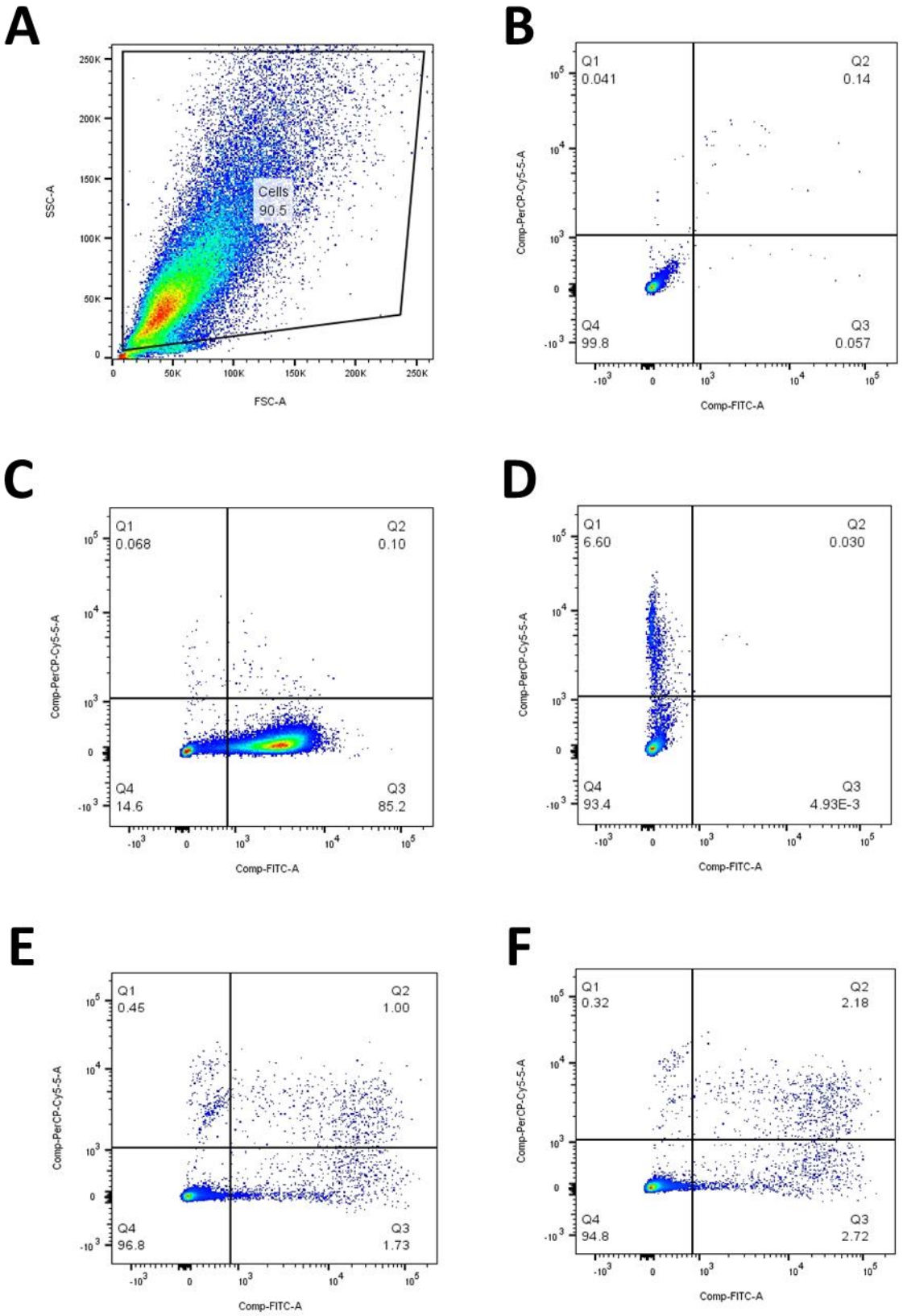

Appendix 4: Representative images of Annexin V/PI staining for apoptosis by flow cytometry. A) Representative scatter plot. B) Unstained control. C) Annexin-V only positive control. D) PI only positive control. E) Unirradiated HCT116 cells 48 h post mock-irradiation. F) HCT116 cells 48 h post exposure to 1.8 Gy radiation.